1-19-2022

Ecology of Periphyton in a Subtropical River Floodplain

Kamela De Gallardo
Louisiana State University and Agricultural and Mechanical College

Recommended Citation

Gallardo, Kamela De, "Ecology of Periphyton in a Subtropical River Floodplain" (2022). *LSU Doctoral Dissertations*. 5741.
https://repository.lsu.edu/gradschool_dissertations/5741

ECOLOGY OF PERIPHYTON IN A SUBTROPICAL RIVER FLOODPLAIN

A Dissertation

Submitted to the Graduate Faculty of the
Louisiana State University and
Agricultural and Mechanical College
in partial fulfillment of the
requirement for the degree of
Doctor of Philosophy

in

The School of Renewable Natural Resources

by
Kamela De Gallardo
B.S., Bowling Green State University, 2012
M.S., Bowling Green State University, 2014
May 2022

ACKNOWLEDGMENTS

I would like to thank my graduate advisors, Drs. William Kelso and Allen Rutherford for their support and instruction. Dr. Kelso’s insight was invaluable. He offered extensive knowledge of floodplain habitats as well as counsel and encouragement. Next, I would like to thank my committee members. Dr. Kaller offered expertise in aquatic ecosystems and statistical methods. I am extremely grateful for his contribution to this dissertation and my development as a researcher and teacher. Dr. Reagan Errera was a great help to me and increased my understanding of plankton ecology. The research associates Tiffany Pasco, Mariah Taylor, Deborah Kelly, and Collen Walsh were such a wonderful help to me. They assisted me in field and laboratory work and became fantastic friends. I would like to thank my fellow graduate students Erin Thayer, Pat Wooden, and Kristy Capelle for their friendship and support. They not only made me laugh and kept me sane, but they also were always willing to lend a hand with field and lab work. I would like to thank all the amazing student workers in the Kelso-Kaller lab, but I want to offer my special appreciation for the exceptional contributions of Allie Davis, Cameron Toerner, Kira Cates, Melanie Bates, and Shae Johnson. This project would not have been possible without their assistance. Next, I would like to thank Thomas Blanchard for his assistance with elemental analysis.

Bill and Versa Stickle should receive special thanks for their above-and-beyond hospitality. I spent countless nights at their house, eating, doing laundry, and using their internet. They also watched my dog for the three long years I commuted to Houston to see my husband on the weekends. Their support, encouragement, and prayers made an enormous impact on me, and I am so very grateful for them in my life. I would like to also thank my family for their support and love. My parents not only fostered a love for

learning and nature in me but also supported me in my college and graduate years, both financially and spiritually. My three fantastic siblings were always there for me, encouraged me when I was down, and made me laugh when I was sad.

Lastly, I would like to thank my wonderful husband, Ricardo, whose unwavering support during my studies is ultimately what made this project possible. Thank you for agreeing to a long-distance marriage, spending hundreds of hours on the midnight bus to be there for me when I had mounds of laboratory work to do. Thank you for the coffee. Thank you for always being there to help me with whatever I needed, whether it was helping me with R codes, cleaning glassware, folding laundry, or giving me a tissue to dry my weepy eyes.

TABLE OF CONTENTS

LIST OF TABLES

LIST OF FIGURES

ABSTRACT

The Atchafalaya River Basin (ARB) in southcentral Louisiana, USA, is a large and biologically diverse floodplain surrounding the Atchafalaya River (AR), which is the largest distributary of the Mississippi River, receiving 30% of the combined daily discharge of the Mississippi and Red Rivers. Annual flooding facilitates exchange between the AR and its floodplain and is thought to give rise to the high productivity of the river-floodplain system. Primary production within the aquatic ARB is driven by periphytic algae, phytoplankton, and aquatic macrophytes, however, very little is known about periphytic algal assemblages in floodplain systems. In this study, artificial substrates were used to sample periphytic algae from several areas across the ARB between 2017- 2019, and environmental variables measured along a spatiotemporal gradient were used to better understand the factors influencing periphytic algal assemblages. Lake Verret, which did not have active AR connections, was also sampled to provide a natural control for the purpose of investigating the effect of an annual flood pulse on periphyton assemblage composition. Algae were classified into seven groups that included chrysophytes, centric diatoms, pennate diatoms, chlorophytes, euglenoids, xanthophytes, and cyanobacteria. Periphytic algal assemblages were dominated by chlorophytes in 2017, but then shifted to mainly diatoms in 2018 and 2019. Canonical correspondence analyses (CCAs) indicated this may have been due to differences in macrophyte abundance among years. Overall, algal densities were higher early in the year and lower during the summer, likely related to greater nutrient levels associated with inundation of the floodplain by the AR. CCAs also indicated spatial effects on ARB periphyton with diatoms dominating assemblages near river water inputs and other groups such as chlorophytes increasing in relative abundance further into the floodplain. This is likely related with associated spatial gradients in nitrogen sources, particularly ammonium. During 2019, the ARB experienced intense flooding, which lasted an unprecedented 329 days. Total algal cell abundance increased substantially during the high magnitude flood but diminished as floodwaters receded during the summer. Although variable across years, the AR flood pulse strongly influenced the composition and dynamics of the ARB periphyton assemblage, with spatial and temporal patterns reflecting interactions of nutrient availability, temperature, distance from source water, macrophyte abundance and composition, and shading.

CHAPTER I. PERIPHYTIC ALGAL ASSEMBLAGES IN THE ATCHAFALAYA RIVER BASIN FLOODPLAIN

The Atchafalaya River Basin (ARB) is a large floodplain in the southeastern United States of America that consists of a network of interconnected channels and bayous, along with seasonally inundated swamps and lakes. The Atchafalaya River (AR) is the fifth-largest river in the USA (combination of the Choctaw words *hacha* meaning “river” and *falaya* meaning “long”) and its floodplain is the largest remaining bottomland hardwood forest in North America. Beginning in central Louisiana near Simmesport, the AR receives 30% of the combined daily discharge from the Mississippi and Red Rivers, and then runs south for over 200 km, where it discharges into the northern Gulf of Mexico (Piazza 2014). The AR and its floodplain support considerable biodiversity as well as significant commercial and recreational fisheries (Piazza 2014). Annual flooding facilitates multiple ecosystem functions, including biochemical cycling and primary production (Pettit et al. 2011, Pettit et al. 2017, Bayley et al. 2018). Although aquatic macrophytes contribute to floodplain primary production, algal production is far greater (Wetzel 1964). These algae can come in two forms, phytoplankton and attached periphyton. Periphyton is comprised of a complex matrix of organic material, fungi, bacteria, and attached algae that accumulate on submerged surfaces (Wetzel 1964). It serves to not only process organic material, but also absorbs and recycles nutrients (Flemming 1993, Battin et al. 2016). Periphytic algae have been identified as important contributors to riverine primary production, with assemblage composition and productivity influenced by seasonal changes environmental drivers such as flow (low flows, Smolar-Žvanut and Mikoš 2014; scouring flows, Hart et al. 2013), nutrient concentrations (Hoyle et al. 2014; Gillett et al. 2016), and invertebrate grazing (Guo et al. 2018). Much less has been published regarding periphytic algal assemblage composition and its response to seasonal changes in environmental drivers in floodplain ecosystems. These systems provide dynamic physicochemical conditions that differ substantially from the adjacent river in terms of flow, temperature, nutrient availability, and grazing assemblages (Lewis et al. 2000, Kaller et al. 2015) and this dissertation aims to improve our understanding of periphyton dynamics in these environmentally complex habitats.

Chapter II

The first research chapter will focus on understanding periphytic algal assemblages in the ARB floodplain. Floodplains play an important role in riverine ecosystems by supporting nutrient cycling and biological production (Junk et al. 1989). During flood events, fish and macroinvertebrates take advantage of newly available habitats to forage and reproduce (Gomes and Agostinho 1997, Agostinho et al. 2004). In addition, river water that moves onto the floodplain facilitates biological exchange (Pettit et al. 2011, Pettit et al. 2017, Bayley et al. 2018). Nutrients and carbon already present in floodplain sediment are released during inundation, and nutrient-rich river moves into the floodplain. The input of nutrients and organic matter from this exchange largely drives algal production. Algae account for the greatest portion of primary production and energy transfer that occurs in river and floodplain habitats (Wetzel 1964). However, very little is known about the factors that influence periphytic algal abundance or assemblage structure in floodplain systems, and even less is known of the role periphyton plays in the highly diverse and productive ARB floodplain. Previous observations made by Prescott (1942), Bryan et al. (1975), and Hern (1978) were mostly in reference to chlorophyll concentrations or local observations of algal blooms. Swamp and floodplain habitats were largely ignored as having poor conditions for algal growth. Colon-Gaud et al. (2004) briefly discussed algal presence during late flood stage in 2001, but this was only in regards to macroinvertebrate dynamics among submerged plant beds. The composition and dynamics of periphytic algal assemblages in the ARB, or what factors might drive changes in assemblage composition, have not yet been studied. Chapter II of this dissertation will discuss how physicochemical and spatiotemporal factors impact periphytic algal assemblages in the ARB floodplain system. To this aim, ARB periphytic algal communities were sampled with artificial substrates between 2017-2018 at differing distances from river input. The goal was to describe ARB periphytic algal assemblages and understand the forces driving spatiotemporal differences in algal assemblage structure.

Chapter III

The second research chapter will discuss the role flood pulses play in floodplain periphyton assemblages. The flood pulse refers to annual river flooding that inundates low-lying floodplain regions adjacent to the river (Junk et al 1989). As mentioned previously, movement of river water onto the floodplain facilitates biological exchange and drives nutrient cycling and production (Pettit et al. 2011, Pettit et al. 2017). It also provides habitat for organisms to forage or reproduce, as well as a sheltered environment rich in food sources where larval fish and invertebrate growth and maturation can occur (Opperman et al. 2010, Bayley et al. 2018). However, floodplains worldwide have been altered by humans, mostly for agricultural land use, navigation, or flood control for urban development. Dams and levees are used to restrict regular flooding and disconnect, sometimes permanently, floodplains from their river sources (Lewis et al. 2000). These modifications can potentially alter biodiversity and ecosystem functions by reducing or stopping the biological and chemical exchange that supports river-floodplain systems (Fernandes et al. 2009, Algarte et al. 2016). Permanently severed floodplain lakes are at risk for lowed biological diversity and production (Beisner et al. 2006, Shurin et al. 2009). The ARB has been constricted to about half of its historic size and has been impacted by multiple, substantial hydrologic changes (Piazza 2014). Many former regions that were seasonally inundated are now permanent floodplain lakes with no hydrologic connection to the AR. Lake Verret (LV), located on the east side of the ARB, was once connected to the AR and received annual river water during seasonal flooding. However, after multiple severe floods in the late 19th and early 20th centuries, levee construction permanently separate LV from AR influences (Report of the Chief of Engineers US Army 1941). Because the purpose of this current work is to better understand floodplain periphytic algal assemblages, LV can serve as a natural control to study flood pulse influences on periphyton assemblages as it no longer receives seasonal pulses of AR water. To this aim, periphytic algae were sampled (January – September 2019) from areas with active river connections and compared to algal assemblages collected from sites with no active river connections. This comparison will allow for a better understanding of the role the flood pulse plays in driving periphytic algal assemblages in river-floodplain systems.

Chapter IV

The third research chapter will discuss the high-magnitude 2019 AR flood, how this historic event impacted periphytic algal assemblages in the ARB, and the implications for periphytic algae in the future. In 2019, the Mississippi River (MR) and Atchafalaya River (AR) experienced unprecedented flooding (NOAA 2019, Reed et al. 2020). The MR was in flood stage for over 150 days and the AR experienced over 300 days of flooding (Pal et al. 2020, Price and Berkowitz 2020). Although the 2019 flood was by far the most extensive, the AR has experienced multiple large flood events in the past (Piazza 2014, Tang et al. 2021). In fact, the frequency at which these severe floods occur has increased in the twentieth century and this phenomenon is being observed across the globe (Muzik 2002). Because climate change threatens to increase the number of severe weather incidents, flooding frequency and severity may increase in the future (Hirabayashi et al. 2008). Periphytic algae play a vital role in river-floodplain ecosystems and the 2019 flood offers an excellent opportunity to observe how these algal assemblages respond to prolonged or severe flooding. To better understand how an atypical flood could affect periphyton composition and abundance in the AR floodplain, periphytic algae samples collected in 2019 were compared to a non-flooded summer in 2017.

CHAPTER II. PERIPHYTON ASSEMBLAGES IN THE ATCHAFALAYA RIVER FLOODPLAIN

INTRODUCTION

Floodplains are an integral part of riverine ecosystems and support a high degree of biodiversity and productivity (Pettit et al. 2011, Jardine et al. 2012, Jardine et al. 2015, Crook et al. 2019). In unmodified systems, seasonal inundation during high water events facilitates the exchange of fish, invertebrates, organic material, and nutrients between the river and its floodplain (Junk et al. 1989, Gomes and Agostinho 1997, Agostinho et al. 2004). This exchange is one of the main drivers of biogeochemical cycling in river ecosystems (Pettit et al. 2011, Pettit et al. 2017, Bayley et al. 2018). Algae play significant roles as primary producers in floodplain and riverine systems, both as phytoplankton and attached periphyton (Wetzel 1964). Periphyton is composed mostly of epiphytic (attached) algae, fungi and bacteria, and forms complex matrixes on submerged surfaces (Wetzel 1964). These sites serve as sites for essential carbon and nutrient cycling by absorbing and processing organic material (Flemming 1993, Battin et al. 2016). Production of epiphytic algae, stimulated by nutrient input and decomposition of organic matter, is a major contributor to aquatic food webs. Together with phytoplankton, this autochthonous production comprises the majority of riverine biomass assimilated into higher trophic levels (Junk et al. 1989, Thorp and Delong 1994, Thorp and Delong 2002, Junk 2005, Doi et al. 2008). Although phytoplankton typically dominates production in lacustrine systems (Vadeboncoeur and Steinmann 2002), particularly in the upper photic zone, epiphytic algae present in periphyton biofilms on submerged surfaces are the principal autochthonous producers in riverine systems (Thorp and Delong 1994, Junk et al. 1989, Doi 2008).

Abiotic influences on riverine algal production, abundance, and community composition include hydrologic regimes, river geomorphology, channel orientation, periodicity of disturbances, and frequency and duration of flooding (Dudgeon 1992, Agostinho et al. 2004, Davies et al. 2008, Julian et al. 2008, Agostinho et al. 2008, Fuller et al. 2011). Changes in flooding regimes can have substantial impacts on algal abundance, richness, and diversity (Leveque 1995, Agostinho et al. 2008, Mihalijevic and Pfeiffer 2012, Bondar-Kunze et al. 2016), with algal species richness and diversity showing positive correlations with high river stage and residence time (Thomaz et al. 1992, Algarte et al. 2009, Fernandes et al. 2009, Adame et al. 2018). Although elevated flow velocities at high river stages can lead to excessive shear stress, dislodgement of attached algae from submerged substrates, and a reduction in overall algal biomass, it also opens up newly available space for recolonization (Biggs et al. 1995, Oliveira and Calheiros 2000). Alterations to natural hydrologic regimes can have deleterious consequences on floodplain algal communities. By constraining and altering natural flooding via dams and levees, changes in the composition and overall abundance of algal species can impact trophic energy and nutrient transfer (Gomes and Agostinho 1997, Fernandes et al. 2009, Algarte et al. 2016). In addition, as the extent of connected floodplains decrease worldwide (e.g., dam construction in Brazil, Nepal, Turkey, India, and China; Zarfl et al. 2015, 2019), it is important that we increase our knowledge of floodplain ecosystem processes and the role epiphytic algae play in floodplain trophic webs (Brinson and Mavarez 2002, Costanza et al. 2014, Batzer et al. 2018).

The Atchafalaya River Basin (ARB), which is the largest remaining bottomland hardwood forest in North America, begins in central Louisiana near Simmesport (Lambou 2020, Piazza 2014). The Atchafalaya River (AR) is regulated to carry an annual average of

30% of the combined daily water discharge of the Mississippi and Red rivers, and flows approximately 220 km to the northern Gulf of Mexico. The ARB consists of a network of canals, backwater lakes, and seasonally inundated swamps that are home to an extremely diverse biota (Piazza 2014). Now only half of its historic size, the ARB has been constrained to 339,100 ha with levees to the east and west (Louisiana Department of Natural Resources 2010). Constriction of natural annual flooding has negatively impacted ecological functions in the ARB and has resulted in nutrient reduction, increased sedimentation rates, and spatially and temporally extensive hypoxia during the latter stages of the flood pulse (Sabo et al. 1999, BryantMason et al. 2013, Baustian et al. 2019, Hupp et al. 2019, Kroes et al. 2019).

Little is known about epiphytic algae in the ARB or how flood pulses impact abundance or species composition. Previous reports on algae in the region avoided bayous and swamps as presumably unfavorable conditions due to high organic matter, turbidity, and shading from tree cover (Prescott 1942, but see Bryan et al. 1975, Hern 1978). The goal of this study was to provide a baseline assessment of the dynamics of ARB periphyton and develop a more comprehensive understanding of the role periphytic algae play in floodplain ecosystems. The specific objectives were to describe i) epiphytic algal assemblages present in the ARB floodplain, and ii) how algal composition changes in response to inundation events that alter floodplain water physicochemistry. As a working hypothesis, I expected periphyton composition would change in response to river flooding and that assemblages would generally homogenize across the floodplain with continued inputs of AR water.

METHODS

Site Locations

The study was conducted at 14 sites in a 50 km^2 section east of the Atchafalaya River, west of Pierre Part, LA and south of Bayou Sorrel in Iberia and St. Martin parishes. Sites were designated along small distributaries of Old River (Figure 2.1), with the northernmost sites located below Bayou Pigeon. Other sites were located in Bayou

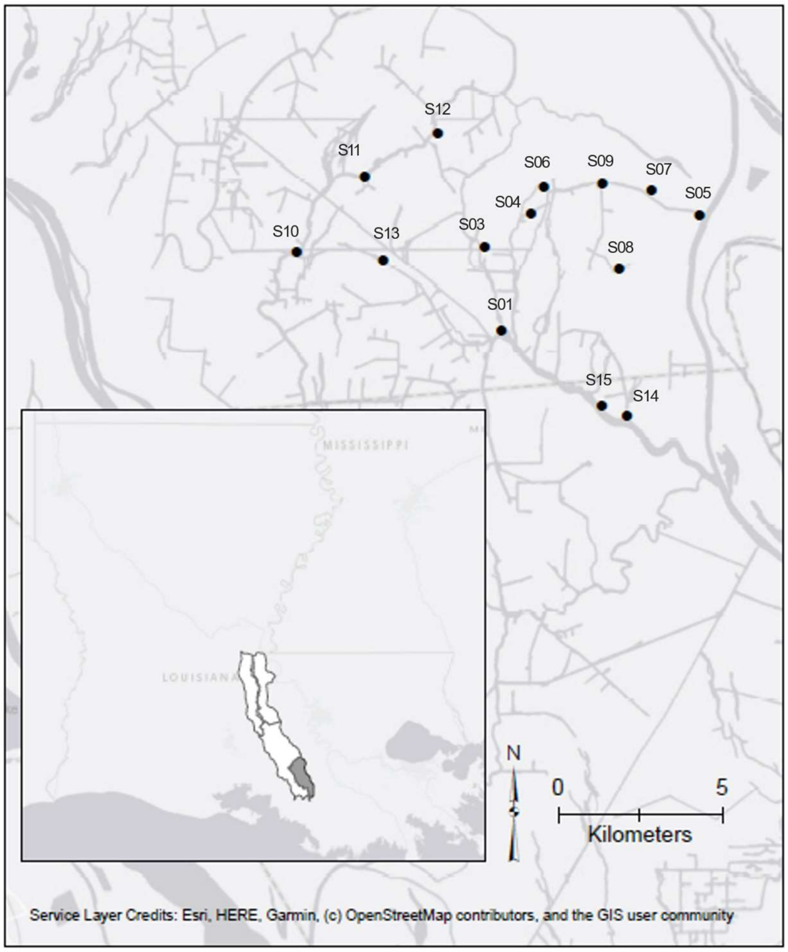

Figure 2.1. Location of periphyton sampling sites in the Atchafalaya River Basin during 2017-2018. Dark grey region in the inset indicates the lower East Grand Lake Water Management Unit within the Atchafalaya River Basin.

Postillion, Bayou Latania, and their connecting tributaries. Three periphyton samplers (periphytometers) were deployed at each site and tethered to trees on shore or baldcypress (*Taxodium distichum*) knees near shore. The inlet of Bayou Postillion at the Gulf Intracoastal Waterway along the eastern Atchafalaya River Basin guide levee was designated as the source of Atchafalaya River water for all sites, except S10-S12, which received water from an inlet further north from Bayou Postillion. The site distribution represented a range of spatial connectivity to source waters (Table 2.1) to examine potential changes in periphyton composition with changes in physicochemistry as floodwaters moved across the floodplain.

Table 2.1. Site locations and distance from the nearest, northward inlet from intracoastal waterway.

Site	Distance (km)	Location
15	5.03	N29° 58.755' W91° 17.646'
14	7.29	N29° 57.595' W91° 17.242'
13	15.21	N30° 01.021' W91° 21.544'
12	18.41	N29° 59.934' W91° 22.668'
11	20.84	N29° 59.827' W91° 21.246'
10	12.87	N30° 01.630' W91° 20.343'
09	1.63	N30° 00.826' W91° 16.830'
08	3.22	N29° 59.693' W91° 17.370'
07	2.89	N30° 00.913' W91° 17.642'
06	4.52	N30° 00.864' W91° 18.601'
05	0.11	N30° 00.466' W91° 16.040'
04	5.1	N30° 00.498' W91° 18.815'
03	7.09	N30° 00.006' W91° 19.576'
01	9.63	N29° 58.811' W91° 19.300'

Periphytometer Design

Periphytometers (15 x 30 cm) were constructed of 1-inch PVC pipe sealed with water-resistant sealant to allow the frame to float at the water surface. Four glass microscope slides

(75 mm x 50 mm x 1 mm) were suspended along the length of the frame within approximately five centimeters of the water surface. Slides were secured with clear fishing line (10 lbs.) and plastic clips spaced five centimeters apart to avoid scraping or transferring biofilm. Glass slides were cleaned thoroughly with 95% ethanol prior to use and replaced with fresh slides biweekly.

Habitat and Water Quality Procedures

Sampling occurred from June 2017 – April 2018 and then during November 2018 to coincide with rising and falling stages in the Atchafalaya River. To assess the effects of local physicochemistry on periphyton composition, I measured surface and bottom temperature, dissolved oxygen (DO), pH, and turbidity at each site with a handheld YSI® multiprobe (Yellow Springs, OH). Water velocity was measured with a handheld velocimeter (SonTek®, YSI, Inc, Yellow Springs, OH). Tree cover and macrophyte cover were also recorded for each periphytometer. Tree cover was scored by a single observer as 0%, 20%, 40%, 80%, or 100%. To estimate macrophyte cover at the time of collection, a 75-cm x 75-cm frame was placed around each periphytometer and photographed from 1 m above. Images were used to estimate the percentage of floating or emergent plants surrounding each periphytometer as well as to identify the presence of invasive plant species. To assess rates of respiration in the surrounding water, I collected water samples for 20-day biochemical oxygen demand (BOD) in 1-L opaque Nalgene bottles once per month (rinsed twice with sample water and filled to the brim before capping) at each site. Samples were stored on ice until processing. Prior to initial dissolved oxygen measurement, samples were raised to room temperature (20° C ± 2) and a nitrogen inhibitor was added. Dissolved oxygen measurements were taken every five days for 20 days; any reading below 3.0 mg L^{-1} was bubbled with atmospheric oxygen for 5 minutes and re-measured prior to further incubation (AMHA 2018).

Algal Identification

Periphytometer slides were collected biweekly. Two of the four slides were removed and placed in individual plastic bags with 10 mL of a 2% glutaraldehyde solution for algal identification. Glutaraldehyde preservative maintains cell color and assists in taxonomic identification (Andersen 2005). Removal of biofilm from the glass surface can result in cell damage, therefore, slides were refrigerated overnight to allow the biofilm to loosen from the surface before scraping. Removal was done with a new, single-edge razor blade and biofilm was transferred into 50 mL centrifuge vials with additional 2% glutaraldehyde to completely cover the algae. Samples were stored at 4° C in the dark. Extremely dense samples were diluted into 250 mL of diluted glutaraldehyde. Prior to enumeration, samples were inverted gently to homogenize the sample. If further homogenization was needed, the sample was sonicated for no more than 15 seconds. This was enough to break up dense clumps but not enough to severely damage or burst a large number of cells. Cell identification and enumeration was made with a Sedgewick-Rafter counting slide and a standard light microscope (Leitz Laborlux K) at 400x magnification. Algal cells were classified into 8 groups (cyanobacteria, centric diatoms, pennate diatoms, xanthophytes, euglenoids, chrysophytes, chlorophytes and unknown/other) and three size classes (pico- (<2 μm), nano- (2–20 μm), and micro- (>20 μm)).

Statistical Analysis

Descriptions of periphyton composition were done with JMP Pro (vers. 15.1.0, SAS Institute, Inc, Cary, NC), and all statistical analyses were performed with R (vers 3.6) R Core Team 2019. I chose canonical correspondence analysis (CCA; R package *vegan*, Oksanen et al. 2019) over other ordination analyses because of the unimodal and constrained nature of the data. My goal was to investigate the environmental variables (temperature, dissolved oxygen, pH, turbidity, water velocity, macrophyte density, tree cover, distance from source, and river stage) influence on periphyton abundance by algal group. Percent tree cover was coded on a scale 0-5. Permutation tests (999 permutations) were used to reduce the number of environmental variables in the CCA for final interpretation. Variables identified as significant in the CCA permutation analysis were subsequently included in generalized linear models (GLMs; package *lme4*, Bates et al. 2015), with individual periphyton groups as a response and the selected environmental variables as fixed effects; collection date was run as a quadratic polynomial to reflect the rising and falling flood waters. Three versions of each generalized linear model (log link-Poisson distribution, log link-negative binomial distribution, inverse link-Gamma distribution) were performed and models with the best fit statistics (quasi $\hat{c}$) were selected for interpretation.

RESULTS

Site Accessibility

Periphytometer sites 05, 06, and 09 were only accessible during parts of the year and became completely dry during low water periods (< 3m, Pasco et al. 2016). Other sites never became dry but were inaccessible due to low water in access channels or movement of floating macrophyte mats into the area. It should be noted that it is a common practice for local crayfish (*Procambarus clarkia* and *P. zonangulus*) harvesters to use their boats to maneuver hyacinth mats in the backwater areas to provide habitat for crawfish (personal observation), and this may have led to site inaccessibility on some occasions. Periphytometers at sites 03, 04, 08, and 10 that could be retrieved during drawdown events were moved (river water receding), following the littoral edge as the river receded away from the floodplain (Keizer et al. 2014). The remaining sites (01, 07, 11, 12, 13, 14, 15) were generally assessable year-round.

Floodplain Inundation

Atchafalaya River flood stage was defined as the period when water levels at the Butte La Rose gauge (USGS 07381515) were > 3 m (Allen et al. 2008, Pasco et al. 2016). The sampling period for this study spanned two river flood pluses (Figure 2.2), with periphytometers deployed near the peak of floodplain inundation in June 2017, removed in April 2018, and re-deployed in November 2018. In 2017, river stages declined from June until July 19 and remained low for 215 days until February 18, 2018. Peak floodplain inundation (5.5

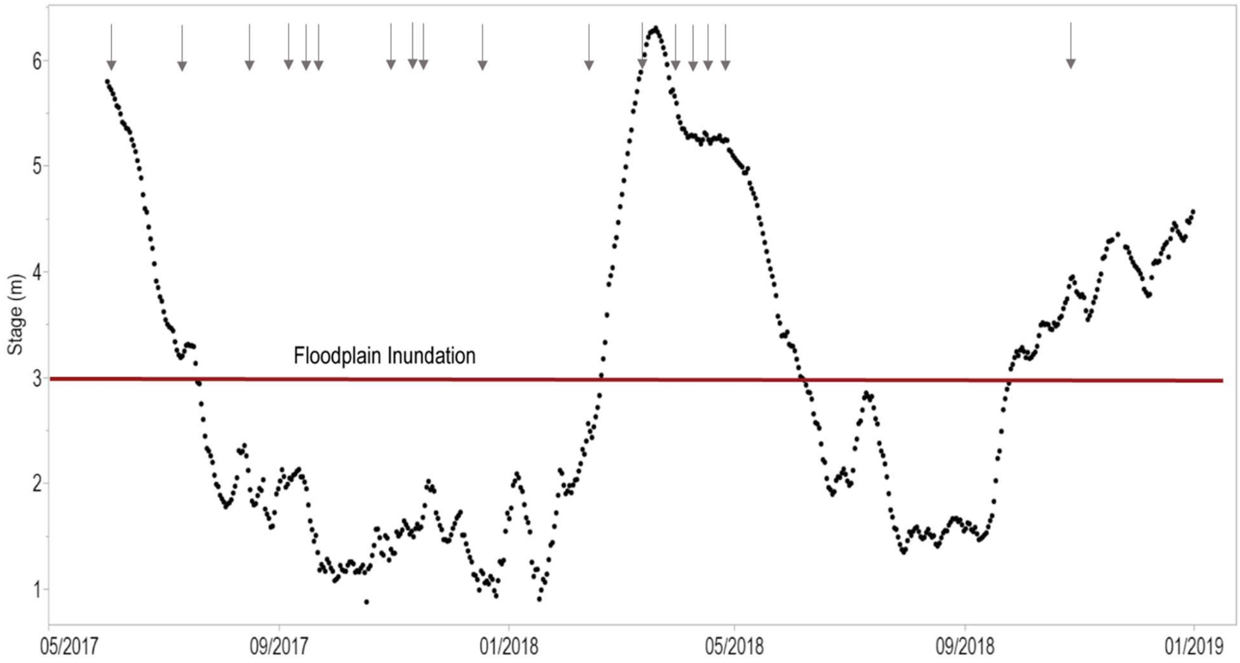

Figure 2.2. The Atchafalaya River stage at Butte La Rose, LA (USGS 07381515). Daily water gauge taken by the USGS Water Science Center. Sampling period spanned from June 2017 – April 2018 and November 2018. Floodplain was considered inundated at 3 meters. Arrows indicate sampling event.

m) was reached in early April 2018 and the floodplain remained inundated until June 7, with water levels once again rising above flood stage 111 days later on September 25.

Physicochemistry

Physicochemistry was typical of the Atchafalaya River basin during the sampling period (Table 2.2). Mean water temperature was 21.58° C ± 0.17 SE with the warmest readings from August 2017 during the low water period and the coolest temperatures from February 2018 (Figure 2.3). Dissolved oxygen (DO) was variable throughout the year and nearly all sites became hypoxic (<2.0 mg L^{-1}; Sabo et al. 1999) during the summer months when the river was below flood stage. The highest DO recordings occurred in the late winter during river inundation. Turbidity was also highly variable, with increases recorded during both rising (January 2017) and falling (April 2017) river stages. Water velocity was relatively stable, as

Table 2.2. Mean (SE), minimum, and maximum values for environmental variables measured at all sites over the 2017-2018 sampling period. Measurements for water quality data are an average of bottom and surface YSI readings. BOD = Biological oxygen demand.

	Mean	Min	Max
Distance from Source (m)	7.72 (0.16)	0.11	20.84
Depth (m)	1.12 (0.02)	0.04	2.51
Temperature (° C)	21.58 (0.17)	7.58	30.17
Dissolved Oxygen (mg L^{-1})	4 (0.08)	0.39	13.7
pH	7.08 (0.01)	5.97	7.84
Turbidity (NTU)	42.74 (1.15)	1.9	179.35
Water Velocity (m sec^{-1})	0.09 (0.00)	0	0.92
BOD (mg L^{-1})	5.03 (0.08)	1.9	10.98
River Stage (m)	3.22 (0.17)	1.13	6.23
Tree Cover (0-5)	2.83 (0.04)	0	5
Macrophyte Cover (%)	62.1 (1.28)	0	100

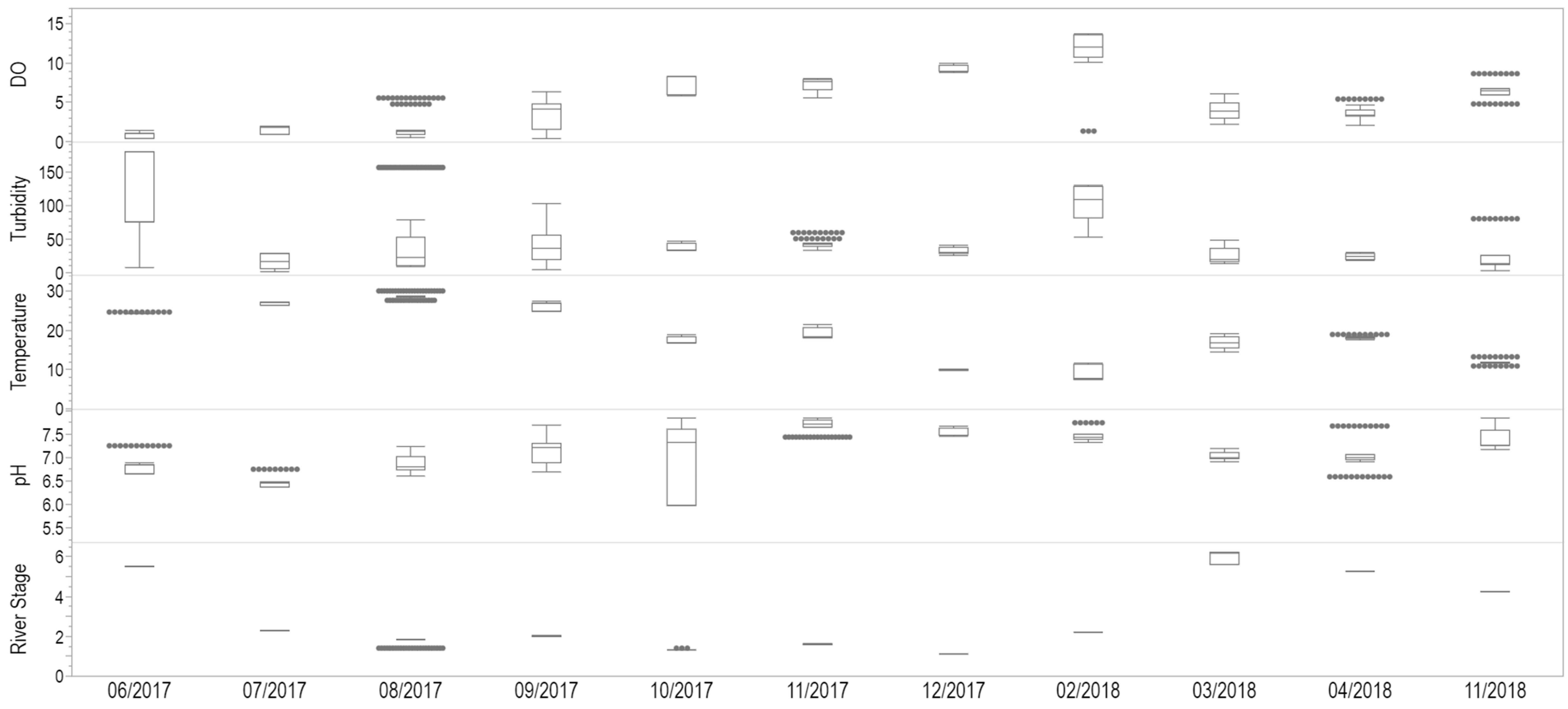

Figure 2.3. Box plots (mean, 25th and 75th quartiles, and range) of dissolved oxygen (mg L-1), turbidity (NTU), water temperature (◦ C), pH, and river stage (m) measurements for all sites sampled in 2017-2018 (sites combined).

periphytometer locations were chosen in backwater areas of the floodplain protected from elevated flows during the flood pulse.

Periphyton Assemblage

Total cell abundance shifted throughout the year (Figure 2.4; cell densities by site can be found in Appendix A.1), with the lowest total cell abundance occurring during the winter months and the highest during the fall and spring. Overall, periphyton assemblage composition also varied over time (Figure 2.5; community by site can be found in Appendix A.2), although diatoms or chlorophytes tended to be the most groups abundant in every month sampled. Chlorophytes dominated the assemblage during the river drawdown and low water (<3 m) periods in 2017, but their numbers declined as water temperature fell in the later months of 2017. Chlorophyte numbers declined further and were replaced as the dominant group by diatoms as river levels began to rise in the early months of 2018, and these remained the dominant group until the end of the sampling period. Centric diatom relative abundance peaked in December 2017 and February 2018. Cyanobacteria showed increases in the warm summer months, but also exhibited a minor increase in November 2018. Chrysophytes and xanthophytes appeared briefly in the summer months, but they represented only a small proportion of algal assemblage (<1%).

Axis 1 of the CCA explained approximately 74% of the variance in periphyton assemblage structure and largely represented spatial variability over time, with pH falling with distance from source water (Table 2.3, Table 2.4, Figure 2.6). CCA axis 2 accounted for 20% of the variance in periphyton composition and was positively associated with river stage, DO, and turbidity, all variables typically related to floodplain inundation. Although CCA axis 3 only

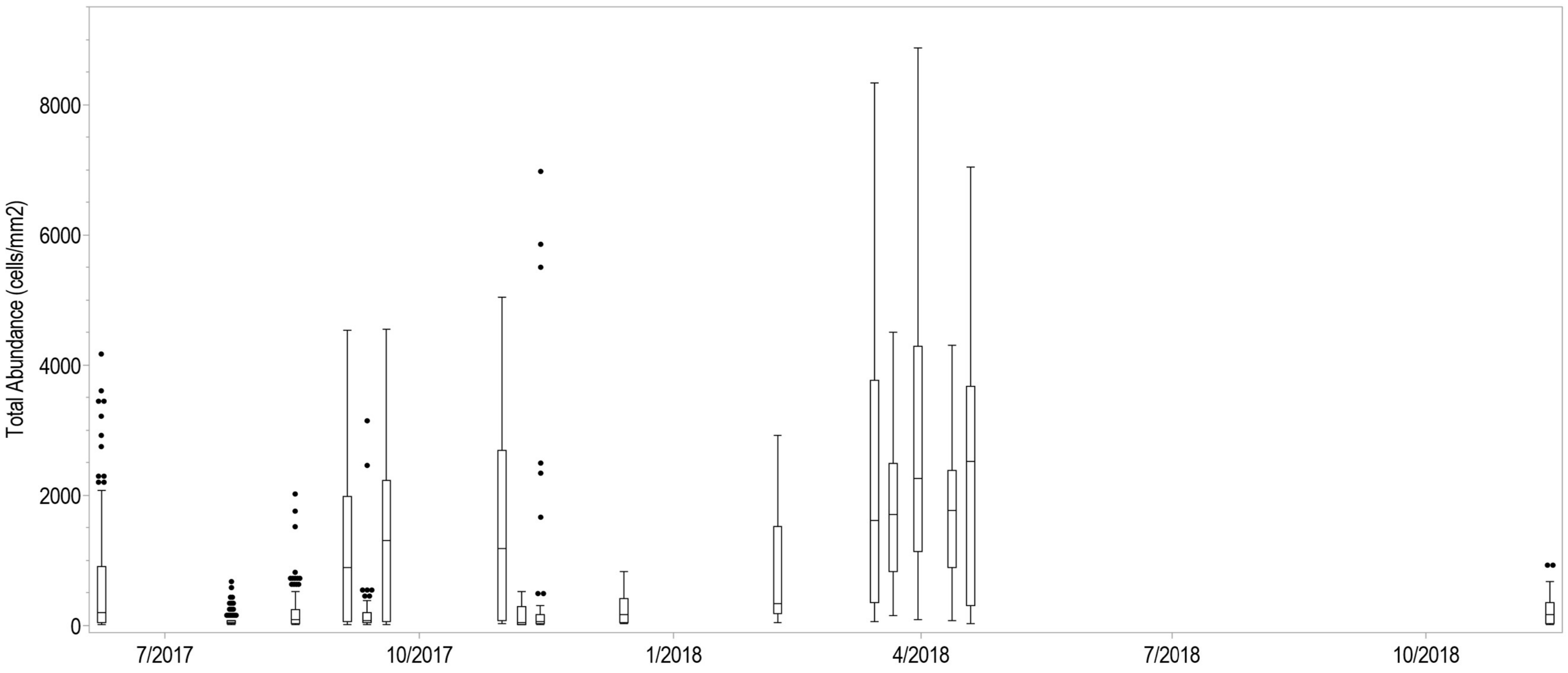

Figure 2.4. Box plots (median, 25th and 75th quartiles, and range) of total cell abundance (cells per mm^2) for all sites sampled during 2017-2018.

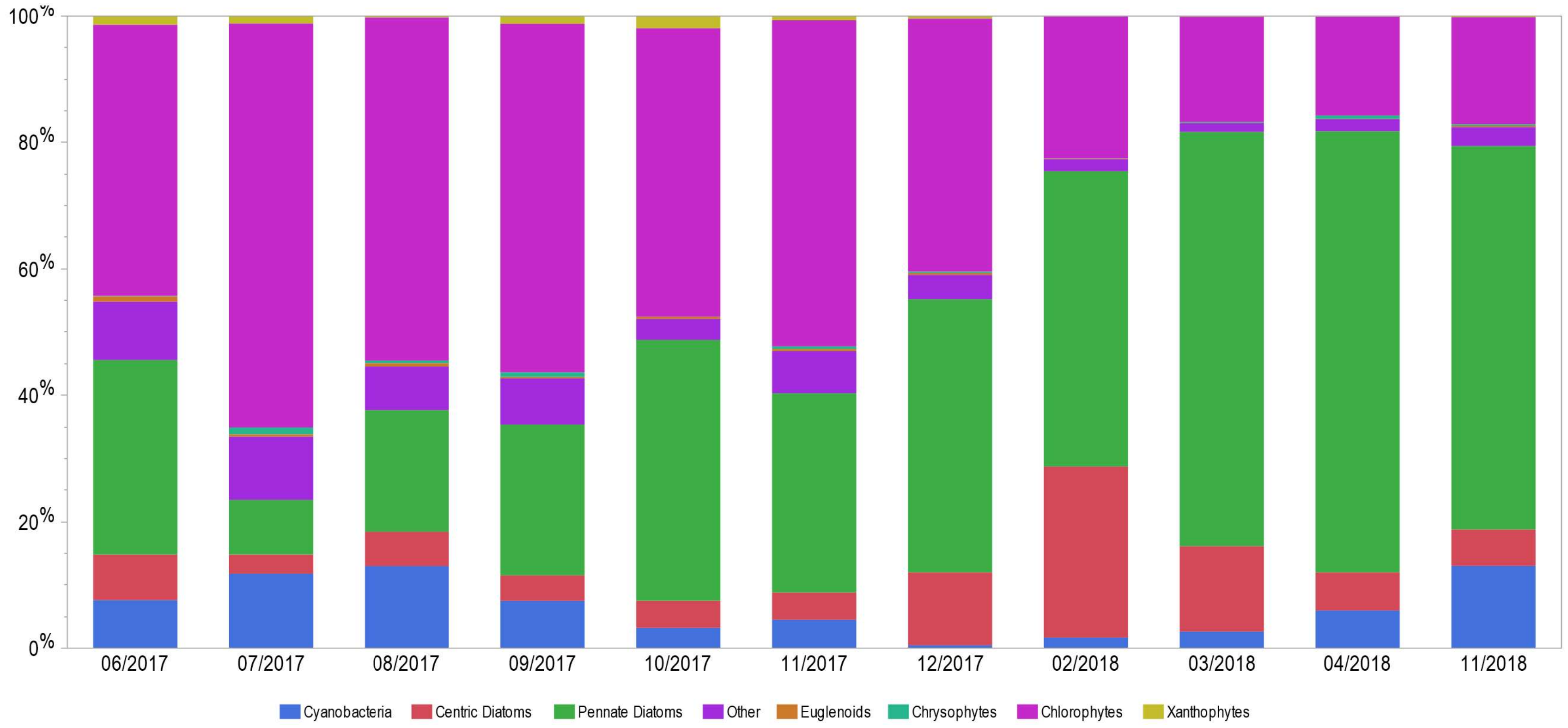

Figure 2.5. Composition (percentage of total cell count) of periphyton assemblages by algal group during the 2017-2018 sampling period.

Table 2.3. Scores from the canonical correlation analysis (CCA; R package vegan, Oksanen *et al.* 2019) for physicochemical and species variables (sites combined) for 2017 and 2018 sampling events. For the first three axes (98% variation explained), CCA correlations ≥ 0.35 are highlighted (Stevens 2012). Eigenvalues, proportion explained, and cumulative proportion explained are indicated at the bottom for each axis.

	CCA1	CCA2	CCA3
Date	-0.43	-0.36	-0.21
Distance	-0.68	0.08	-0.39
Depth	-0.34	0.12	0.08
Temperature	-0.43	-0.52	-0.25
DO	0.07	0.72	0.03
pH	0.35	0.22	-0.11
Turbidity	0.26	0.50	-0.06
Water Velocity	-0.34	-0.06	-0.54
BOD	-0.26	-0.32	-0.55
River Stage (m)	-0.13	0.74	0.30
Tree Cover	-0.25	-0.22	0.46
Macrophyte Cover	0.10	0.11	-0.50
Cyanobacteria	0.15	-0.44	-0.36
Centric Diatoms	-0.58	0.12	-0.02
Pennate Diatoms	0.08	-0.09	0.02
Euglenoids	0.08	0.48	-0.63
Chrysophytes	0.30	0.75	-0.47
Chlorophytes	0.43	0.31	-0.03
Xanthophytes	-0.59	-0.27	0.65
Eigenvalue values	0.10	0.03	0.00
Proportion Explained	0.74	0.20	0.03
Cumulative Proportion	0.74	0.95	0.98

accounted for a small proportion of variance, it did appear to represent biologically meaningful associations [macrophyte cover, tree cover, and oxygen consumption (BOD)] that exerted an influence on periphyton abundance and composition. Algal group scores for CCA1 included positive associations with chlorophytes, and negative associations with centric diatom and xanthophytes. For CCA 2, chrysophytes and euglenoids showed positive relationships, while cyanobacteria showed a negative association. Xanthophytes were positively related to CCA3, whereas chrysophytes, cyanobacteria, and euglenoids were negatively associated with this axis.

The GLMs performed on variables identified in the CCA as important in structuring the algal assemblage provided greater detail on the nature of the relationships (Table 2.5). ARB euglenoids, xanthophytes, and centric and pennate diatoms were more abundant during the early part of the year, whereas cyanobacteria, chrysophyte, chlorophyte, and euglenoid abundance increased in the latter part of the flood pulse. CCA1 revealed strong positive relationships between distance from the water source and xanthophytes and centric diatoms.

Table 2.4. Following CCA, a permutation test (999 permutations) was performed to determine significance of each explanatory variable (α = 0.05).

	Df	ChiSquare	F	Pr(>F)	
Date	1	0.023	15.36	<0.01	*
Distance	1	0.033	22.20	<0.01	*
Depth	1	0.003	1.72	0.18	
Temperature	1	0.013	8.74	<0.01	*
DO	1	0.007	4.46	0.01	*
pH	1	0.020	13.70	<0.01	*
Turbidity	1	0.007	4.67	<0.01	*
Water velocity	1	0.002	1.41	0.24	
BOD	1	0.004	2.50	0.06	
River stage	1	0.004	2.88	0.04	*
Tree cover	1	0.005	3.42	0.03	*
Macrophyte cover	1	0.015	10.12	<0.01	*
Residual	71	0.104			

However, GLMs indicated that all algal groups, except for chrysophytes and chlorophytes, showed positive associations with distance from source water. Chlorophytes showed a negative relationship with distance from source water, i.e., abundance decreased at increasing distances, while chrysophytes were not significantly related to distance. Xanthophytes and centric diatoms did not show significant relationships with DO, whereas euglenoids, centric diatoms, and chrysophytes showed large negative relationships with pH.

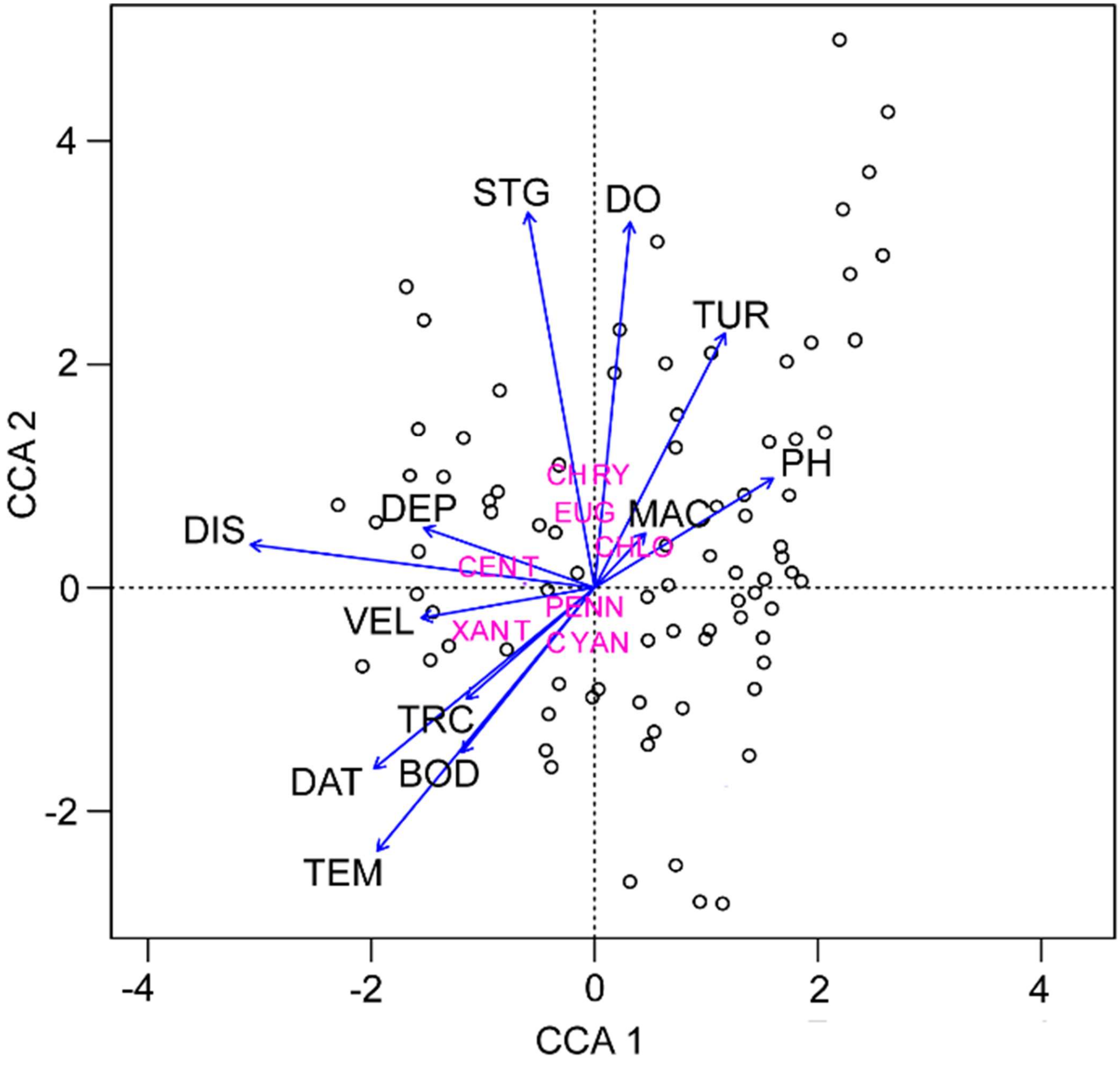

Figure 2.6. Canonical correspondence analysis (CCA) plot for sites. Abbreviations: Date = DAT, Distance = DIS, Biological oxygen demand = BOD, Temperature = TMP, Dissolved Oxygen = DO, pH = PH, Turbidity = TRB, Water velocity = VEL, River stage = STG, Tree cover = TRC, Macrophyte abundance = MAC. Cyanobacteria = CYANO, Pennate Diatoms = PENN, Centric Diatoms = CENT, Chrysophytes = CHRY, Euglenoids = EUGL, Xanthophytes = XANT, Chlorophytes = CHLO.

As expected, abundances of all algal groups, except for euglenoids, were reduced from shading by macrophytes, most commonly floating water hyacinth (*Eichhornia crassipes*) and common salvinia (*Salvinia minima*).

Table 2.5. Generalized linear models (GLMs; Vers. 3.6; R Core Team 2019; package *lme4*) were constructed for each algal group separately and included only the explanatory variables indicated to be significant by the CCA. Date was run as a polynomial to account for seasonality. All GLMs used the Poisson distribution (link=log) at α = 0.05.

Chrysophytes	Estimate	Std. Error	z value	Pr(>|z|)	
(Intercept)	90.17	15.67	5.76	<0.01	*
$Date^1$	-99.92	13.42	-7.45	<0.01	*
$Date^2$	-95.88	12.72	-7.54	<0.01	*
Distance	0	0.04	0.06	0.95	
Temperature	1.26	0.23	5.51	<0.01	*
DO	2.74	0.34	7.98	<0.01	*
pH	-18.29	2.44	-7.49	<0.01	*
Turbidity	-0.17	0.03	-6.65	<0.01	*
River Stage	1.21	0.16	7.68	<0.01	*
Tree Cover	-0.79	0.09	-8.6	<0.01	*
Macrophyte Cover	-0.01	0	-3.73	<0.01	*

Centric Diatoms	Estimate	Std. Error	z value	Pr(>|z|)	
(Intercept)	71.51	0.93	76.89	<0.01	*
$Date^1$	15.84	0.35	45.11	<0.01	*
$Date^2$	-4.51	0.31	-14.51	<0.01	*
Distance	0.29	0	93.26	<0.01	*
Temperature	-0.21	0.01	-19.51	<0.01	*
DO	0	0	-1.72	0.09	
pH	-7.76	0.1	-78.27	<0.01	*
Turbidity	-0.06	0	-52.77	<0.01	*
River Stage	-0.35	0.01	-55.83	<0.01	*
Tree Cover	-0.25	0	-59.42	<0.01	*
Macrophyte Cover	-0.03	0	-85.78	<0.01	*

Table 2.5. Continued.

Pennate Diatoms	Estimate	Std. Error	z value	Pr(>|z|)	
(Intercept)	6.39	0.43	14.99	<0.01	*
$Date^1$	-0.58	0.18	-3.26	<0.01	*
$Date^2$	-0.99	0.2	-5.02	<0.01	*
Distance	0.01	0	6.31	<0.01	*
Temperature	-0.1	0.01	-16.93	<0.01	*
DO	-0.15	0	-88.29	<0.01	*
pH	0.71	0.04	16.26	<0.01	*
Turbidity	-0.03	0	-58.61	<0.01	*
River Stage	-0.01	0	-4.25	<0.01	*
Tree Cover	-0.11	0	-49.54	<0.01	*
Macrophyte Cover	-0.03	0	-212.66	<0.01	*

Euglenoids	Estimate	Std. Error	z value	Pr(>|z|)	
(Intercept)	-11.73	16.29	-0.72	0.47	
$Date^1$	-42.88	12.56	-3.41	<0.01	*
$Date^2$	-67.86	11.54	-5.88	<0.01	*
Distance	0.45	0.08	5.72	<0.01	*
Temperature	1.23	0.25	4.84	<0.01	*
DO	-0.28	0.06	-4.42	<0.01	*
pH	-3.84	1.67	-2.31	0.02	*
Turbidity	0.13	0.02	5.45	<0.01	*
River Stage	0.92	0.19	4.87	<0.01	*
Tree Cover	0.2	0.11	1.84	0.07	
Macrophyte Cover	0	0	-0.41	0.68	

Chlorophytes	Estimate	Std. Error	z value	Pr(>|z|)	
(Intercept)	-9.27	0.6797	-13.64	<0.01	*
$Date^1$	-11.48	0.4202	-27.31	<0.01	*
$Date^2$	-0.95	0.4214	-2.26	0.02	*
Distance	-0.12	0.0029	-39.88	<0.01	*
Temperature	-0.18	0.0098	-18.5	<0.01	*
DO	-0.01	0.0033	-2.95	<0.01	*
pH	2.41	0.0743	32.42	<0.01	*
Turbidity	-0.01	0.0009	-16.32	<0.01	*
River Stage	0.16	0.0057	28.17	<0.01	*
Tree Cover	-0.12	0.0046	-26.65	<0.01	*
Macrophyte Cover	-0.02	0.0002	-87.63	<0.01	*

Table 2.5. Continued.

Cyanobacteria	Estimate	Std. Error	z value	Pr(>|z|)	
(Intercept)	31.71	2.18	14.52	<0.01	*
Date^1	8.69	0.82	10.62	<0.01	*
Date^2	9.23	0.93	9.88	<0.01	*
Distance	0.02	0.01	2.71	<0.01	*
Temperature	-0.26	0.03	-9.1	<0.01	*
DO	-0.07	0.01	-9.32	<0.01	*
pH	-2.51	0.23	-10.81	<0.01	*
Turbidity	-0.03	0	-12.66	<0.01	*
River Stage	-0.23	0.01	-15.79	<0.01	*
Tree Cover	-0.24	0.01	-20.96	<0.01	*
Macrophyte Cover	-0.02	0	-31.58	<0.01	*

Xanthophytes	Estimate	Std. Error	z value	Pr(>|z|)	
(Intercept)	-24.17	12.52	-1.93	0.05	
Date^1	14.05	6.75	2.08	0.04	*
Date^2	-17.48	8.1	-2.16	0.03	*
Distance	0.18	0.06	3.26	<0.01	*
Temperature	0.48	0.26	1.83	0.07	
DO	-0.29	0.16	-1.81	0.07	
pH	2.24	1.28	1.75	0.08	
Turbidity	-0.06	0.02	-3.04	<0.01	*
River Stage	0.05	0.11	0.48	0.63	
Tree Cover	0.53	0.08	6.5	<0.01	*
Macrophyte Cover	-0.02	0	-6.48	<0.01	*

Algal Cell Size

Date, distance from water source, and their interaction were significantly related to changes in algal cell size (Table 2.6.). Nano-periphyton was by far the most abundant size class (Mean = 628.9 cell/mm^2 ± 30.09 SE) compared to pico-plankton (266.3 cells/mm^2 ± 11.5) and micro-plankton (19.9 cells/mm^2 ± 1.5). Nano-periphyton were positively associated with months later in the year and were negatively associated with distance from source water (Table 2.7.). Pico-plankton were abundant all year and showed little association with distance from source water; however, there did seem to be an interaction later in the year.

DISCUSSION

Temporal Periphyton Assemblage Dynamics

Algal taxonomic composition and abundance in the ARB is influenced by light availability, temperature, water flow, turbidity, pH, and, although not measured in the current study, the concentration of dissolved organic material and nutrients present in backwater areas (Tillman 1982, Reynolds 1984, Dodds and Welch 2000). Although highly variable in magnitude and timing among years (Piazza et al. 2015, Baustian et al. 2019), the annual ARB flood pulse typically has three main periods: rising river stages with low temperatures and elevated floodplain nutrient availability in the fall and winter; falling stages in late spring with pervasive hypoxia if water temperatures reach 20° C; and low water during the summer characterized by high temperatures (> 30° C) and normoxia within weeks of the cessation of AR water input (Sabo et al. 1999). During all three periods, chlorophytes or diatoms were the dominant

Table 2.6. The (a) intercepts and (b) coefficients (SE) from multinomial regression (Vers. 3.6; R Core Team 2019; package *MASS*) of total abundance of each cell size (pico- <2 µm, nano- 2-20 µm, micro- >20 µm) versus date and distance from the water source during 2017-2018.

	Value	Std. Error	t value
Micro|Nano	-3.52	0.02	-212.62
Nano|Pico	0.88	0.01	93.96

Table 2.7. The coefficients (SE) from multinomial regression (Vers. 3.6; R Core Team 2019; package *MASS*) of total abundance of each cell size (pico- <2 µm, nano- 2-20 µm, micro- >20 µm) versus date and distance from the water source during 2017-2018.

	Value	Std. Error	t value
$Date_1$	2.46	0.41	5.99
$Date_2$	-5.92	0.43	-13.84
Distance	0.09	0.00	55.02
$Date_1$*Distance	1.13	0.07	15.02
$Date_2$*Distance	-2.87	0.07	-39.94

algal groups, although changes in periphyton composition were evident as river stages rose and fell. During the river drawdown period (starting in June 2017), chlorophytes were the most prevalent periphytic group, followed by diatoms (pennate and centric) and cyanobacteria. Although present in low numbers, euglenoids and xanthophyte abundances were positively associated with low DO levels, which can become widespread as the floodplain dewaters due to increased decomposition on the floodplain associated with rising temperatures (Sabo et a. 1999, Pasco et al. 2016). Surprisingly, xanthophytes occurred at sites with elevated pH, which was unexpected given their loading on CCA1, as well as their typical occurrence in acidic or dystrophic waters (Holmes and Whitton 1977, Stein and Borden 1979, Findlay et al. 2005, Ott et al. 2015). Hypoxic receding floodwaters would have exhibited low pH from organic decomposition, so it is surprising that xanthophytes showed positive relationships to pH in the GLM. This could be more a product of their location at increasing distances to source water or temporal changes related to seasonal changes in floodplain inundation.

Changes in water circulation on the ARB floodplain over the last few decades have increased the spatial magnitude and temporal duration of hypoxia in the ARB [conditions reported in Sabo et al. (1999) versus Pasco et al. 2016)], which may have improved conditions for xanthophytes. The occurrence of xanthophytes at ARB sites with elevated pH is in contrast to their association with lower pH levels in other systems, such as periphytic xanthophytes found in streams throughout the Western Allegany Plateau (Verb and Vis 2004) and the free-floating xanthophyte *Gonyostomum semen* in shallow boreal lakes in NW Ontario (Findlay et al. 2005). In contrast, chrysophyte abundance was greater at sites with lower pH, which was expected given their prevalence in cooler and slightly acidic water (Findlay et al. 2005, Ott et al. 2015).

During low-water periods (< 3m), cyanobacteria became more abundant, though never dominated the assemblage. This slight increase occurred during the warm summer months, even though GLMs indicated significant negative associations with water temperature, and likely reflected increased cyanobacteria abundance at sites with lower water temperatures. This is in contrast to observations of cyanobacteria associations with warmer water in other floodplain ecosystems (Mihaljevic and Stevic 2011, O'Farrell et al. 2015). Cyanobacteria can flourish in low-light conditions (Necchi 2004, Chakdar and Pabbi 2016) and can be found in areas with abundant tree cover. In addition, cyanobacteria are frequently observed in areas of standing water where dissolved nutrients are limiting, such as during river low-water periods (Oliveira and Calheiros 2000, Yang et al. 2015). Given that these conditions likely characterized many of the ARB sample sites in backwater areas with dense overstory shade, I expected cyanobacteria would completely dominate the periphytic community in the summer months. Some cyanobacteria, such as *Anabanea* and *Aphanizomenon*, have the ability to fix nitrogen during nutrient-limiting periods (Paerl et al. 2020), however, high light intensity is required for this process. Given the amount of tree and macrophyte cover present at the floodplain sites, the high levels of light required may have rarely occurred, which may explain why cyanobacteria numbers were unexpectedly low. It is also possible that cyanobacteria were more abundant in the phytoplankton assemblage rather than periphyton, however, there were no visible indications of cyanobacteria blooms in the water column. Further, I did not observe a large number of cyanobacteria filaments with heterocysts (nitrogen-fixing cells) during this time, indicating minimal levels of nitrogen fixation.

Chlorophytes, particularly flagellated or coccoid, are known to become dominant during summer months and prefer standing water high in nitrogen (Wehr et al. 2015). In large Alpine lakes, chlorophytes were observed to increase during summer periods after diatom-dominance depleted silica and dissolved nutrients (Salmaso 2000). Chlorophytes showed negative estimates for temperature in the GLM, indicating that their dominance during summer months was less related to water temperatures and more related to preferences for higher light intensities as seen in other lotic systems (Okada and Watanabe 2002, Necchi 2004, Tonetto et al. 2012, Peres et al. 2017).

In February 2018, the river pulse likely introduced nutrient-rich river water onto the floodplain, causing a shift in the dominant algal taxa to diatoms, with other algal groups declining to very low numbers or disappearing completely (xanthophytes and euglenoids). Diatoms remained the dominant periphytic algal taxa until the end of sampling. Typically, diatoms require high levels of nutrients and prefer cooler temperatures than cyanobacteria or chlorophytes (Reynolds et al. 2002, Svensson et al. 2014). In both rivers and lakes, algal assemblage succession generally begins with diatoms colonizing an area first, when nutrients are readily available (Dai et al. 2012, Bellinger and Sigee 2015), although in lentic systems that experience distinct dry and rainy seasons, succession can differ (Franca et al. 2011). Centric diatoms, in particular, require higher levels of nutrients, and their abrupt decline in March 2018 (after peak inundation) is consistent with literature from Reynolds et al. (2002) and Kiss et al. (2012). Although the current study did not measure dissolved nutrients, it is likely that as algal density increased, nutrients became limited, and diatoms were replaced by other taxa that were better competitors for scarce resources, such as chlorophytes and cyanobacteria, as has been reported from drawdown events as seen in other systems (Reynolds et al. 2002, Bellinger and Sigee 2015). It should also be noted that although macroinvertebrates were not collected during this study, herbivore grazing also likely increased as algal densities began to rise with increased nutrient input (e.g., similar to invertebrate grazing in the tropical and temperate streams Moulton et al. 2015, Calapez et al. 2019).

Inundation patterns appeared to drive the relative abundance of chlorophytes and diatoms in the ARB. Chlorophytes dominated periphytic assemblages during river recession and low-water periods (< 3m), whereas diatom relative abundance increased as floodplains became inundated with rising river levels. Although no prior data exists for ARB periphyton, Hern (1978) observed contrasting trends for phytoplankton in the Buffalo Cover Water Management Unit (located on the western side of the ARB). Despite seasonal fluctuations in water depth, as well as water temperature and dissolved nutrients, chlorophytes dominated algal assemblages year-round. Hern's (1978) observations undoubtedly occurred during seasonal changes in water quality, so the lack of an apparent influence of the AR flood pulse on phytoplankton contrasts sharply with the seasonal trends in periphyton composition in observed in the current study that appeared to be closely tied to changes in river stage and floodplain inundation.

Floodplain inundation and variation in water quality also influence the abundance and distribution of macrophytes in the ARB, which can further impact algal biomass and assemblage composition (Tesolin and Tell 1996, Ward et al. 2016, Silva et al. 2020) due to competition for resources, such as light and nutrients (Souza et al. 2015, Santos and Ferragut 2018). Longer flood inundation periods (as seen in 2017) likely provide longer and more spatially extensive inputs of nutrients, which would promote higher lateral/vertical expansion of macrophyte beds in the backswamp area. This phenomenon has been seen in other floodplain systems including the Murray River and Amazon River (Robertson et al. 2001, Silva et al. 2013). Macrophyte composition and richness can influence periphyton assemblage composition (Rodrigues dos Santos and Ferragut 2018, Cao et al. 2019) because of macrophyte-induced physicochemical changes in water quality or leachate excretion (Morin and Kimball 1983). Dissolved organic matter excretion from water lettuce (*Pistia stratiotes*) has been observed to differentially impact attached algae, reducing the growth rate of the cyanobacteria *Anabaena* sp. while at the same time increasing internal chlorophyll *α* concentration in the chlorophyte *Chlamydomonas moewusii* (Bottino et al. 2018). The floating macrophyte *Salvinia* spp., which is invasive in many parts of the US, has been found to be associated largely with chlorophytes over other taxa, such as diatoms, which are more nutritious to grazing macroinvertebrates (Fernandes et al. 2016). In a Brazilian reservoir, macrophyte richness had positive impacts on diatom densities and negative impacts chlorophyte abundance (Rodrigues dos Santos and Ferragut 2018); however, these results were contrary to trends observed in a nearby reservoir system (Pellegrini and Ferragut 2018). Although allelopathic interactions between periphytic algae and aquatic macrophytes were not included in the current study, such interactions certainly contribute to temporal and spatial trends present in periphytic assemblages and should be considered in further ARB periphyton research. Differential responses by periphytic algae to changes in macrophyte abundance and composition could have substantial impacts on higher trophic levels, particularly given differences in algal nutritional content and consumability to invertebrate grazers and their predators (do Nascimento Filho and do Nascimento Moura 2021). More long-term studies are needed on the effects of flood duration and intensity on vegetation in order to better understand the dynamics and interactions of macrophytes, periphyton, and phytoplankton in permanently inundated floodplain habitats and the resulting effects on secondary productivity in higher trophic levels.

Distance from Source Water

In addition to seasonal trends, periphyton assemblage composition also shifted along a longitudinal gradient away from the source of river water. Although the CCAs indicated that centric diatoms and xanthophytes had positive associations with distance (i.e., increased at further distances) and chlorophytes showed negative associations, GLMs indicated that all groups, except for chlorophytes and chrysophytes, had positive relationships with distance from source water, with chlorophytes declining with distance and chrysophytes showing no significant relationship. Although nutrient concentrations also likely changed with distance to Atchafalaya River source water, as was subsequently seen in 2019 nutrient analysis (ammonium and phosphorus were higher nearest to river sources; unpublished data), other factors may have also significantly influenced periphyton composition. Billabongs in the furthest reaches of Murray River Basin, Australia floodplains differed slightly in water quality parameters, such as specific conductance, pH, and turbidity, but these factors had less influence on diatom assemblages than did river reach location, hydrology, or the amount of vegetation present (Reid and Ogden 2009). The authors speculated that temporal variations in water quality promoted species turnover and could be amplified at near-river sites because of intermittent hydrologic connections that facilitate recolonization. Similarly, Philibert et al. (2006) found the strongest predictive models for diatom assemblages among streams in southeastern Australia, included non-water quality parameters, such as longitude. Diatom assemblages in the Mackenzie Delta Lakes, Canada, were shown to be most strongly impacted by the degree of river connectivity (Hay et al. 2000). Additionally, the authors noted that the distribution of aquatic macrophytes on the floodplain was directly related to flood duration, which also appeared to be the case in the ARB. Distance from river sources is related to the degree of river connectivity and is an important factor influencing the abundance and composition of periphyton assemblages in this, and other, river floodplains. Changes in the level of river connectivity can ultimately influence water quality in backwater areas and alter the fate of nitrogen sources, affecting primary production from periphytic algae and macrophytes (Scott et al. 2014).

Algal Cell Size

Cell size has important implications for metabolic processes, light absorption, as well as nutrient uptake and processing, and shifts in the dominant size class can affect nutrient cycling and carbon transfer to higher trophic levels (Marrase et al. 1989, Litchman et al. 2009, see references in Finkel et al. 2010, Maranon 2014). As expected, the most abundant size class was nano-periphyton (2-20 μm; Chetelat et al. 2006), although pico-periphyton (<2 μm) increased in abundance at sites further from river inputs, whereas nano-periphyton declined. Because smaller cells have higher surface area:volume ratios and smaller diffusion boundary layers, they can uptake nutrient resources more efficiently with lower light levels and nutrient concentrations, as frequently seen in backwater swamp areas during summer months (Reynolds et al. 1994, Chetelat et al. 2006, Maranon 2014, Svensson et al. 2014). Smaller cells proliferate in environments with low dissolved nutrients (Jiang et al. 2005; but also see Raven 1994) but are more prone to grazing by herbivores (Sunda and Hardison 2010). Cells larger than 2 μm typically have higher rates of phosphorus uptake (Stolte and Reigman 1996, Chetelat et al. 2006), and this may explain why nano-periphyton occur closer to river-water inputs, where phosphorus is likely higher. Nitrate has also been linked to increase in diatom size (Stolte et al. 1994). Nitrate concentration, similar to phosphorus, would likely be negatively related to distance from source water and may explain why nano-plankton abundance was higher closer to river inputs. River flood pulses can contribute to shifts in algal size classes as well. Dunck et al. (2013) found that during low-water periods, smaller cells with strong surface attachments (e.g., adnate diatoms) tended to dominate, whereas metaphyton periphyton was dominant during flood pulses.

CONCLUSION

Periphytic algae present in the Atchafalaya River Basin floodplain represent a diverse group of primary producers that exhibited both temporal and spatial variability driven by physicochemical and biotic changes in the floodplain throughout the annual AR flood pulse. All groups showed seasonal variation in abundance related to high-water and low-water physicochemistry during floodplain inundation events. Increased distance into the floodplain also substantially impacted periphyton assemblage composition, but water parameters and spatial factors were not sufficient to explain variation in community composition between flood years, which may have been related to substantial differences in macrophyte bed development. As seen in other systems, variability in floodplain inundation period and frequency of flooding influences water quality as well as macrophyte abundance and composition, which then interacts with the periphyton grazing assemblage to ultimately determine the seasonal progression of dominant algal groups.

CHAPTER III. THE INFLUENCE OF THE ATCHAFALAYA RIVER FLOOD PULSE ON BASIN PERIPHYTON ASSEMBLAGES

INTRODUCTION

River-floodplain systems are ecologically and economically important and fulfill a number of ecosystem services, including primary and secondary production, as well as sediment and nutrient storage (Junk et al. 1989, Jardine et al. 2012, Jardine et al. 2015, Pettit et al. 2017, Crook et al. 2019). Floodplains consist of a network of adjacent terrestrial habitats, as well as seasonally disconnected lakes and channels that become inundated during river flooding. Lateral connectivity between a river and its floodplain facilitates exchange of nutrients and organic material, as well as fish and other organisms that can move into newly available habitat (Junk et al. 1989, Pettit et al. 2017, Bayley et al. 2018). Macrophytes present in floodplain lakes and channels serve as refugia for macroinvertebrates, which are valued prey items for riverine fishes. The abundance of food sources and reduced water flow make floodplain systems ideal for fish spawning and juvenile development. Thus, floodplains typically are highly productive and can support lucrative commercial fishing operations (Opperman et al. 2010).

In these systems, basal resources, like aquatic macrophytes and algae, are responsible for carbon fixation and incorporation of inorganic nutrients to upper trophic levels (Wetzel 1964, Campos-Silva et al. 2020, Cazzanelli et al. 2021). Algae, in particular, contribute substantially to production in rivers and lakes (Junk et al. 1989, Thorp and Delong 1994, Doi 2009). Historically, algal primary production was thought to be dominated mostly by phytoplankton (Reynolds 1994, Kalff 2002). However, the role of epiphytic algae has emerged as equally important (Wetzel 1983, Liboriussen and Jeppesen 2006, Adame et al. 2017). In some temperate lakes, attached algae have been observed to account for 50-90% of total lake production, depending on lake depth and surface area (Vadeboncoeur and Steinman 2002, Vesterinen et al. 2015). In river-floodplain systems, the role of epiphytic algae has not been widely studied, but the influx of inorganic nutrients (i.e., nitrate, nitrite, ammonium, phosphorus) onto the floodplain during the flood pulse (Bortolini et al. 2016) provides resources needed for growth and production of photosynthetic algae (Lewis et al. 2000, Ahearn et al. 2006). Attached algae coexist with bacteria and organic material in complex matrices, creating a thin biofilm (i.e., periphyton) layer on submerged surfaces. Periphytic biofilms are the site of carbon and nutrient absorption and cycling (Wetzel 1964, Flemming 1993, Battin et al. 2016) and are sensitive to environmental changes. Alterations to river hydrologic regimes, such as frequency and duration of flooding, can impact periphytic algal abundance, assemblage composition, and production (Agostinho et al. 2004, Agostinho et al. 2008).

Nearly all floodplains in the Northern Hemisphere have been anthropogenically altered (Lewis et al. 2000), mostly for navigation or agricultural purposes or for flood control. Modifications to river-floodplain systems can have deleterious consequences for aquatic productivity and biodiversity. When floodplains become disconnected from their river sources through dam or levee construction, biological and chemical exchange between the river and floodplain is greatly reduced, threatening ecological integrity (Fernandes et al. 2009, Algarte et al. 2016). Isolation from nearby water sources can severely limit organismal dispersal and can even lead to extirpation of sensitive species

(Beisner et al. 2006, Shurin et al. 2009). The Yangtze River, for example, has been substantially altered to accommodate rising population needs, and many of its seasonally inundated lakes have been permanently severed from their river connections. These disconnected lakes show a substantial reduction in the diversity of riverine fishes, largely because of reduced access to habitat, complete loss of fluvial environments, and limited access to spawning grounds (Liu and Wang 2010). Jiang and colleagues recently studied fish populations in connected and disconnected lakes in the Yangtze River floodplain and found that fish populations in disconnected lakes had lower levels of taxonomic distinctiveness than populations inhabiting lakes with active river connections (Jiang et al. 2020).

In the Paraná River, Brazil, isolated lakes had greater environmental heterogeneity and higher levels of dissimilarity in macrophyte composition relative to seasonally connected lakes (Quirino et al. 2019). In addition, the diet of the invertivorous fish *Moenkhausia bonita* differed among isolated lakes, but not in connected lakes, indicating river connectivity was essential to food dispersal in these aquatic systems (Quirina et al. 2019). River connectivity is important for algal communities as well. In floodplain lakes with active riverine connections, periphyton communities had a higher degree of species richness compared to isolated lakes (Agostinho et al. 2008). Similar results were found for species composition of free-floating algae (Lansac-Toha et al. 2016) as well as zooplankton, which feed on phytoplankton and have the potential to significantly influence plankton assemblage dynamics (Li et al. 2019). In Brazil, phytoplankton richness and diversity were larger in lakes with active river links due to increased exchange of riverine algal species and transfer of nutrients (Bortolini et al. 2016).

The Atchafalaya River is the fifth largest river on the North American continent and is the main distributary of the Mississippi River (Ford and Nyman 2011, Piazza 2014). The Atchafalaya River Basin (ARB) supports a tremendous diversity of terrestrial, semi-aquatic, and aquatic species, thought to be fueled by river flooding events (Rutherford et al. 2001, Colon-Gaud et al. 2004, Troutman et al. 2007). These flood pulses vary annually in degree and magnitude, but will typically inundate floodplain habitats, such as bayous, floodplain lakes, and excavated canals, for periods ranging from weeks to months. This pulse facilitates nutrient and organism exchange and drives the enormous production and biodiversity characteristic of this system, which supports numerous commercial fishing enterprises that generate approximately $17 million in fish and crayfish annually (NOAA 2018). Over the last several decades, the Atchafalaya River and its basin have undergone substantial hydrologic modification. Once over 8,000 km^2, the ARB has been constricted to just half of its historic size (Sabo et al. 1999, Piazza 2014). Lakes, bayous, and dredged channels on the Atchafalaya River floodplain support a diverse assemblage of native and exotic macrophytes (Walley 2007), which in turn provide substrate for highly productive periphyton assemblages, as well as the organisms that exploit this rich food source (e.g., Colon-Gaud et al. 2004; Fisher et al. 2012).

In this study, I explored how river flood pulses in this modified system impacted periphytic algal assemblages. I compared periphyton composition in ARB sites with active floodplain connections to a permanently-isolated floodplain lake, Lake Verret

(LV). I hypothesized that, relative to sites receiving no annual water inputs from a flood pulse, floodplain sites will: 1) have substantially greater periphyton abundance, 2) exhibit different temporal trends in assemblage composition, and 3) exhibit spatial differences in periphyton composition related to distance from the floodwater source.

METHODS

Site Locations

The study took place in Iberia and St. Martin parishes and consisted of five ARB sites located in a 50-km^2 section east of the Atchafalaya River, west of Pierre Part, LA and south of Bayou Sorrel (Fig. 3.1). The inlet of Bayou Postillion at the Gulf Intracoastal Waterway along the eastern Atchafalaya River Basin guide levee was designated as the source of Atchafalaya River water for five sites. Five additional sites were located in LV, an historic floodplain lake that has been disconnected from the Atchafalaya River since the 1940's (Report of the Chief of Engineers US Army 1941). Three periphyton samplers (periphytometers) were deployed at each site and tethered to trees on shore or on bald cypress (*Taxodium distichum*) knees near shore. Sites were sampled biweekly from January 2019 – September 2019, although high water in the ARB precluded launching a boat to access sites in March and April.

Periphytometer Design

Periphytometers (15 x 30 cm) were constructed of 1-inch PVC pipe and sealed with water-resistant sealant, allowing the frame to float at the water surface. Four glass microscope slides (75 mm x 50 mm x 1 mm) were suspended along the length of the

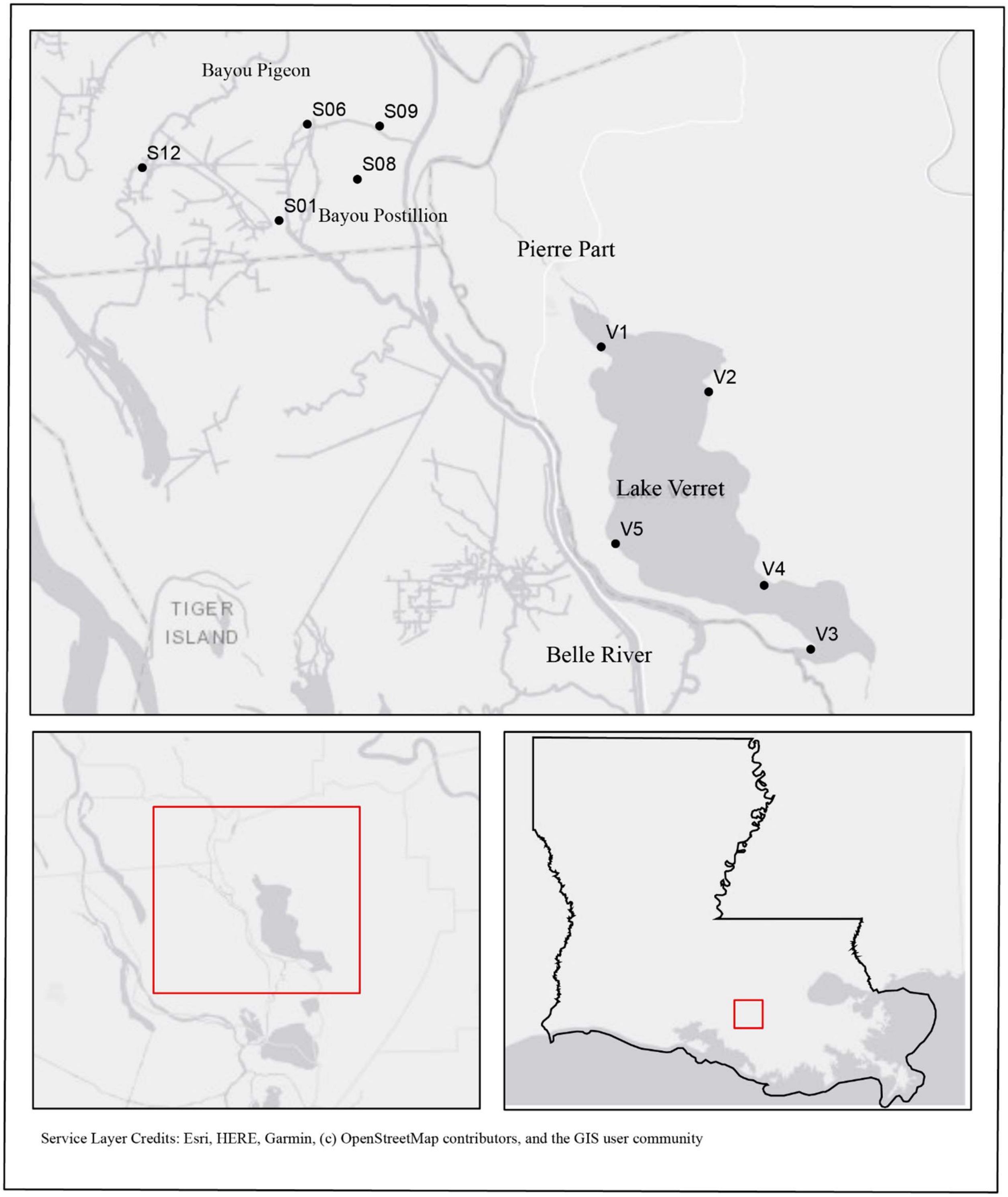

Figure 3.1. A map showing the major bayous and periphyton sampling sites in the Atchafalaya River Basin and Lake Verret during 2019.

frame within approximately five centimeters from the surface of the water. Slides were secured with clear fishing line (10 lbs) and plastic clips spaced five centimeters apart to avoid loss or transfer of biofilm. Glass slides were cleaned thoroughly with ethanol prior to use and replaced with fresh slides biweekly.

Habitat and Water Quality Procedures

Sampling occurred for six months during 2019 at roughly the same time (± 1 hour). Maintaining consistent sampling times was important because algal chlorophyll expression changes throughout the day (Gargas et al. 1979, Owens et al. 1980). An *Aqua*Fluor Handheld Fluorometer (Turner Designs, San Jose, CA) was used to measure chlorophyl (CHL) and phycocyanin (PC) concentration of algal samples (sterile, buffer dilution water was used as blank). Surface and bottom temperature measurements, dissolved oxygen (DO), specific conductance, pH, and turbidity were recorded at each site with a handheld YSI® multiprobe (Yellow Springs, OH). Water velocity was measured with a handheld velocimeter (SonTek®, YSI, Inc, Yellow Springs, OH). Tree cover and macrophyte cover were also recorded for each periphytometer. Tree cover was scored by a single observer as 0%, 20%, 40%, 80%, or 100%. To estimate macrophyte cover at the time of collection, a 75-cm x 75-cm frame was placed around each periphytometer and photographed from 1 m above. Images were used to estimate the percentage of floating or emergent plants surrounding each periphytometer.

To measure inorganic nutrients, water samples were collected in 1-L glass amber bottles that had been combusted at 550° C for 5 hours to remove any residual carbon (rinsed twice with sample water and filled to the brim). Samples were immediately filtered through 0.45-μm pore filter, and spectrophotometry was used to determine nutrient concentration (Nitrite, NO_2^-N, Method 8507; Nitrate, NO_3^-N Method 8192; Phosphorus PO_4^{3-} , Method 8048; Ammonia, NH_3^-N, Method 8155; APHA 2018).

To determine rates of respiration, samples for 20-day biochemical oxygen demand (BOD; unfiltered sample) were collected in 1-Liter, opaque Nalgene bottles once per month at each collection site (rinsed twice with sample water and filled to brim before capping). Samples were stored on ice until processing. Prior to initial dissolved oxygen measurement, samples were raised to room temperature (20° C ± 2) and a nitrogen inhibitor was added. Dissolved oxygen measurements were taken every five days for 20 days; any bottle reading below 3.0 mg L^{-1} was bubbled with atmospheric oxygen for 5 minutes and re-measured before further incubation (APHA 2018).

Samples were also taken from algae scrapings to estimate heterotrophic bacterial abundance. One glass slide was removed, and a new, single-edge razor blade rinsed in 95% ethanol solution was used to scrape one-half of the slide into a sterile centrifuge vial filled with 50 mL of sterile, phosphate-buffered dilution water, put on ice for transportation back to the laboratory, and inoculated onto AR-2 agar for heterotrophic plate counts (HPC; APHA 2018). Plates were inverted and incubated at 35° C for 48 hours prior to enumeration (APHA 2018) with a standard darkfield colony counter (Reichert Darkfield Quebec®, 220V; Depew, NY).

To measure periphyton carbon and nitrogen content, a single periphytometer slide was placed (algae-side up) in an individual plastic box for transport. Samples were dried for 30 min at 60° C, scraped, weighed, and wrapped in tin capsules for processing. Carbon and nitrogen were measured by heating the tin/sample unit and measuring the gas products (N^2 and CO^2) from the combusted material via gas chromatography (Costech 1040 CHNOS Elemental Combustion, Valencia, CA; Matejovic 1993).

Algal Identification

Periphytometer slides were collected biweekly and two were placed in individual plastic bags with 10 mL of a 2% glutaraldehyde solution for algal identification. Glutaraldehyde preservative maintains cell color very well, which assists in taxonomic identification (Andersen 2005). The bags were refrigerated overnight so the glutaraldehyde would loosen the biofilm from the glass slide surface, reducing cell damage when scraped. Periphyton was scraped from the glass slides with a new, single-edge razor blade into centrifuge vials with additional 2% glutaraldehyde that completely covered the algae. Samples were refrigerated at 4° C in the dark. Extremely dense samples were diluted into 250 mL of glutaraldehyde. Prior to enumeration, samples were inverted gently to homogenize. If further homogenization was needed, the sample was sonicated for no more than 15 seconds. This was enough to break up dense clumps, but not enough to severely damage or burst a large number of cells. A Sedgewick-rafter counting slide observed at 400x magnification (Leitz Laborlux K) was used to classify periphyton cells into 8 groups (cyanobacteria, centric diatoms, pennate diatoms, xanthophytes, euglenoids, chrysophytes, chlorophytes and unknown/other) and three size classes [pico- (<2 µm), nano- (2–20 µm), and micro- (>20 µm)].

Statistical Analysis

Descriptive analyses of periphyton composition were completed with JMP Pro (vers. 15.1.0, SAS Institute, Inc, Cary, NC), and all statistical analyses were performed with R (vers 3.6; R Core Team 2019) based on periphyton composition and measured environmental variables [nutrient concentrations, temperature, dissolved oxygen, pH, turbidity, water velocity, specific conductance, biochemical oxygen demand (BOD) colony-forming units (CFU), total organic carbon (TC), total nitrogen content (TN), carbon:nitrogen ratio (C:N), chlorophyll a (CHL α), phycocyanin (PC), macrophyte density, tree cover (0-5 scale), distance from the source, and river stage]. I used a log link- Poisson distribution general linear model (GLM; Vers. 3.6; R Core Team 2019) to analyze differences in total algal abundance between ARB and LV sites. It is important to note only a single basin and lake were included in this study, spatial autocorrelation is present (see Hurlbert 1984). However, useful information from this investigation can still be gleaned by observing differences between the two systems (Davies and Gray, 2015). To assess temporal and spatial trends in algal assemblage composition, Lake Verret and ARB data were analyzed independently with separate canonical correspondence analyses (CCA; R package *vegan*, Oksanen et al. 2019); the explanatory variable distance refers to the straight-line distance to river source for ARB sites and was excluded from the LV analysis. CCA permitted identification of relationships between periphyton assemblage composition and measured environmental variables. I chose CCA over other ordination methods because of the unimodal and constrained nature of the data. Components identified from the CCAs were then used in log link-Poisson distribution generalized linear models with the package lme4 (Vers. 3.6; R Core Team 2019; Appendix A) to further investigate trends in periphyton assemblage composition.

RESULTS

Physicochemistry

The 2019 flood began on January 25 when the Atchafalaya River exceeded 3 m at the Butte la Rose (Gauge 07381515; Allen et al. 2008, Pasco et al. 2016), and ended on August 21, 2019. Sampling began on January 30 and continued biweekly until September 25, 2019, after the river entered the low-water stage (Figure 3.2). LV did not experience a spring flood pulse, but lake height and water flow were influenced by local wind and rain events. In both ARB and LV sites (Table 3.1), dissolved oxygen (DO; Figure 3.3) showed higher concentrations early in the year, which declined in the summer months. In contrast, differences in the temporal patterns of nutrient concentrations were evident between ARB and LV sites (Figure 3.4). Nitrate (NO_3) concentration was relatively low in LV compared to ARB sites, which exhibited higher

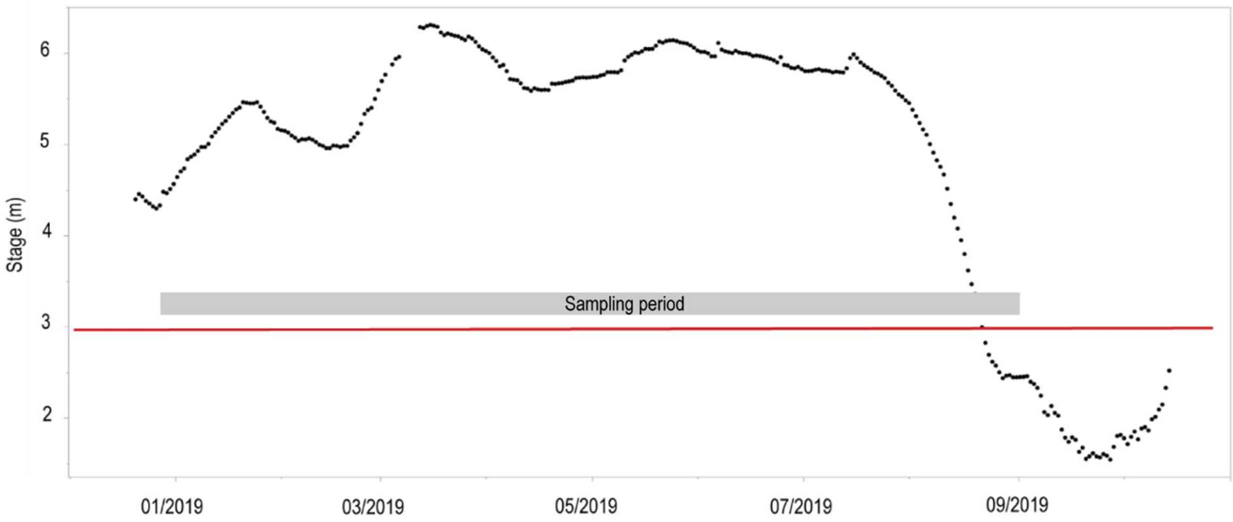

Figure 3.2. Daily Atchafalaya River stage obtained from the Butte la Rose water gage (USGS 07381515) from Jan 2019 to Sep 2019. Horizontal line indicates flood stage (Pasco et al. 2016).

Table 3.1. Summary of physicochemical, chlorophyll, and habitat variables for ARB and Lake Verret sampling sites from January–September 2019.

	Region					
	Basin			Lake Verret		
	Mean (SE)	Min	Max	Mean (SE)	Min	Max
River Stage (ft)	16.38 (0.25)	5.16	19.89	13.74 (0.32)	5.16	19.05
Depth (m)	1.43 (0.03)	0.10	2.81	0.48 (0.01)	0.00	0.86
Temperature (C)	21.91 (0.38)	8.70	29.15	25.03 (0.36)	9.30	31.55
Dissolved Oxygen (mg L^{-1})	2.982 (0.15)	0.17	8.73	4.87 (0.13)	0.14	11.20
pH	7.18 (0.01)	6.83	8.19	7.57 (0.04)	5.55	9.05
Turbidity (NTU)	14.99 (0.63)	0.36	51.19	15.42 (0.64)	1.96	64.60
Specific Conductance	0.33 (0.0)	0.25	0.46	0.22 (0.0)	0.11	0.33
Water Flow (m sec^{-1})	0.03 (0.0)	-	0.18	0.02 (0.0)	-	0.22
BOD (mg L^{-1})	6.56 (0.08)	2.45	9.95	10.29 (0.16)	4.85	16.95
Nitrate (mg L^{-1})	0.04 (0.0)	0.01	0.13	0.02 (0.0)	-	0.08
Nitrite (mg L^{-1})	0.01 (0.0)	0.00	0.02	0.01 (0.0)	-	0.07
Phosphorus (mg L^{-1})	0.34 (0.01)	0.12	0.59	0.42 (0.01)	0.13	1.25
Ammonium (mg L^{-1})	0.06 (0.0)	0.01	0.11	0.07 (0.0)	-	0.34
Colony Forming Units	50264.77 (6698.55)	365.00	1,175,500.00	63229.83 (4752.82)	185.00	612,750.00
Phycocyanin	0.99 (0.06)	0.06	8.20	0.66 (0.03)	0.06	1.99
Chlorophyll	29546.48 (3087.68)	220.00	373,700.00	10823.45 (863.00)	262.20	88,682.00
TN(mg)	0.09 (0.0)	0.01	0.42	0.21 (0.01)	0.00	0.63
TC(mg)	0.59 (0.03)	0.04	2.57	1.09 (0.04)	0.02	3.04
C/N	6.55 (0.04)	4.66	11.02	5.27 (0.03)	4.09	7.42
Tree Cover (0-5)	3.56 (0.05)	1.00	5.00	3.78 (0.05)	2.00	5.00
Macrophyte Cover (%)	45.42 (2.12)	-	100.00	21.93 (1.57)	-	-

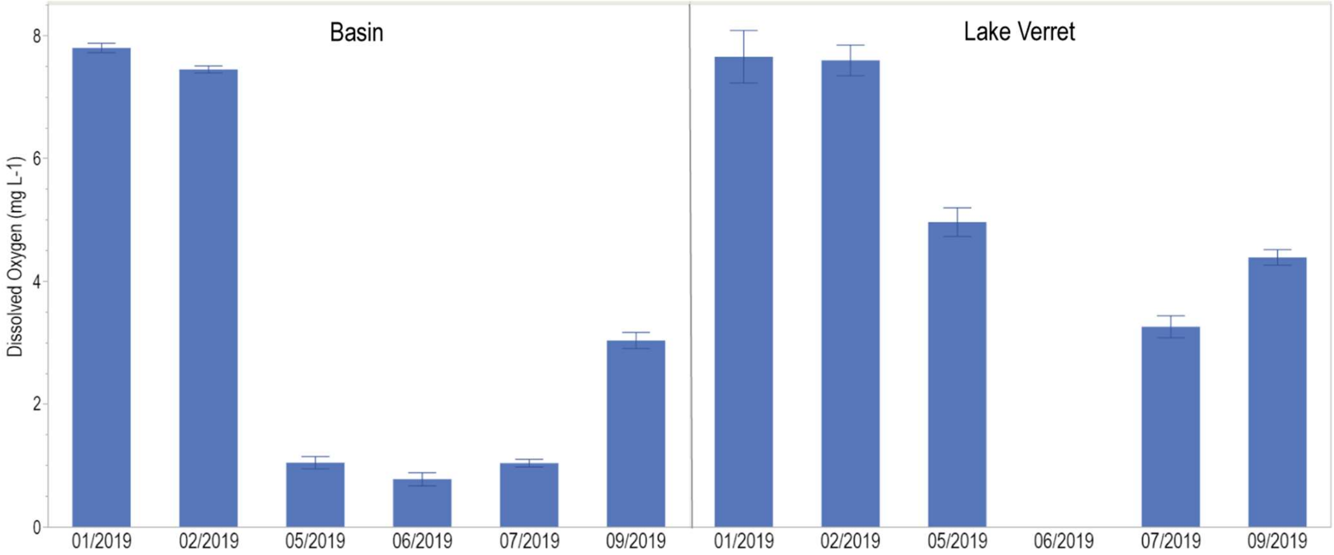

Figure 3.3. Dissolved oxygen concentration averaged over all sites for the ARB (left) and Lake Verret (right). Error bars represent one standard error.

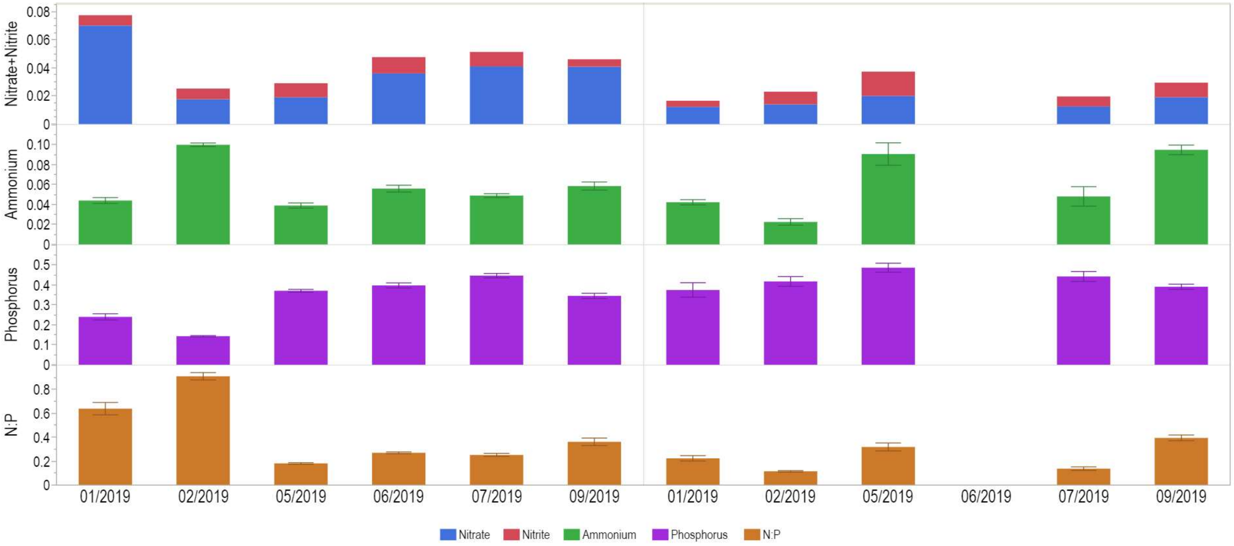

Figure 3.4. Nitrate (blue), nitrite (red), ammonium (green), phosphorus (purple), N:P ratio (orange) concentrations (mg/l) averaged over all sites for ARB (left) and Lake Verret (right) from January 2019 – September 2019. Error bars represent one standard error.

nitrate values throughout the sampling period, particularly in January. Nitrite (NO_2) concentrations were similar between the two sampling periods, whereas ammonium (NH_4) was more variable in LV. Ammonium peaked twice in LV in May and September but was in low concentration during the other months. In the ARB, there was a single ammonium peak in February, with all other months exhibiting similar values. Temporal trends in phosphorus concentrations were similar in LV and ARB sites, although ARB sites exhibited lower concentrations in January and February. N:P ratios indicated nitrogen limitation (ratio < 13; Hillebrand and Sommer 1999) in LV year-round and in the late spring and summer months in the ARB.

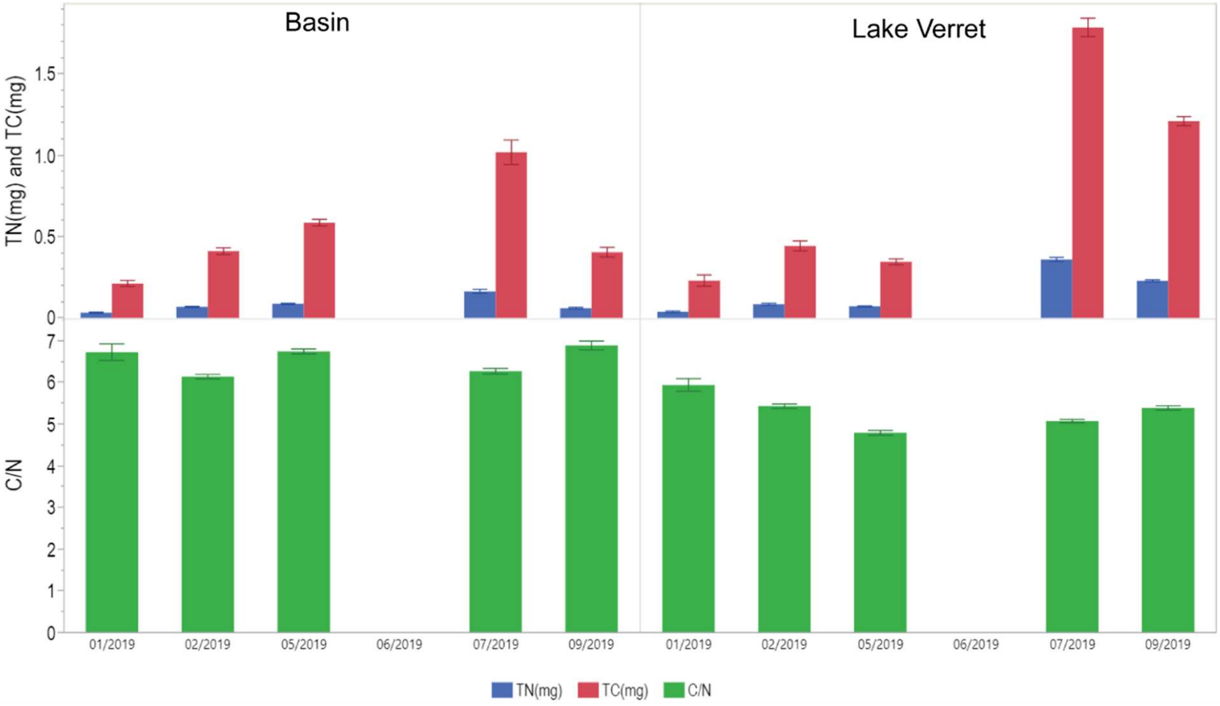

Figure 3.5. Total carbon (TC), total nitrogen (TN), and Carbon:Nitrogen Ratio (C/N) averaged over sites for ARB (left) and Lake Verret (right) sites sampled in 2019. Error bars represent one standard error.

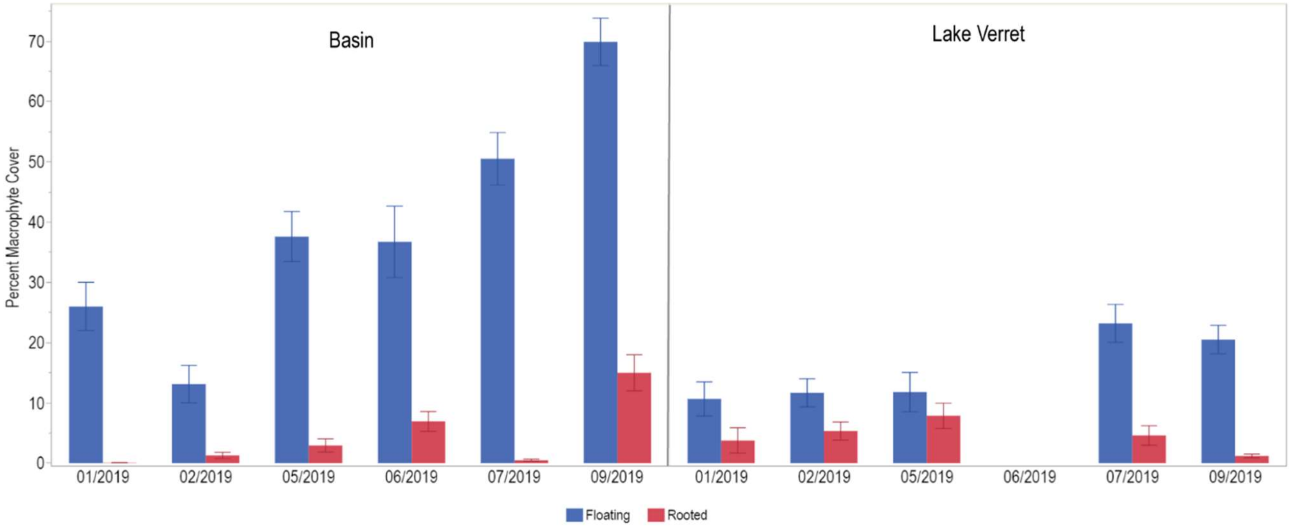

Figure 3.6. The average percentage of floating (blue) and rooted (red) macrophyte coverage at the time of periphyton collection averaged across sties for ARB (left) and Lake Verret (right). Error bars represent one standard error.

On average, both Total Carbon (TC) and Total Nitrogen (TN) were higher for Lake Verret relative to ARB sites, but both locations showed similar temporal concentration patterns (Figure 3.5), with peaks in TC and TN during July and lows in January. However, the C/N ratio was slightly higher for ARB sites. Macrophyte cover was also higher in the ARB compared to LV (Figure 3.6), although peak macrophyte abundance occurred in the summer months at both locations and was dominated by floating taxa like salvinia and water hyacinth. Overall, ARB sites located nearer to water sources supported higher macrophyte densities than sites located deeper in the floodplain.

Periphyton Assemblage

Periphytic algae abundance was significantly greater at ARB sites compared to LV sites (Basin: Mean = 2,358.12 cells/mm^2, SE = 209.09; Verret: Mean = 896.86 cells/mm^2, SE = 41.99; SE = 222; $P < 0.01$) and overall community composition was

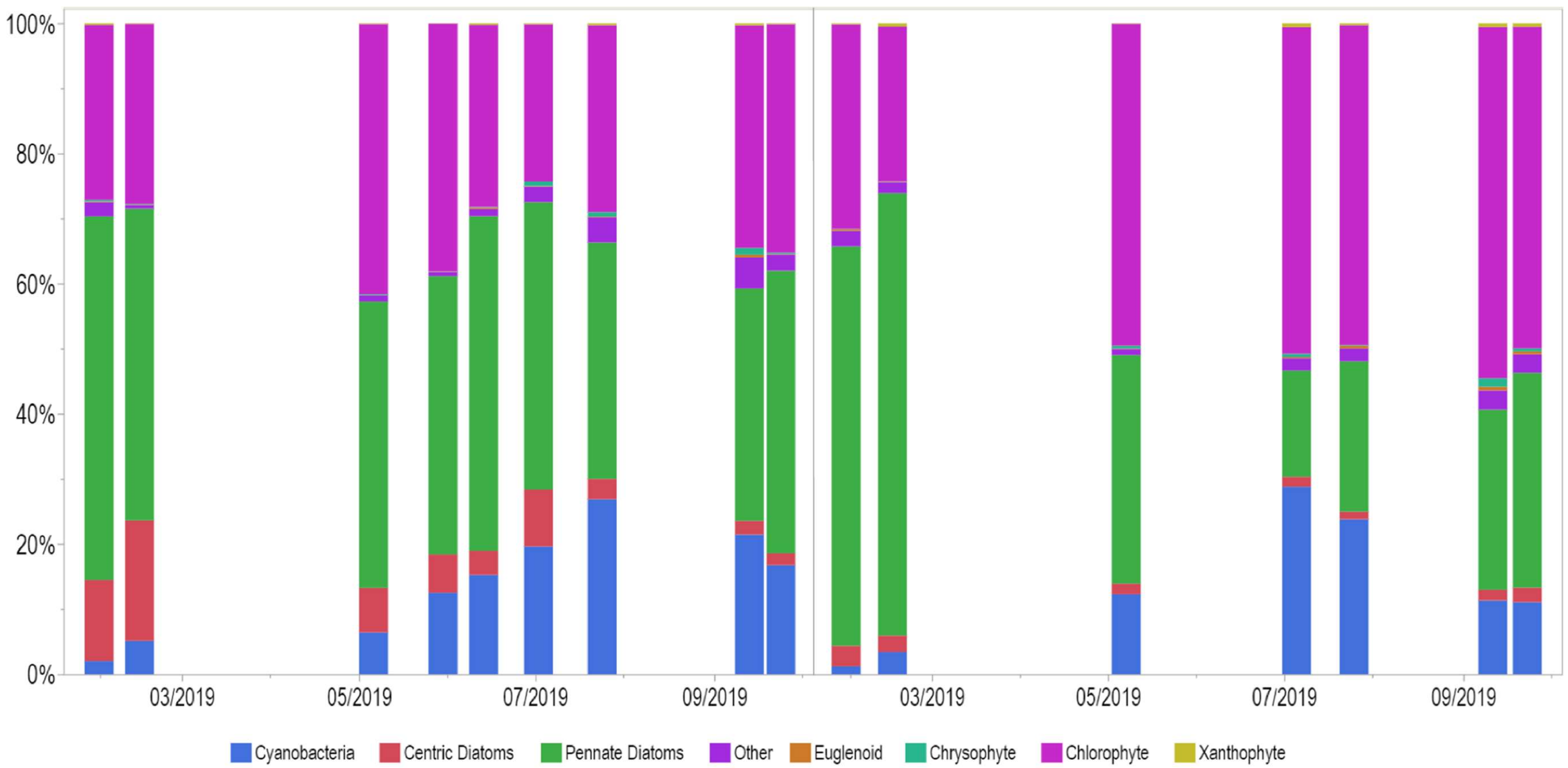

Figure 3.7. Percent abundance of each algal group from the ARB (left) and Lake Verret (right) during 2019.

very different between the two regions (Figure 3.7). Periphyton assemblages in the ARB were dominated by diatoms in all months sampled. The relative abundance of centric diatoms was between 12-18% in January and February, then declined to less than 7% for the rest of the sampling period, whereas pennate diatom relative abundance was between 40-56% in all months. Chlorophytes usually did not exceed 30% of the total community assemblage. All other algal groups remained below 1%. In LV, the periphyton assemblage was dominated by chlorophytes in all months except January and February, when pennate diatoms were highest (61% and 68%, respectively). Centric diatoms never exceeded 3%. In both LV and ARB assemblages, cyanobacteria increased in the summer months, reaching over 20% in July.

Multivariate Analysis: ARB Sites

The first three components of the canonical correspondence analysis (CCA; Table 3.2; Figure 3.8) explained the majority (99%) of variation in the data. Component 1 represented mostly temporal changes in periphyton assemblages (CCA1; 45% of the variation) and was positively associated with cyanobacteria and xanthophytes and a negatively associated with centric diatoms. Environmental variables positively associated with CCA1 included specific conductance, water temperature, sampling date, TC, TN, and phosphorus and had a negative association with DO. The second component represented primarily spatial features of environmental data and algal assemblages at ARB sites (CCA2; 42% of variation). Overall, total algal abundance was higher closer to river water input (SE = 0.0002; Chi-square = 2401.56; $P<0.01$), with sites near the Gulf Intracoastal Waterway (GIWW) supporting higher cyanobacteria and centric diatom abundances, greater ammonium concentrations, and

Table 3.2. Scores from the canonical correlation analysis for ARB sites for physicochemical and algal group variables (sites combined). Only the first three axes were considered (99% variation explained). Matrix loadings > 0.35 were considered interpretable and highlighted (Stevens 2012). Eigenvalues, proportion explained, and cumulative proportion explained are indicated at the bottom for each axis.

	CCA1	CCA2	CCA3
Date	0.62	0.32	-0.27
SiteS06	-0.18	-0.01	0.08
SiteS08	-0.33	0.05	-0.59
SiteS09	0.18	-0.18	0
SiteS12	0.09	-0.54	-0.16
Distance	0.09	-0.39	-0.04
Temperature	0.51	0.29	-0.26
Dissolved Oxygen	-0.45	-0.13	0.04
pH	-0.09	0.3	-0.42
Turbidity	-0.32	-0.35	0.04
Specific Conductance	0.43	0.48	-0.28
CFU	-0.3	0	-0.12
Water Velocity	0.29	0.58	0.22
BOD	-0.05	-0.57	0.19
Nitrate	-0.07	0.31	-0.15
Nitrite	0.04	0.35	0.01
Phosphorous	0.68	0.39	-0.22
Ammonium	-0.08	0.51	-0.16
PC	-0.02	-0.14	-0.01
CHL	-0.07	-0.34	0.1
TN	0.57	0.61	-0.31
TC	0.54	0.62	-0.31
C:N	-0.29	-0.26	0.2
Tree Cover	0.21	-0.4	0.19
Macrophyte Cover	-0.07	-0.02	-0.51
Cyanobacteria	0.54	0.59	-0.25
Centric Diatom	-1.04	0.41	-0.17
Pennate Diatoms	0.03	0.06	0.2
Euglenoids	-0.32	0.03	-0.62
Chrysophytes	0.18	0.27	-0.38
Chlorophytes	0.03	-0.47	-0.14
Xanthophytes	0.63	0.24	-0.23
Eigenvalue	0.14	0.13	0.04
Proportion Explained	0.45	0.42	0.12
Cumulative Proportion	0.45	0.87	0.99

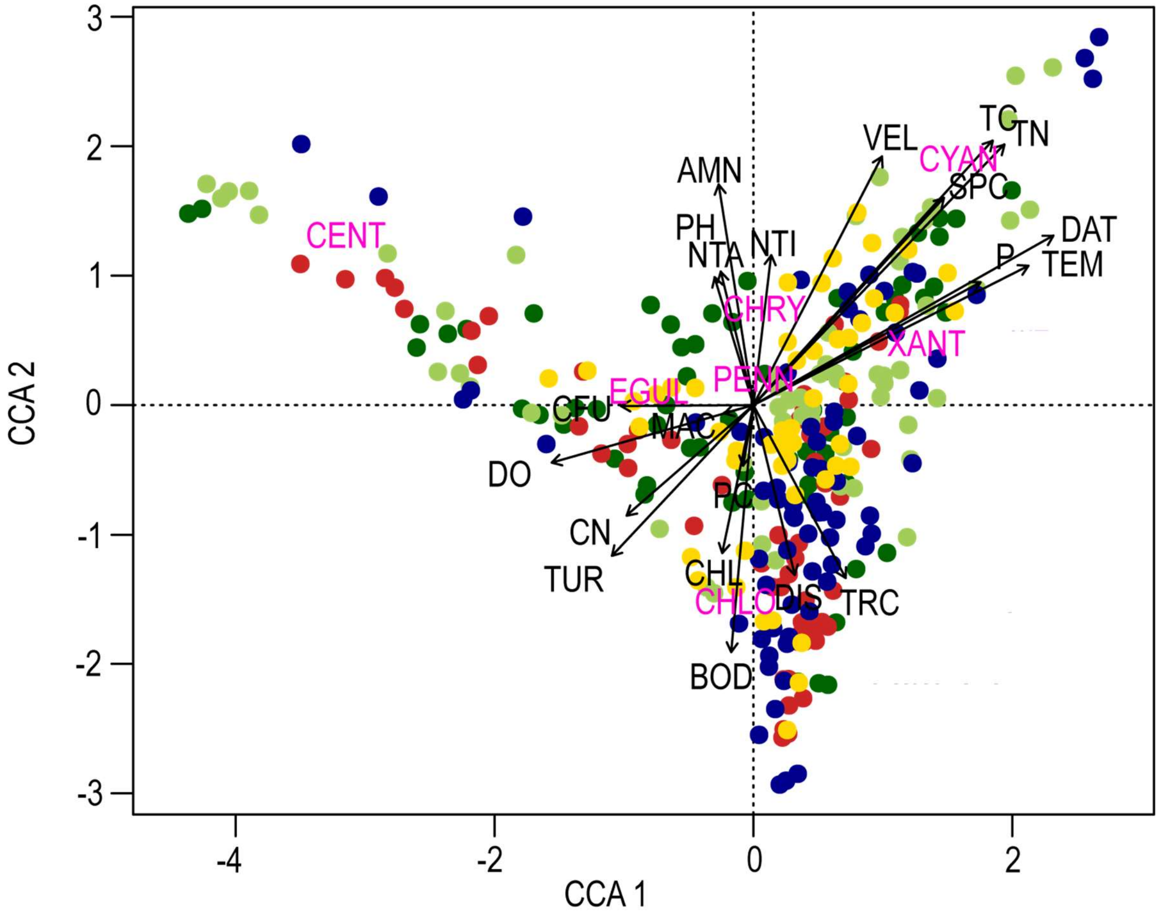

Figure 3.8. Canonical correspondence analysis (CCA) plot for sites in the ARB. Variables include date (DAT), distance from water source (DIS), temperature (TMP), dissolved oxygen (DO), pH (PH), turbidity (TRB), water velocity (VEL), tree cover (TRC), macrophyte abundance (MAC), Nitrate (NTA), Nitrite (NTI), biological oxygen demand (BOD), total carbon (TC), total nitrogen (TN), carbon:nitrogen ratio (CN), specific conductance (SPC), colony forming units (CFU), chlorophyll a (CHL), and phycocyanin (PC), chrysophytes (CHRY), centric diatoms (CENT), pennate diatoms (PENN), euglenoids (EUGL), chlorophytes (CHLO) xanthophytes (XANT), cyanobacteria (CYANO). Sites are S01 (dark green), S06 (light green), S08 (blue), Site09 (yellow), and S12 (red).

Table 3.3. A permutation test (999 permutations) was performed with all explanatory variables to determine significance of each variable (α = 0.05).

	Df	ChiSquare	F	Pr(>F)	
Date	1	0.07	137.11	<0.01	*
Site	4	0.09	45.78	<0.01	*
Distance	1	0.01	22.47	<0.01	*
Temperature	1	0.00	1.96	0.12	
Dissolved Oxygen	1	0.03	52.23	<0.01	*
pH	1	0.01	12.74	<0.01	*
Turbidity	1	0.01	21.93	<0.01	*
Specific Conductance	1	0.01	15.48	<0.01	*
CFU	1	0.02	33.53	<0.01	*
Water Velocity	1	0.01	24.65	<0.01	*
BOD	1	0.00	2.83	0.04	*
Nitrate	1	0.01	14.21	<0.01	*
Nitrite	1	0.01	26.76	<0.01	*
Phosphorous	1	0.01	24.82	<0.01	*
Ammonium	1	0.00	5.29	<0.01	*
PC	1	0.01	10.03	<0.01	*
CHL	1	0.00	1.03	0.34	
TN	1	0.00	5.71	<0.01	*
TC	1	0.00	2.56	0.06	
C:N	1	0.00	4.16	0.01	*
Tree Cover	1	0.00	0.84	0.46	
Macrophyte Cover	1	0.00	2.04	0.11	
Residual	288	0.15			

higher flow rates. Chlorophytes were lower in abundance closer to river inputs, but increased in abundance further into the floodplain, where tree cover and microbial activity (BOD) were higher. The last component (CCA3, variation 12%) represented the presence or absence of macrophytes. Sites heavy in aquatic vegetation tended to have higher pH levels and showed higher densities of both chrysophytes and euglenoids compared to sites with less macrophyte cover. Permutation tests completed after the CCA (Table 3.3) indicated algal abundance was particularly influenced by sampling date, site, and DO, although all variables with the exception of water temperature, CHL, TC, tree cover, and macrophyte cover were related to periphyton abundance.

General linear models for each algal group included only those variables that were significant in the permutation test, although variables varied by algal group. Euglenoids, chrysophytes, and xanthophytes did not show significant relationships for distance from source water (parameter estimates -937.10 ± 52080.00 SE; 3.79 ± 17.40; 2.64 ± 10.66; respectively; Table B.1), whereas cyanobacteria, chlorophytes and centric and pennate diatoms did (-2.60 ± 1.05; -4.83 ± 1.47; -170.10 ± 8.11; -13.88 ± 0.90; respectively). The negative correlation with distance to the water source exhibited by chlorophytes was contrary to loadings in the CCA. Both pennate and centric diatoms showed negative estimates for distance, indicating that they were more abundant near river inputs. Centric and pennate diatoms also showed large positive relationships with nitrate (2.33 ± 0.66; 13.81 ± 0.19, respectively) and nitrite (188.60 ± 3.02; 193.70 ± 0.93, respectively). Chlorophytes showed positive estimates for only nitrite (77.11 ± 1.03).

Multivariate Analysis: Lake Verret Sites

Periphyton assemblages at LV sites differed substantially from sites located in the ARB. The first three components of the CCA explained 96% of the variability in the data (Table 3.4; Figure 3.9). The first component (CCA1; 73% of variation) described mostly seasonal variation in the data, with positive loadings for BOD, water flow, and temperature, along with CFU, TC, and TN. Algal groups that also positively loaded on

Table 3.4 Scores from the canonical correlation analysis for Lake Verret sites for physicochemical and algal group variables (sites combined). Only the first three axes were considered interpretable (96% variation explained). Matrix correlations > 0.35 were highlighted (Stevens 2012). Eigenvalues, proportion explained, and cumulative proportion explained are indicated at the bottom for each axis.

	CCA1	CCA2	CCA3
Date	0.48	-0.2	0.2
SiteV02	-0.13	-0.52	-0.18
SiteV03	-0.16	0.64	-0.24
SiteV03	0.31	-0.14	0
SiteV05	0.13	0.22	0.14
Temperature	0.69	-0.1	0.09
Dissolved Oxygen	-0.73	0.2	0.16
pH	-0.12	0.14	-0.2
Turbidity	-0.57	0.32	0.05
Specific Conductance	0.1	-0.14	0.22
CFU	0.39	0.1	-0.12
Water Velocity	0.42	0.49	0.21
BOD	0.64	0.36	-0.15
Nitrate	-0.15	0.03	-0.04
Nitrite	0.04	-0.11	-0.05
Phosphorous	0.03	-0.39	-0.19
Ammonium	0.13	0	0.23
PC	-0.32	-0.23	-0.06
CHL	-0.48	-0.22	-0.11
TN	0.66	0.37	0.02
TC	0.65	0.34	0.03
C:N	-0.39	-0.2	0
Tree Cover	0.3	0.18	0.05
Macrophyte	0.16	0	0.39
Cyanobacteria	0.63	0.46	0
Centric Diatom	-0.23	-0.16	0.43
Pennate Diatom	-0.61	0.09	-0.01
Euglenoids	0.27	-0.37	0.44
Chrysophytes	0.26	-0.15	1.94
Chlorophytes	0.27	-0.22	-0.02
Xanthophytes	0.43	0.11	0.4
Eigenvalue	0.23	0.06	0.01
Proportion Explained	0.73	0.19	0.04
Cumulative Proportion	0.73	0.92	0.96

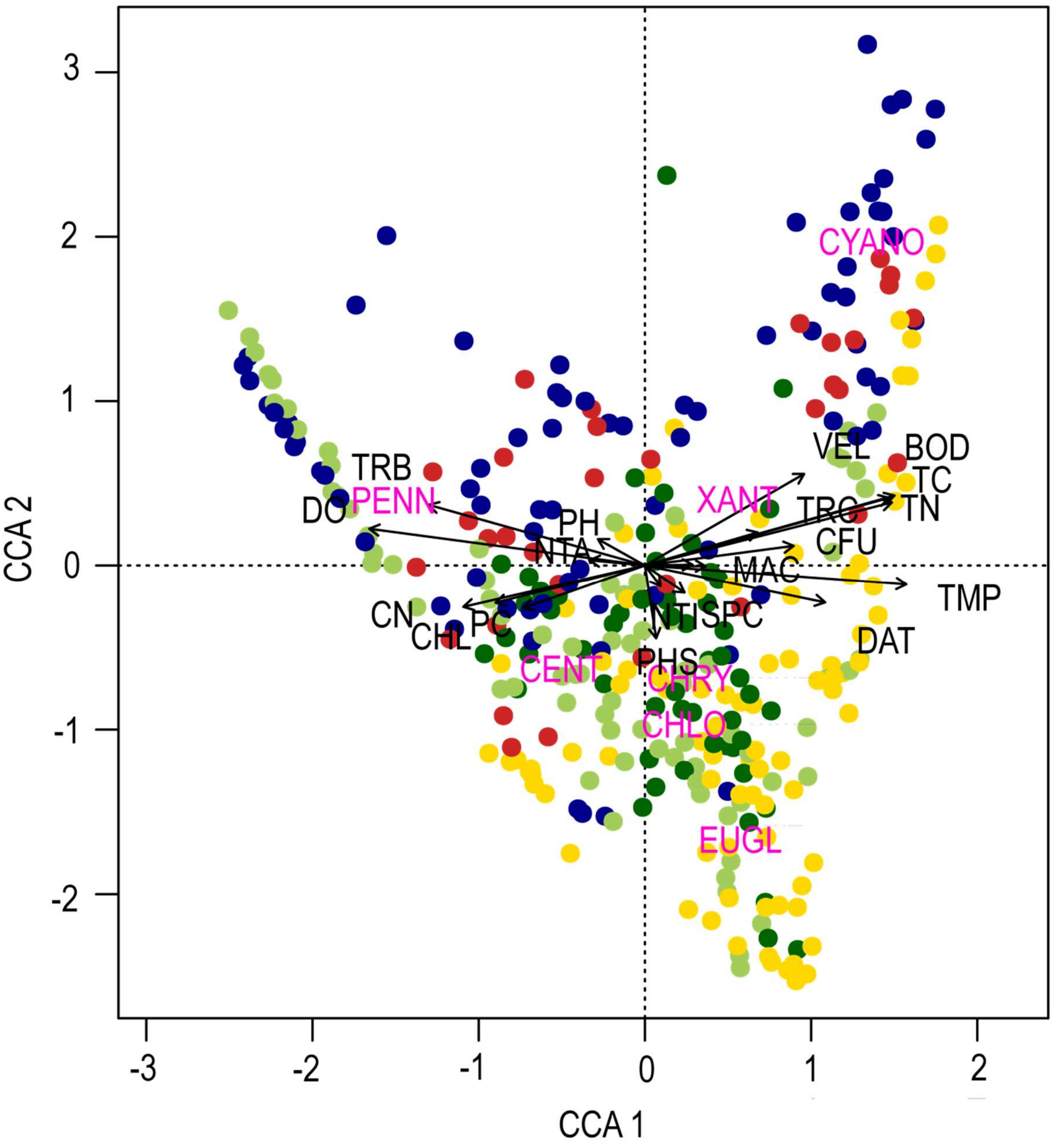

Figure 3.9. Canonical correspondence analysis (CCA) for Lake Verret Sites. Variables include date (DAT), temperature (TMP), dissolved oxygen (DO), pH (PH), turbidity (TRB), water velocity (VEL), tree cover (TRC), macrophyte abundance (MAC), nitrate (NTA), Nitrite (NTI), phosphorus (PHS), biological oxygen demand (BOD), total carbon (TC), total nitrogen (TN), carbon:nitrogen ratio (CN), specific conductance (SPC), colony forming units (CFU), chlorophyl (CHL), and phycocyanin (PC). Sites are V01 (dark green), V02 (light green), V03 (blue), V04 (yellow), and V05 (red).

CCA1 were xanthophytes and cyanobacteria. Negative associations with CCA1 included pennate diatoms, DO, turbidity, CHL and C:N. The second component (CCA2; 19% variation) reflected areas that favored euglenoids, specifically sites high in phosphorus. The third component represented sites high in macrophyte cover (CCA3; 4% of variation) and was also positively related to chrysophytes, xanthophytes, centric diatoms, and euglenoid abundances. The permutation test (Table 3.5) indicated that all the environmental variables were significant to periphytic algal assemblages except nitrate, nitrite, PC, and C:N ratios. General linear models based on significant variables I the CCA (Table B.2) indicated most taxa were more abundant earlier in the year,

Table 3.5. A permutation test (999 permutations) was performed with all explanatory variables to determine significance of each variable (α = 0.05).

	Df	ChiSquare	F	Pr(>F)	
Date	1	0.05	110.71	<0.01	*
Site	4	0.06	32.11	<0.01	*
Temperature	1	0.07	147.38	<0.01	*
Dissolved Oxygen	1	0.03	63.68	<0.01	*
pH	1	0.01	14.54	<0.01	*
Turbidity	1	0.01	18.61	<0.01	*
Specific Conductance	1	0.00	2.85	0.05	*
CFU	1	0.01	19.38	<0.01	*
Water Velocity	1	0.01	21.57	<0.01	*
BOD	1	0.01	21.77	<0.01	*
Nitrate	1	0.00	1.65	0.16	
Nitrite	1	0.00	2.25	0.09	
Phosphorous	1	0.01	16.12	<0.01	*
Ammonium	1	0.00	7.92	<0.01	*
PC	1	0.00	1.60	0.16	
CHL	1	0.00	4.88	<0.01	*
TN	1	0.01	13.09	<0.01	*
TC	1	0.00	8.57	<0.01	*
C:N	1	0.00	1.15	0.29	
Tree Cover	1	0.01	13.56	<0.01	*
Macrophyte	1	0.01	12.25	<0.01	*
Residual	309	0.15			

although sample date was not significant for all groups. Chrysophytes showed large positive associations with specific conductance (parameter estimate 15.46 ± 2.81 SE) whereas other groups showed no significant, or negative relationships. Pennate diatoms and xanthophytes were negatively related to water flow (-5.79 ± 0.16; -3.87 ± 1.42; respectively), but centric diatoms, chlorophytes, and cyanobacteria were not (7.11 ± 0.86; 2.28 ± 0.12; 2.38 ± 0.22; respectively).

DISCUSSION

Because of its central position in the trophic web of littoral aquatic communities, periphyton has a strong influence on the composition, functional structure, and dynamics of littoral aquatic communities (Wetzel 1964, Adame et al. 2017, Doi 2009). Spatial and temporal shifts in the composition of these basal resources impact nutrient and energy flow and are likely reflected in the distribution and growth of invertebrate and vertebrate grazers and predators (Jones and Sayer 2003, Chessman et al. 2009, Tonkin et al. 2014). Periphyton assemblages in the ARB were found to be significantly influenced by many environmental factors, including distance to the water source, temperature, nutrients, and macrophyte abundance. Importantly, changes to historical flooding regimes in the ARB and other floodplain rivers could significantly alter floodplain productivity, and flood pulse relationships to floodplain trophic webs should be considered in the management of floodplain river systems.

Temporal Effects on Algal Assemblages

Seasonal effects were important in determining periphyton growth and assemblage composition at ARB and LV sites. For ARB sites, CCA1 represented temporal trends in periphyton composition related to annual inundation and dewatering events. High water turbidity and increases in DO concentration and periphyton C/N ratio indicated periods of floodplain inundation, which typically occurs in the early months of the year depending on the timing and magnitude of the Atchafalaya River flood pulse (Piazza 2014). Later in the season, usually in May and June, Atchafalaya River stages decline, and inundated floodplains drain into canals and bayous, eventually entering the Atchafalaya River to the west or the GIWW to the east. Temporal changes in periphyton composition were also evident in LV but were not related to seasonal rising and falling water levels. The early part of the year for these non-floodplain sites was characterized by increased DO levels and high chlorophyll-a concentrations. As temperatures increased later in the year, there was an increase in algal and bacterial growth, as indicated by TN correlations, as well as respiration rates (BOD) and microbial associations (CFU). Although LV does slowly drain into Grassy Lake, directional north-to-south flow is negligible, and water movement is largely due to local wind action. Interestingly, cyanobacteria were highly correlated with increased water movement in Lake Verret, even though cyanobacteria in lotic systems have been reported to prefer little to no water movement (Bellinger and Sigee 2015, Pacheco and Neto 2017, Giblin and Gerrish 2020). Most likely, greater abundances of cyanobacteria later in the year were more related to elevated temperatures than the influence of increased water movement, as seen in other freshwater lake systems (Beaulieu et al. 2013, Mullin et al. 2020)

Pennate diatoms were largely ubiquitous at ARB sites, as in other riverine ecosystems (Finlay et al. 2002, Snell et al. 2019) and did not appear on any CCA components, although centric diatoms were associated with CCA1 and CCA2. In LV, diatoms, particularly pennate diatoms, exhibited seasonal trends and significantly declined in abundance during the warmer parts of the year. This is similar to observations from another group of floodplain lakes in the Yangtze River system. There, diatoms dominated phytoplankton assemblages in lakes with active river connections, such as the ARB. However, unlike the LV results where chlorophytes were the dominant taxa, isolated lakes in the Yangtze River floodplain were dominated by cyanobacteria (Liu et al. 2016), which might be related to higher nutrient concentrations in the isolated system. In ARB and LV, diatoms were closely associated with turbidity and high DO, characteristic of ARB flooding conditions and extensive rainfall in both locations early in the year. Although high levels of turbidity generally reduce photosynthetic activity by blocking incoming light (Bellinger and Sigee 2015), it may be that turbidity levels at this time, although elevated relative to other parts of the year, were not high enough to impact photosynthesis on the shallowly suspended (5 cm) periphytometers. In addition, diatoms can be highly sensitive to DO levels (Brett et al. 2009), which are highest during river rising events and may provide optimal conditions for periphyton growth, at least near the water surface. Interestingly, diatoms typically have high TC and TN content and are a valued consumer resource (Brett et al. 2009, Guo et al. 2016). Therefore, I expected they would have loaded with TC and TN on the CCA axes. Prior to elemental analysis, periphyton growth slides were viewed under a dissecting microscope and large macroinvertebrates, such as chironomid larvae, were removed. However, smaller grazers, like Cladocera and rotifers, may have been included and confounded results.

Xanthophytes also varied temporally in their contribution to the periphyton assemblages at both locations. Xanthophytes can be single-celled or colonial and appear yellow-green in color due to the accessory pigment diatoxanthin (Bellinger and Sigee 2015). Members of this algal group, such as *Botrydiopsis arrhizal*, are commonly found in muddy habitats near littoral edges (Bellinger and Sigee 2015; Reynolds 2006), in small water bodies, or in soil (Reynolds 2006, Bellinger and Sigee 2015, Zhang et al. 2015, Costa et al. 2020). In both regions, this group made up less than 1 percent of the periphytic algal assemblage but exhibited its highest abundances in the late summer months in both regions. Xanthophytes prefer cool, free-standing, slightly acid water (Gabyshev and Gabysheva 2010), therefore, their appearance in Lake Verret later in the season was somewhat unexpected. However, Reynolds (2006) reported xanthophyte abundance could be driven by low turbidity levels, which may explain their relative loadings on CCA1.

Distance from River Source Impacts Algal Assemblages

Although the timing of the flood pulse emerged as an important determinant of algal community assemblages, there were also significant spatial effects on periphyton assemblage composition in the ARB. During flood events, areas closer to river water input showed biotic and abiotic trends that differed from areas deeper within the floodplain. During floodplain inundation, rising water crests natural levees and begins to move onto the floodplain. Water velocity increases differentially as river water moves onto the floodplain, with sites nearer river water sources showing higher water velocities than more distant sites. Dry floodplain areas with accumulated organic matter during low-water are inundated with nitrogen-rich river water, while hydrologic mixing occurs in floodplain lakes. Newly available nutrients (NO_3, NO_2, NH_4) fuel algal and bacterial growth. In the ARB sites, nitrogen and phosphorus sources were inversely related to distance from the river source and would have been readily taken up by early colonizers, such as diatoms. In rivers and lakes, diatoms, particularly large centric diatoms, are typically the first to exploit influxes of nutrients (Brett et al. 2009, Dai et al. 2012, Bellinger and Sigee 2015, Reynolds et al. 2002, Kiss et al. 2012), explaining why centric diatoms loaded on the first and second components of the CCA. Chlorophytes, in contrast, did not exhibit substantial seasonal trends observed in other riverine and lake systems (Sheath and Burkholder 1983, Andersen et al. 2020), but did appear to be more abundant at sites located further from river sources, where inorganic nitrogen was lower. In the ARB, back-water swamps are characterized by high amounts of canopy cover and decomposition due to microbial activity (BOD; Battle and Mihuc 2000). Greater chlorophyte abundance at more distant sites was unexpected given their requirements for high light intensity and low shade tolerance (Lemes-da-Silva et al. 2010, Tonetto et al. 2012, Peres et al. 2017). However, it is likely that chlorophytes were simply more abundant later in the year when flood-related turbidity had declined and light levels were sufficient for photosynthesis, regardless of shading. This is also supported by their association with BOD, which was also higher later in the year when water temperatures and microbial activity increased. The magnitude and duration of floodplain inundation can vary substantially in the ARB given annual variability in the Atchafalaya River flood pulse (e.g., Pasco et al. 2016). In 2019, the river remained in flood stage until nearly September. This prolonged inundation, particularly in the backwater regions most distant from river inputs, could have provided particularly suitable environmental conditions for chlorophyte growth for an extended period relative to more typical flood years.

Macrophytes

Macrophytes are essential to aquatic ecosystems because they influence habitat and water quality, which determines organism abundance and distribution (Caraco and Cole 2002, Dodds and Biggs 2002, Kaller et al. 2011, Pasco et al. 2016), as well as also serving as substrate for basal resource development (Cazzanelli et al. 2021). As such, in both ARB and LV CCA3, macrophyte cover appeared influential in driving periphytic algal assemblages, but only emerged significant for LV. Specifically, chrysophytes, euglenoids, and xanthophytes in LV sites were positively associated with macrophytes. These taxa are generally present in small numbers but can become dominant under favorable conditions. Chrysophytes, which can be unicellular, colonial, or filamentous (Reynolds 2006), tend to be found in cooler, oligotrophic waters that are low pH, specific conductance, and alkalinity. There have been very few observations of freshwater chrysophytes associated with macrophytes, therefore their correlation with aquatic macrophytes in LV was unexpected (Siver and Hamer 1989, Siver and Hammer 1992, Bellinger and Sigee 2015). However, *Chrysomorula choaerens* has been observed previously to form dense colonies on aquatic macrophytes (Wujek 2013), and Tunca et al. (2014) found several taxa in northern Turkey that commonly occurred with aquatic macrophytes (i.e. *Chromulina* sp., *Ochromonas* sp. *Psuedokephyrion* sp.). In 2018, Cao and colleagues noted that when P was abundant in heavily vegetated ponds, algal communities tended to be dominated by chrysophytes, rather than cyanobacteria as generally seen (Cao et al. 2018). More studies are needed to better understand the occurrence of chrysophytes in floodplain lakes like LV, as the current study did not identify chrysophytes to genera or species. Xanthophytes also generally constitute only a small portion of the periphytic community, and similarly to chrysophytes, are rarely found among aquatic plants. The few occurrences that have been observed tended to be filamentous (*Trebonema* sp.) or coccoid (*Mischococcus* sp.; Ott and Oldham-Ott 2003, Salmaso and Tolotti 2009). Euglenoids are far more common among aquatic vegetation and can be found in small ponds or areas with high amounts of decaying organic matter (Bellinger and Sigee 2015, Wehr et al. 2015, Cao et al. 2018), particularly those dominated by submerged macrophytes (Dokulil and Padisak 1994). Thus, it was not unexpected to observe euglenoids among macrophyte beds in LV. In fact, it has been reported that when macrophyte abundance exceeded 40%, euglenoids consistently dominated algal assemblages (Borics et al. 2003). One of the reasons why euglenoids can thrive in vegetated areas, where competition for light and nutrients is high, is because of their mixotrophic strategies that allow for proliferation in resource-limiting environments. Mixotrophy is also common xanthophytes and chrysophytes, so it is possible that this strategy is what allowed them to thrive in competitive environments with euglenoids among aquatic macrophytes (Tunca et al. 2014, Pribyl and Cepak 2019).

CONCLUSIONS

Alterations to river-floodplain systems threatens habitat integrity and can contribute to the loss of ecosystem function and biodiversity. Disconnection of floodplain lakes from their rivers by installing dams and levees (as seen in Lake Verret) causes changes in hydrology that can significantly alter macrophyte and fish assemblage composition and function (Liu and Wang 2010, Quirino et al. 2019, Jiang et al. 2020). Periphytic algal assemblages in the ARB differed from LV, particularly in overall higher cell abundance, pennate diatom-dominated assemblages, a seasonal shift from pennate diatoms to chlorophytes, and a gradient of decreasing overall cell abundance and a shift from centric diatoms to chlorophytes at increasing distances into the floodplain. In contrast, in LV samples, pennate diatoms were replaced by cyanobacteria and xanthophytes and in the absence of a floodplain gradient, assemblages were similar among sites. However, in both systems, vegetated areas were regularly associated with three algal groups: euglenoids, chrysophytes, and xanthophytes (only LV). Importantly, distance from the water source had a substantial effect on both algal community composition and environmental variables in the ARB floodplain. Overall cell abundance decreased further into the floodplain, with centric diatoms showing higher prevalence closer to river water sources, characterized by greater flow velocity and nitrogen concentrations. Deeper into floodplain habitats, tree cover and microbial activity were greater, favoring chlorophytes. To the author's knowledge, this is the first study to investigate periphytic algal community composition at differing distances from river sources in floodplain regions in the southeastern USA. Because shifts in the composition of basal resources could impact higher trophic levels, changes to historical flooding regimes and their impact on floodplain trophic webs should be considered in future floodplain management decisions.

CHAPTER IV. THE IMPACT OF HISTORIC FLOODING ON ATCHAFALAYA RIVER BASIN PERIPHYTIC ALGAL ASSEMBLAGES

INTRODUCTION

The Mississippi (MR) and Atchafalaya (AR) Rivers experienced extensive flooding in 2019 due to extreme rainfall and snowmelt (NOAA 2019, Reed et al. 2020). The catastrophic flooding resulted in staggering economic loss, estimated at 20 billion dollars (NOAA 2020), and over a million acres of destroyed cropland along the MR (Reed et al. 2020). The MR remained in flood stage for over 150 days (Price and Berkowitz 2020), the longest floodplain inundation since the Great Flood of 1927 (Pal et al. 2020). The Bonnet Carré Spillway, which channels Mississippi River water into the Lake Pontchartrain Estuary, was open for record-breaking 23 days (Parra et al. 2020). The AR is the major distributary of the MR, accepting 30% of the combined daily discharge of the Mississippi and Red Rivers (Lambou 2020, Piazza 2014). The AR begins near Simmesport, LA, and runs south for over 200 km towards the Gulf of Mexico, providing approximately 200 km^3 of freshwater into the Gulf annually (Rosen and Xu 2015). With a watershed that spans 162,000 ha, the AR is the fifth largest river in North America (Piazza 2014, Piazza et al. 2015). The Atchafalaya River Basin (ARB) is the largest bottomland hardwood forest remaining in North American and consists of meandering bayous and backwater lakes that are inundated annually by the AR (Lambou 2020, Piazza, 2014). This flood pulse drives a highly productive and diverse environment by introducing nutrients and organic material into the floodplain (Pettit et al. 2017). Fish and other aquatic organisms use floodplain habitats for feeding and reproduction (Crook et al. 2019). Floodplain habitats also make excellent refugia for larval fish and invertebrates, and many species time their reproductive events with the hydrology of the flood pulse (Bonvillian 2013, Bayley et al. 2018).

Coincident with the 2019 MR flood, the AR received a record amount of water and remained in flood stage for 329 days, with >50% of the river's water moving onto the floodplain (Pal et al. 2020). Over the last several decades, flooding frequency in Louisiana has increased substantially (Wang et al. 2020, Tang et al. 2021). In fact, the AR has experienced several major flood events, notably in 2008 and 2011 (Piazza 2014), with eleven major flood events in the ARB since 1983 (Tang et al. 2021). Nearly all floodplains in the northern hemisphere have undergone anthropogenic alterations for flood mitigation (Lewis et al. 2000), and the ARB is currently only half its historic size due to construction of guide levees for flood control (Hupp et al. 2008, Louisiana Department of Natural Resources 2010).

In unmodified floodplain systems, regular intervals of high- and low-water periods support substantial biodiversity and aquatic productivity (Junk et al. 1989, Jardine et al. 2012, Jardine et al. 2015, Pettit et al. 2017, Crook et al. 2019). However, extreme floods can substantially impact ecosystem functions (Talbot et al. 2018). Floodplain connectivity facilitates exchanges of fish, invertebrates, and organic material, which drives important biochemical cycles (Pettit et al. 2017, Bayley et al. 2018). Large floods reduce the ability of a system to cycle nutrients and export organic material (Price and Berkowitz 2020), which increases as heavy precipitation facilitates excess terrestrial runoff from urban or agricultural areas (Devlin et al. 2012, D'Sa et al. 2019, Clemenston et al. 2021). With excess nutrient input and reduced processing ability, extreme hydrologic events also can affect algal production and community composition (Francoeur and Biggs 2006, Hintz and Willnitz 2013, Tang et al. 2013).

Periphytic, or attached, algae and bacteria in biofilms absorb organic material and nutrients and facilitate biochemical processing in freshwater ecosystems (Flemming 1993, Battin et al. 2016). These algae are responsible for a substantial amount of autochthonous primary production and serve as major contributors to riverine food webs (Junk et al. 1989, Thorp and Delong 1994, Thorp and Delong 2002, Junk et al. 2005, Doi et al. 2008). Production and community composition can be affected by a number of factors, including hydrologic regimes, frequency of disturbances, and the duration of flooding events (Agostinho et al. 2004, Davies et al. 2008, Agostinho et al. 2008, Fuller et al. 2011). Changes in these factors can lead to changes in algal abundance, richness, and diversity (Mihalijevic and Pfieffer 2012, Algarte et al. 2016, Bondar-Kunze et al. 2016), which may impact the transfer of energy and nutrients to higher trophic levels.

The objective of this chapter is to compare periphytic algal community assemblages and environmental conditions in the lower ARB during a typical low-water summer in 2017 to an atypical summer in 2019 where flood conditions were sustained. This unprecedented flood event provided an opportunity to understand how algal communities respond to extreme inundation. Because these events may become more frequent in the future, understanding how communities respond is important to flood remediation and ecosystem management. My main goal was to compare spatial and temporal differences in algal community composition between the non-flooded summer of 2017 and the flooded summer of 2019. Specifically, I investigated differences in periphytic algal total cell abundance and relative abundance between the typical and atypical summer. I hypothesized that extended flood conditions would substantially alter periphyton community composition in regard to total algal abundance and relative abundance of algal groups. In addition, I hypothesized that periphyton assemblages would change with increasing distance from the water source.

METHODS

Site Locations

The study took place in Iberia and St. Martin Parishes and consisted of five ARB sites located in a 50-km^2 section east of the Atchafalaya River, west of Pierre Part, LA, and south of Bayou Sorrel (Fig. 4.1). The inlet of Bayou Postillion at the Gulf Intracoastal Waterway along the eastern Atchafalaya River Basin guide levee was designated as the source of Atchafalaya River water for all sites, except S12, which received water from an inlet north of Bayou Postillion. Three periphyton samplers (periphytometers) were deployed at each site and tethered to trees on shore or on bald cypress (*Taxodium distichum*) knees near shore. Biweekly sampling occurred from June - October 2017 and then from May – September 2019.

Periphytometer Design

Periphytometers (15 x 30 cm) were constructed of 1-inch PVC pipe sealed with water-resistant sealant, allowing the frame to float at the water surface. Four glass microscope slides (75 mm x 50 mm x 1 mm) were suspended along the length of the frame within approximately five centimeters from the surface of the water. Slides were spaced five centimeters apart and secured with clear fishing line and plastic clips to

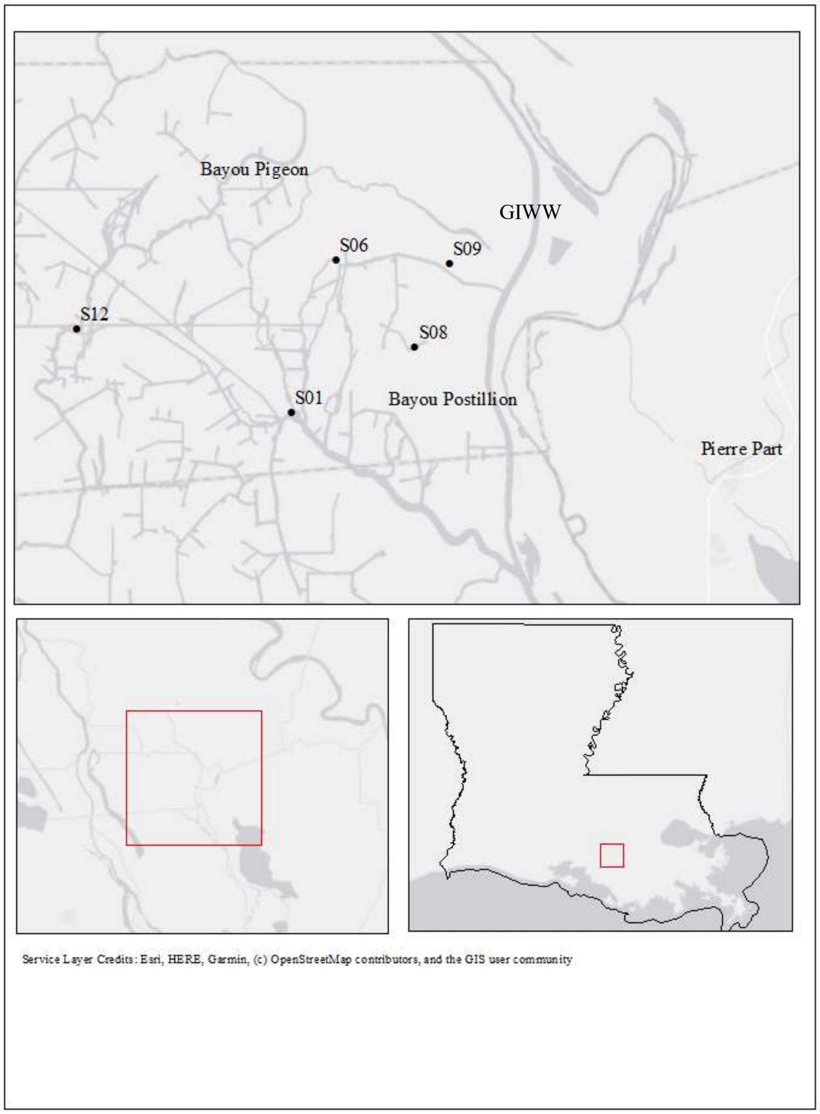

Service Layer Credits: Esri, HERE, Garmin, (c) OpenStreetMap contributors, and the GIS user community

Figure 4.1. A map showing the sampling locations in the Atchafalaya River Basin along with prominent bayous.

avoid loss or transfer of biofilm. Glass slides were cleaned thoroughly with ethanol prior to use and were replaced with fresh slides biweekly.

Habitat and Water Quality Procedures

Surface and bottom measures of temperature, dissolved oxygen (DO), pH, and turbidity were recorded at each site with a handheld YSI (Yellow Springs, OH). Water velocity was measured with a handheld velocimeter (SonTek, YSI, Inc, Yellow Springs, OH). Tree cover and macrophyte cover were also recorded for each periphytometer. Tree cover was scored by a single observer as 0%, 20%, 40%, 80%, or 100%. To estimate macrophyte cover at the time of collection, a 75-cm x 75-cm frame was placed around each periphytometer and photographed from 1 m above. Images were used to estimate the percentage of floating or emergent plants surrounding each periphytometer.

Algal Identification

Periphytometer slides were collected biweekly and two were placed in individual plastic bead bags with 10 mL of a 2% glutaraldehyde solution for algal identification. Glutaraldehyde preservative maintains cell color very well, which assists in taxonomic identification (Andersen 2005). The bags were refrigerated overnight so the glutaraldehyde would loosen the biofilm from the glass slide surface, reducing cell damage when scraped. Periphyton was scraped from the glass slides with a new, single-edge razor blade into centrifuge vials with additional 2% glutaraldehyde that completely covered the algae. Samples were refrigerated at 4° C in the dark. Extremely dense samples were diluted into 250 mL of glutaraldehyde. Prior to enumeration, samples were inverted gently to homogenize. If further homogenization was needed, the sample was sonicated for no more than 15 seconds. This was enough to break up dense clumps, but not enough to severely damage or burst a large number of cells. A Sedgewick-rafter counting slide observed at 400x magnification (Leitz Laborlux K) was used to classify periphyton cells into 8 groups (cyanobacteria, centric diatoms, pennate diatoms, xanthophytes, euglenoids, chrysophytes, chlorophytes and unknown/other) and three size classes [pico- (<2 μm), nano- (2–20 μm), and micro- (>20 μm)].

Statistical Analysis

Descriptions of periphyton composition were completed with JMP Pro (vers. 15.1.0, SAS Institute, Inc, Cary, NC), and all statistical analyses were performed with R (vers 3.6; R Core Team 2019) based on periphyton composition and measured environmental variables (temperature, dissolved oxygen, pH, turbidity, water velocity, total macrophyte density, tree cover, distance from source, and river stage). Tree cover was coded on a scale 0-5. Periphytic algae were grouped into cyanobacteria, centric diatoms, pennate diatoms, xanthophytes, euglenoids, chrysophytes, and chlorophytes for analyses. I used a log link, Poisson distribution general linear model (GLM; Vers. 3.6; R Core Team 2019) to analyze differences in total algal abundance between a normal flood summer (i.e., 2017) versus a flooded summer (i.e., 2019). It is important to note only a single basin and lake were included in this study, spatial autocorrelation is present (see Hurlbert 1984). However, useful information from this investigation can still be gleaned by observing differences between the two systems (Davies and Gray, 2015). To assess temporal and spatial trends in algal community assemblage, I conducted a canonical correspondence analysis (CCA; R package *vegan*, Oksanen et al.2019; permutations=999; $\alpha=0.05$) for each summer separately. The CCA permitted identification of relationships between periphyton assemblage composition and measured environmental variables. I chose the CCA over other ordination methods based on the unimodal and constrained nature of the data.

RESULTS

Sampling and Physicochemistry

In contrast to 2017, when floodplain inundation lasted 133 days, flooding conditions in 2019 persisted for a total of 329 days (Figure 4.2). This prolonged flood resulted in substantial differences in floodplain physicochemistry and habitat conditions relative to 2017 (Table 4.1). In June 2017, DO was below 2.0 mg/L (1.05 + 0.0 SE), and hypoxia continued until September, when some concentrations increased to 4.0 mg/L (2.23 + 0.20). Turbidity was relatively low (< 35 NTU) at all sites (Figure 4.3) in 2017, except for S06 in the month of September where turbidity jumped to >100 NTU. In 2019, average turbidities were under 10 NTU until September, when

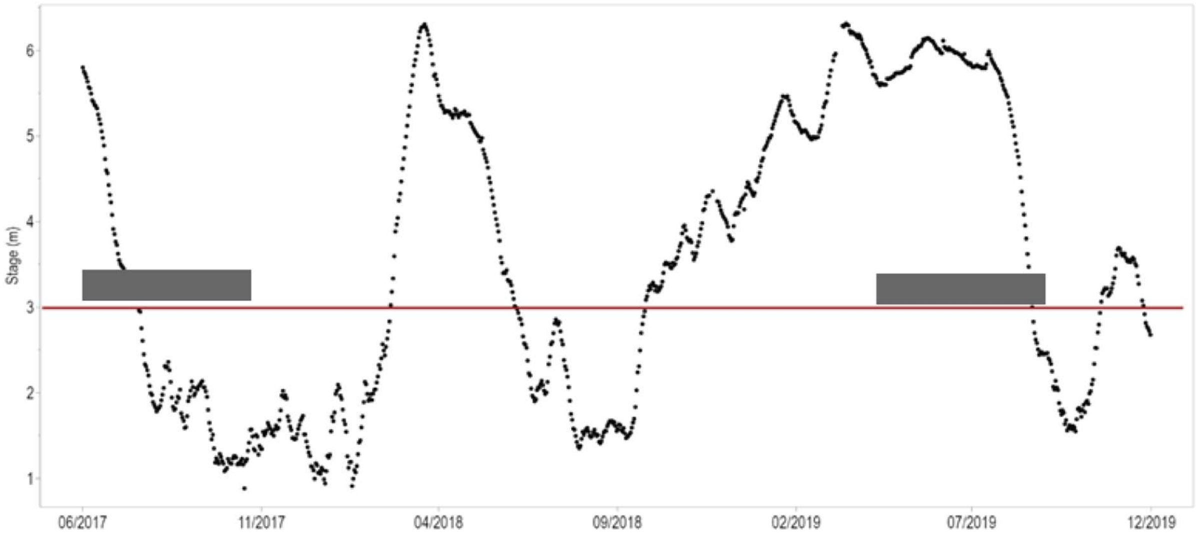

Figure 4.2. Butte la Rose water gauge (07381515) daily water level readings (stage) from June 2017 – September 2019. Red line indicates flood stage level (Pasco et al. 2016). Grey boxes indicate period sampled in 2017 (June-October) and 2019 (May – September.

Table 4.1. Summary statistics for the normal (2017) and flooded (2019) summer for all sites (combined). Standard error (SE) in parentheses.

	2017			2019		
	Mean (SE)	Min	Max	Mean (SE)	Min	Max
Depth (m)	0.92 (0.02)	0.16	1.47	1.42 (0.03)	0.1	2.81
Temperature (C)	24.37 (0.34)	9.85	28.51	21.82 (0.39)	8.7	29.15
DO (mg L^{-1})	2.95 (0.18)	0.39	8.96	3.03 (0.15)	0.17	8.73
pH	7.04 (0.03)	6.36	7.8	7.19 (0.01)	6.83	8.19
Turbidity (NTU)	24.31 (1.42)	1.9	102.6	15.22 (0.64)	0.36	51.19
Water Flow (m sec^{-1})	0.04 (0.00)	0	0.09	0.02 (0.00)	0	0.18
BOD (mg L^{-1})	4.08 (0.16)	2.35	8.35	6.57 (0.08)	2.45	9.95
River Stage (m)	2.02 (0.05)	1.13	5.5	4.98 (0.08)	1.57	6.06
Tree Cover (0-5)	2.32 (0.06)	1	4	3.58 (0.05)	1	5
Macrophyte Cover (%)	73.80 (2.02)	0	100	46.06 (2.14)	0	100

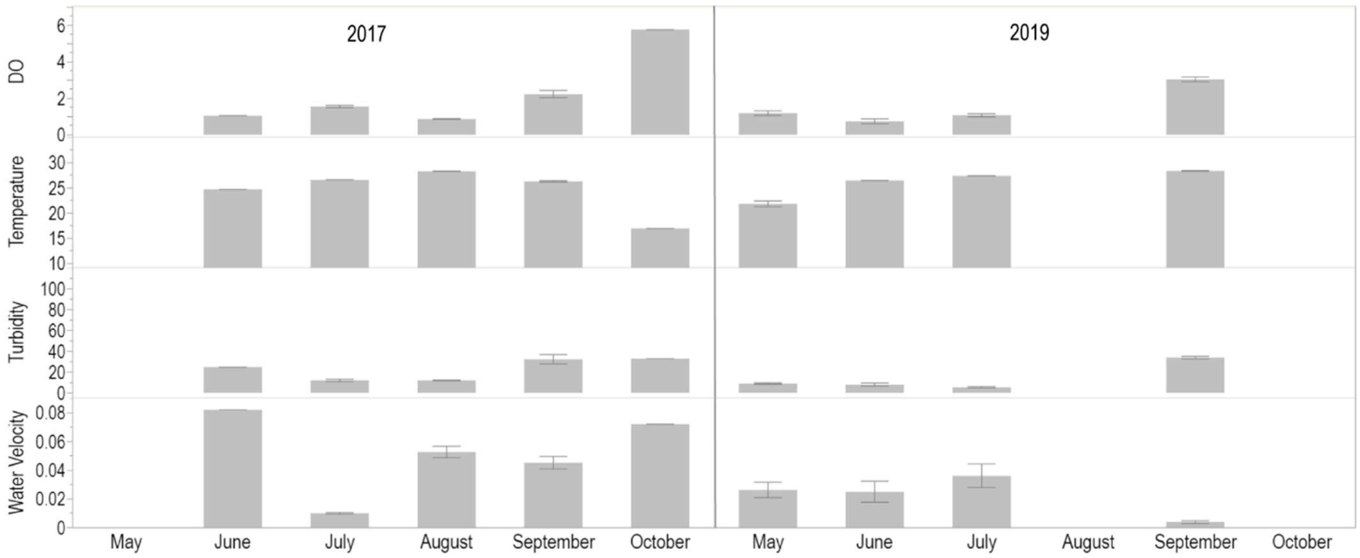

Figure 4.3. Dissolved oxygen (DO), temperature, turbidity (NTU), and water velocity differences between a normal (2017, left) and a highly flooded (2019, right) summer. Error bars represent standard error.

turbidities increased to 34 NTU. Temperature in 2017 and 2019 was highest during the months of August (28.3° C ± 0.04 SE) and September (28.39° C ± 0.06), respectively. During both summer periods, average water velocity was minimal (2017, 0.05 m sec^{-1} ± 0.003; 2019, 0.02 ± 0.003) at most sites, with the exception of S01 (near an open channel), where average water flow reached 0.07 m sec^{-1} ± 0.002 in 2017 and 0.08 m/s ± 0.007) in 2019. Total macrophyte cover was highest in 2017 (Figure 4.4), with July and October exhibiting 100 percent macrophyte coverage at all sites sampled. July coverage was composed of mostly floating macrophytes (>80%), whereas October beds supported equal coverages of floating and submerged plants. This was the highest percentage of submerged plants in either summer, as submerged plants typically were responsible for less than 30 percent of the macrophyte coverage. In 2019, total macrophyte cover was highest in September (70% coverage), with submerged plants accounting for about 15%.

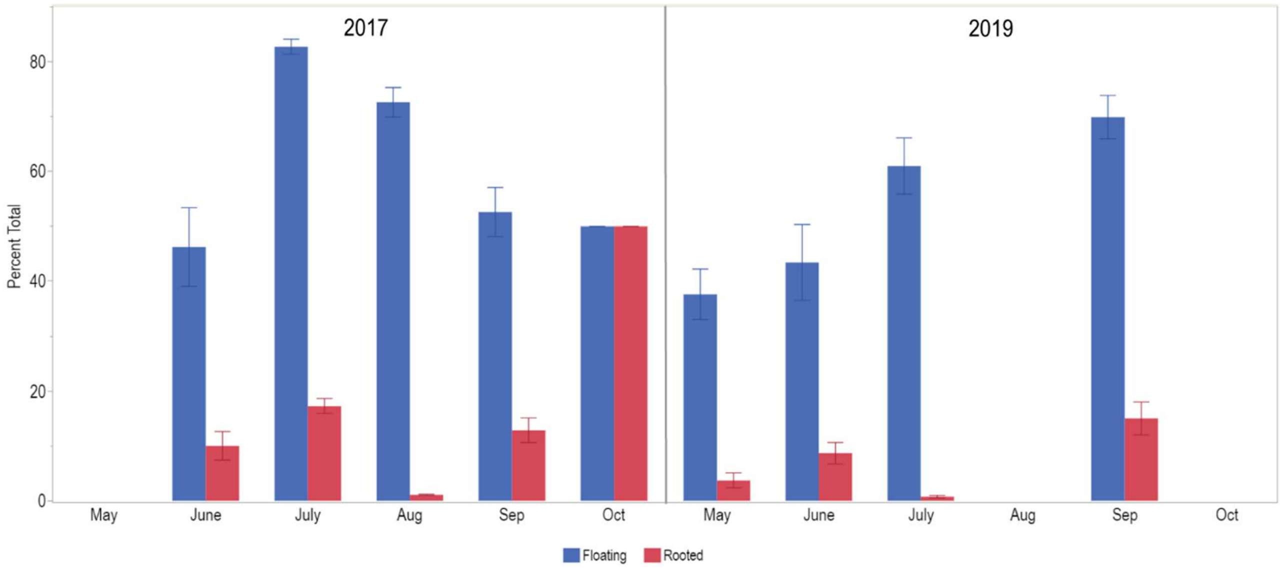

Figure 4.4. The percent of floating (blue) and rooted (red) plants visible from above in a 1m x 1m frame (photographed at time of periphyton collection) for summer 2017 (left) and summer 2019 (right). Error bars represent standard error.

Algal Assemblages

Overall cell totals for summer 2019 were significantly higher (Deviance = 543.64, P<0.01) than for summer 2017 (Figure 4.5). Total cell density for 2019 peaked in May

(5,578 cells per mm^2 ± 762.42 SE) which corresponded to the peak of the extended flood (approx. 6 m at Butte la Rose gauge USGS 07381515). Cell counts for June and July were much lower (1,843 cells per mm^2 ± 249, 1,667 cells per mm^2 ± 429, respectively), but reached their lowest level in September (604 cells per mm^2 ± 101). In contrast, September 2017 exhibited the highest mean cell count (669 cells per mm^2 ± 134) recorded that summer. The lowest cell count was seen in July (30.4 cells per mm^2 ± 5.8). In addition to total cell count, there were also differences in cell size distributions between the two summers. Overall, all size classes were more abundant in 2019 summer (Figure 4.6), with intermediate-sized (2-20 μm) algal cells being the most prevalent every month sampled. However, in 2017, intermediate-sized cells only dominated during June, all other months were dominated by smaller (<2 μm) algal species. Larger (>20 μm) algae were uncommon both years.

In addition to differences in total cell counts and size distributions, the two sampling years also exhibited different algal assemblage compositions. Chlorophytes made up a much higher proportion of the periphytic algal assemblage in 2017 (Figure 4.7), comprising 37% of the assemblage in June and 74% by October. In 2019, chlorophytes did not exceed 42% of the total periphytic assemblage on any date. In contrast, pennate and centric diatoms were much more prevalent in the summer compared to 2017. From May to July 2019, pennate and centric diatoms together accounted for 51-55% of the

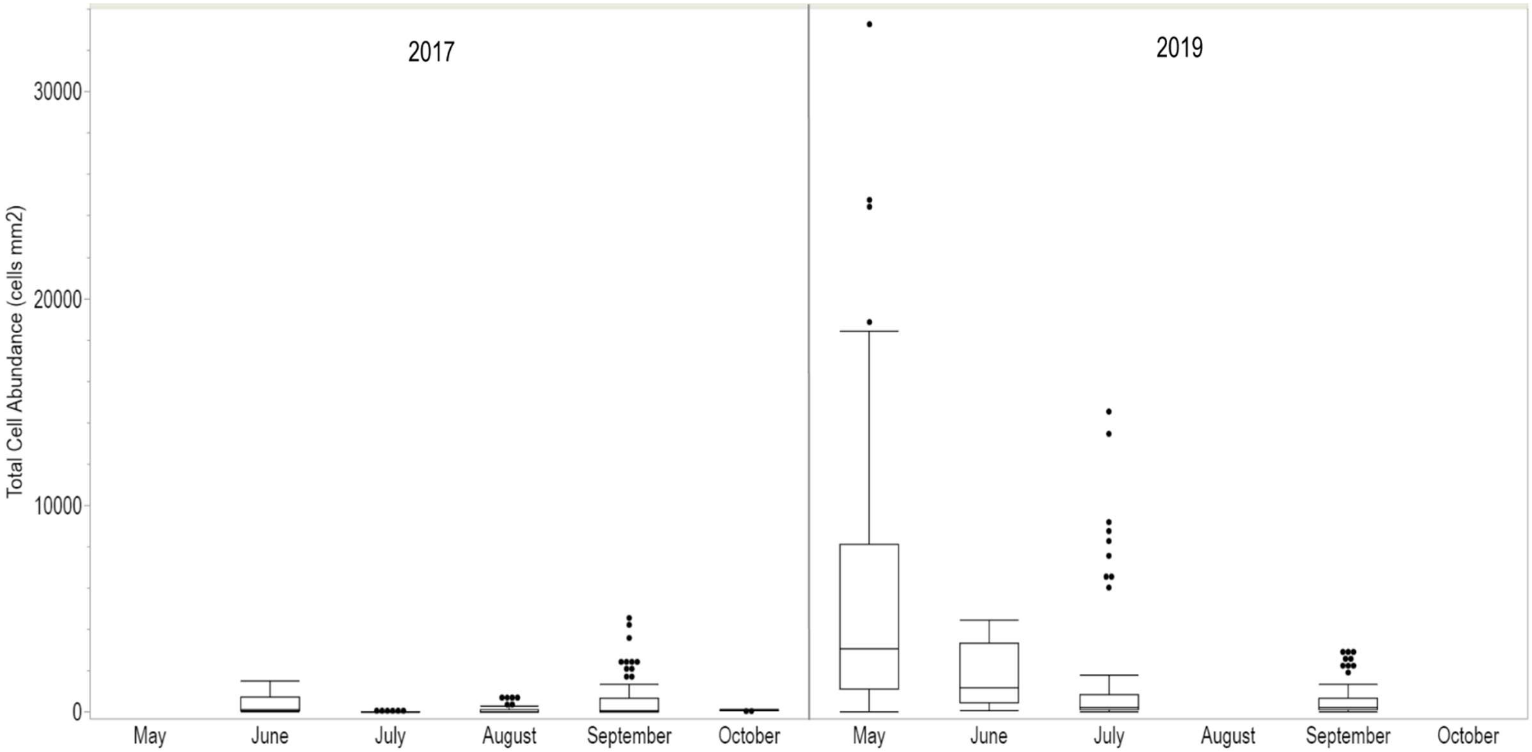

Figure 4.5. Total cell abundance (cells/mm^2) for all sites sampled in 2017 (left) and 2019 (right) for each month.

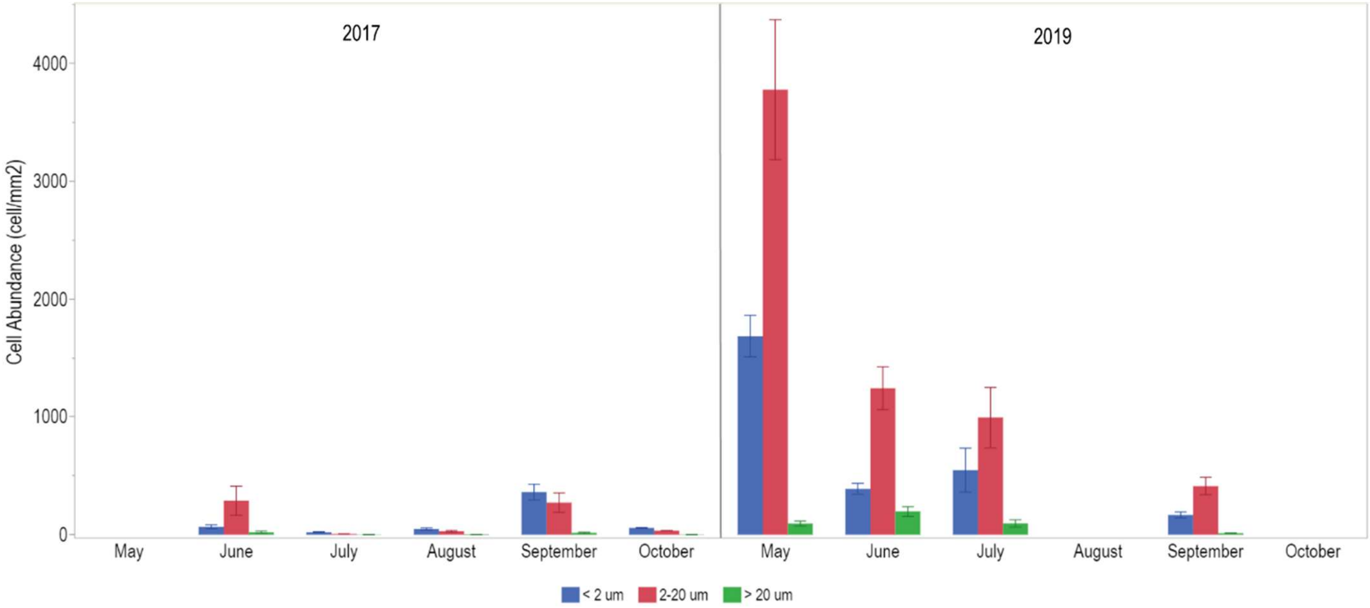

Figure 4.6. Cell abundance for each size class (<2 μm = blue, 2-20 μm, = red, >20 μm = green) were graphed for each month for summer 2017 (left) and 2019 (right). Sites combined). Error bars represent standard error.

periphyton assemblage. In June 2017, these two diatom groups made up less than 40% of the assemblage, with pennate and centric groups declining to 7 and 2%, respectively, in July. Xanthophytes were very rare in both summers, contributing less than 0.30% in 2019 and less than 5% in 2017. Similarly, chrysophytes and euglenoids were uncommon in both summer samples, although chrysophytes displayed a brief abundance increase (8%) in September 2017. Cyanobacteria abundances were similar between the two years, ranging between 5% and 25% across the summer sampling periods.

For the 2017 and 2019 summer periods, the first three axes of the CCAs explained 97% and 99% of the variation, respectively. For the non-flooded 2017 summer (Figure 4.8; Table 4.2.a, Table 4.2.b), the first axis was positively correlated with chlorophytes, tree cover, date, and DO, and negatively correlated with pennate

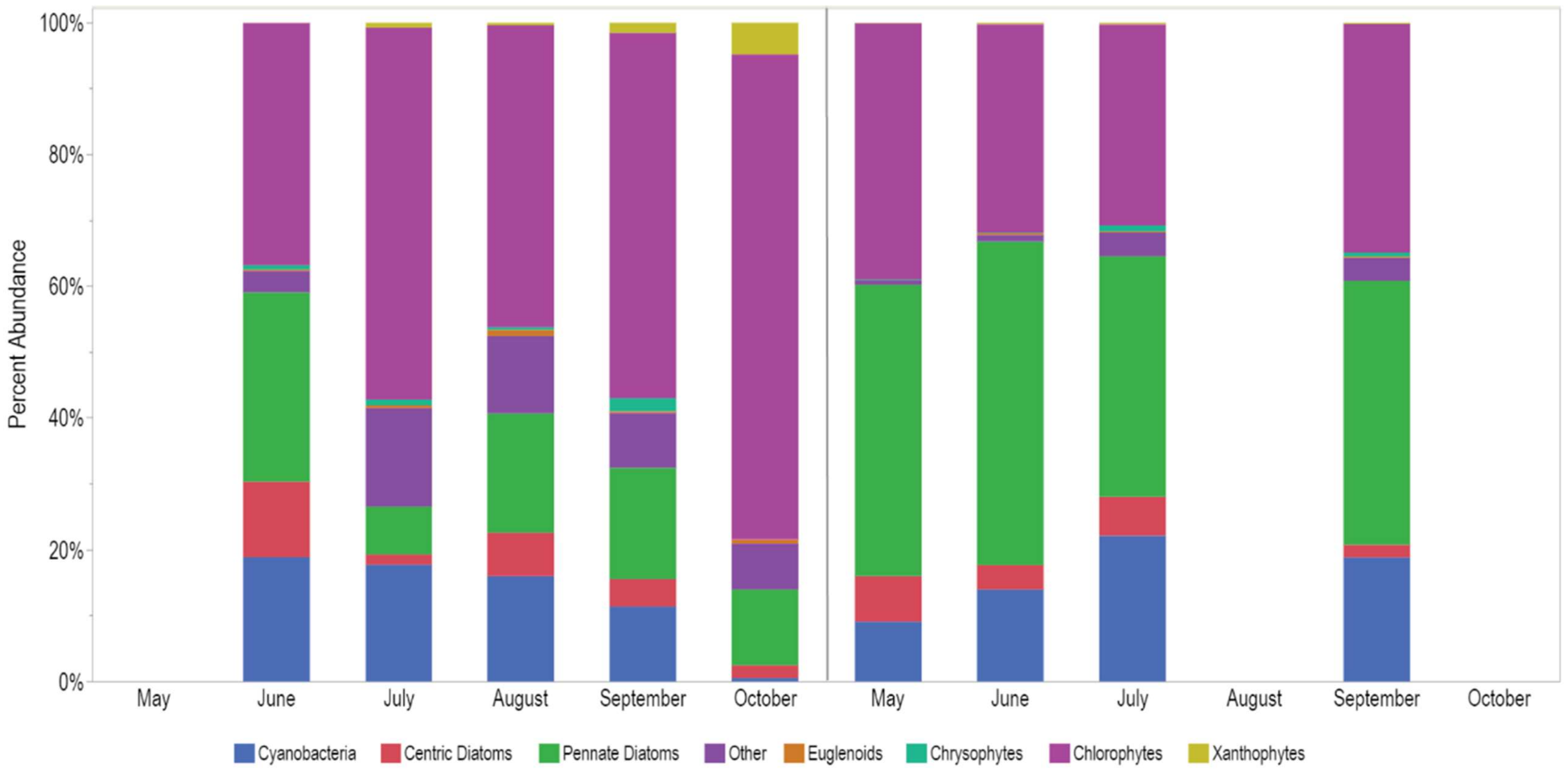

Figure 4.7. The percent abundance of all algal groups for the four sites (S01, S06, S08, and S12) sampled each month for 2017 (left) and 2019 (right). summers.

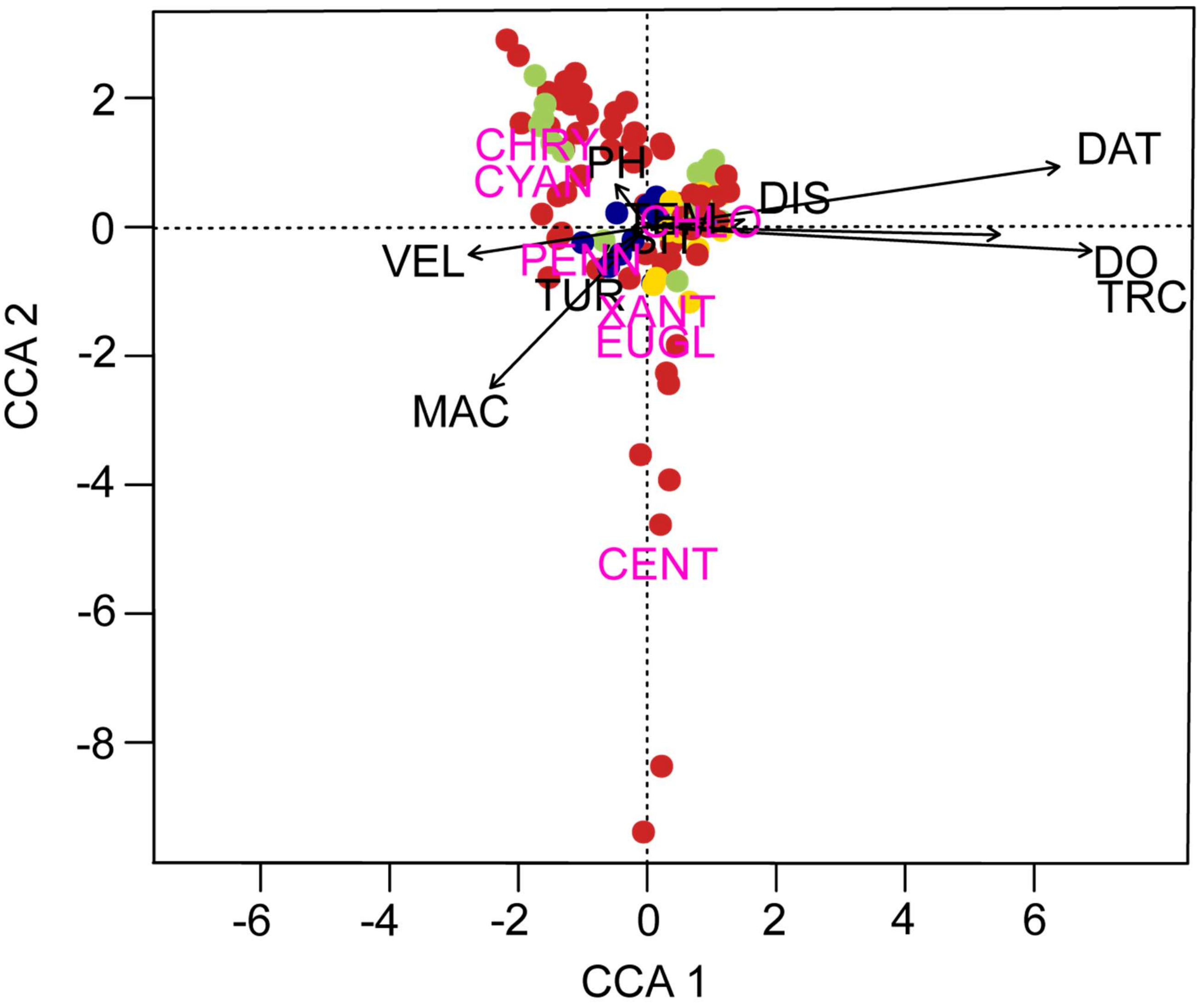

Figure 4.8. Canonical correspondence analysis (CCA) plot showing distribution of explanatory variables for all sites. ARB in 2017. Abbreviations: Date = DAT, Distance = DIS, Site = SIT, Temperature = TEM, Dissolved Oxygen = DO, pH = PH, Turbidity = TUR, Depth, Water velocity = VEL, Tree cover = TRC, Macrophyte abundance = MAC, Cyanobacteria = CYANO, Pennate Diatoms = PENN, Centric Diatoms = CENT, Chrysophytes = CHRY, Euglenoids = EUGL, Xanthophytes = XANT, Chlorophytes = CHLO. Sites are colored as follows: S01 = red, S06 = light green, S08 = blue, S12 = yellow.

diatoms, chrysophytes, and cyanobacteria. Axis 2 was positively related to chrysophytes and negatively related to macrophytes and centric diatoms. Site 01 was particularly variable along this axis, reflecting substantial changes in macrophyte cover and the two algal groups throughout the year. The third axis showed a small (<0.4) positive relationship with Site 06 and turbidity, as well as euglenoids and cyanobacteria. The flooded summer of 2019 showed an entirely different trend in the algal assemblage composition (Figure 4.9, Table 4.3.a, Table 4.3.b). Axis 1 showed positive associations between temperature, water flow, date, and the algal groups cyanobacteria, chrysophytes, and xanthophytes. Distance from the water source, turbidity, and DO were associated with chlorophyte appearance. The second axis showed a positive association with centric diatoms and euglenoids, which appeared to be inversely related to distance from source water. On the third axis, xanthophytes and cyanobacteria were associated with S08, but also with DO, date, and pH.

DISCUSSION

In this study, I compared summer periphytic algal assemblages and environmental variables in permanently-inundated floodplain channels during a low-water year (2017) and a year when flood conditions extended into late summer (2019). Habitat conditions in 2017 reflected temperature and flow conditions typical of annual floodplain inundation and recession (Pasco et al. 2016). Chlorophytes and cyanobacteria dominated for most of the summer, largely associated with shade from

Table 4.2. Scores from the canonical correspondence analysis for all sites for 2017 summer (CCA; R package vegan, Oksanen *et al.* 2019) for physicochemical and species variables. The first three axes explained 97% of variation. Matrix loadings > 0.35 were considered interpretable and highlighted (Stevens 2012). Eigenvalues, proportion explained, and cumulative proportion are indicated at the bottom for each axis.

	CCA1	CCA2	CCA3
Date	0.56	0.18	-0.20
Distance	0.13	0.02	0.05
S06	0.04	0.11	0.32
S08	-0.06	-0.09	-0.09
Temperature	0.05	0.01	0.05
DO	0.47	-0.02	0.09
pH	-0.04	0.13	-0.31
Turbidity	-0.06	-0.09	0.32
Water Velocity	-0.24	-0.08	-0.07
Tree cover	0.60	-0.07	0.00
Macrophyte	-0.21	-0.48	0.29
Cyanobacteria	-0.93	0.25	0.65
Centric Diatom	-0.01	-1.32	0.25
Pennate Diatom	-0.70	0.00	-0.20
Euglenoid	0.11	-0.28	0.50
Chrysophytes	-0.88	0.37	0.15
Chlorophyte	0.52	0.07	0.01
Xanthophyte	0.33	-0.28	-0.07
Eigenvalue	0.37	0.08	0.05
Proportion Explained	0.73	0.15	0.09
Cumulative Proportion	0.73	0.88	0.97

tree cover and high DO levels. Diatoms were in low abundance, but pennate taxa tended to occur at sites with low tree cover, and centric taxa preferred sites with high macrophyte cover. Conversely, diatoms were the dominant algal group in summer 2019. Water flow and water temperature were important environmental factors structuring algal assemblages, as well as distance from source water, indicating

Table 4.3. A permutation test (999 permutations) was performed with all explanatory variables to determine significance of each variable (α = 0.05).

	Df	ChiSquare	F	Pr(>F)	
Date	1	0.12	107.95	<0.01	*
Distance	1	0.01	8.55	<0.01	*
Site	2	0.02	7.87	<0.01	*
Temperature	1	0.00	1.73	0.16	
DO	1	0.21	192.83	<0.01	*
pH	1	0.04	34.24	<0.01	*
Turbidity	1	0.02	14.82	<0.01	*
Water Flow	1	0.01	4.74	0.02	*
Tree cover	1	0.03	27.59	<0.01	*
Macrophyte	1	0.05	45.81	<0.01	*
Residual	159	0.18			

prolonged inundation substantially altered the structure of periphytic algal assemblages relative to a typical flood year (Figure 4.8 and 4.9).

Flooding Impacts Periphytic Algal Assemblage

The extended flood in 2019 (Price and Berkowitz 2020) resulted in a substantial increase in total algal cell abundance compared to summer 2017. There was also a higher relative abundance of pennate diatoms compared to the chlorophyte dominance in 2017. Because of the extended inundation, access to backwater areas created a spatial gradient, with chlorophytes, turbidity, and DO being positively related to distance from river source, which was not seen in summer 2017. In contrast, centric diatom abundance in 2019 was negatively associated with distance from the source. This spatial trend was likely related to continued nutrient inputs from the GIWW, which

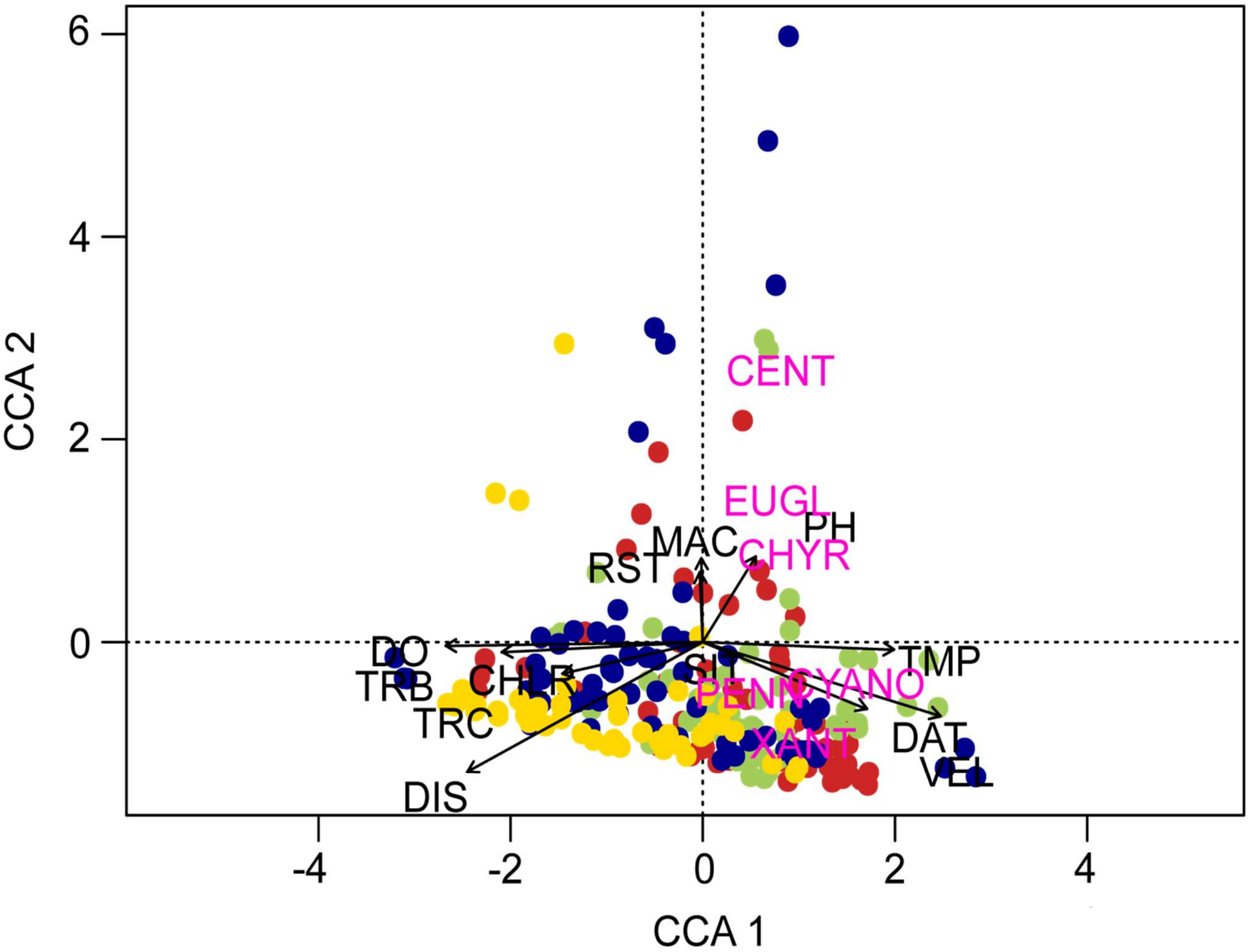

Figure 4.9. Canonical correspondence analysis (CCA) plot showing distribution of explanatory variables for all sites in 2019. ARB. Abbreviations: Date = DAT, Distance = DIS, Site = SIT, Temperature = TEM, Dissolved Oxygen = DO, pH = PH, Turbidity = TUR, Water velocity = VEL, river stage (STG), Tree cover = TRC, Macrophyte abundance = MAC, Cyanobacteria = CYANO, Pennate Diatoms = PENN, Centric Diatoms = CENT, Chrysophytes = CHRY, Euglenoids = EUGL, Xanthophytes = XANT Sites are colored as follows: S01 = red, S06 = light green, S08 = blue, S12 = yellow.

Table 4.4. Scores from the canonical correlation analysis for all sites for 2019 summer (CCA; R package vegan, Oksanen *et al.* 2019) for physicochemical and species variables. The first three axes explained 99% of variation. Matrix loadings > 0.35 were considered interpretable and highlighted (Stevens 2012). Eigenvalues, proportion explained, and cumulative proportion are indicated at the bottom for each axis.

	CCA1	CCA2	CCA3
Date	0.44	-0.22	-0.52
Distance	-0.63	-0.44	-0.24
S06	0.01	-0.05	0.18
S08	-0.07	0.70	-0.37
Temperature	0.51	-0.03	-0.28
DO	-0.69	-0.01	-0.40
pH	0.14	0.29	-0.70
Turbidity	-0.54	-0.03	-0.16
Water Flow	0.64	-0.25	0.06
Water Gage	-0.01	0.23	0.15
Tree cover	-0.38	-0.11	0.30
Macrophyte	0.00	0.28	-0.17
Cyanobacteria	0.59	-0.12	-0.42
Centric Diatom	0.16	0.88	0.04
Pennate Diatom	0.14	-0.12	0.18
Euglenoid	0.29	0.44	-0.30
Chrysophyte	0.50	0.24	-0.35
Chlorophyte	-0.51	-0.02	-0.12
Xanthophyte	0.45	-0.23	-0.83
Eigenvalue	0.13	0.08	0.04
Proportion Explained	0.52	0.30	0.17
Cumulative Proportion	0.52	0.83	0.99

would have promoted increased abundances of these fast-growing taxa (Reynolds et al. 2006, Kiss et al. 2012).

In stream systems, high water flows resulting from flood disturbances typically remove algal biomass via scouring (Francoeur and Biggs 2006, Hintz and Willnitz 2013, Tsai et al. 2014, Townsend et al. 2017), which can reduce overall algal abundance and lead to lower species richness (Izagirre and Elosegi 2005, Schneider and Petrin 2017).

Table 4.5. A permutation test (999 permutations) was performed with all explanatory variables to determine significance of each variable (α = 0.05).

	Df	ChiSquare	F	Pr(>F)	
Date	1	0.04	43.66	<0.01	*
Distance	1	0.07	77.60	<0.01	*
Site	2	0.06	33.35	<0.01	*
Temperature	1	0.01	12.55	<0.01	*
DO	1	0.01	9.39	<0.01	*
pH	1	0.02	22.63	<0.01	*
Turbidity	1	0.02	21.30	<0.01	*
Water Flow	1	0.00	4.68	<0.01	*
Water Gage	1	0.00	2.52	0.05	*
Tree cover	1	0.00	1.90	0.12	
Macrophyte	1	0.00	5.24	<0.01	*
Residual	214	0.20			

In contrast, smaller flood events that are short in duration with lower water velocities can benefit algal growth by increasing nutrient inputs (Weilhoefer et al. 2008), with scour-resistant benthic algae tending to fare better than other taxa (Mihaljevic et al. 2013). On the ARB floodplain, water movement was evident throughout the 2019 flood pulse, but water velocities were not high at most sites due to distance from the source channel, and flow reductions related to the abundance of submerged aquatic vegetation (Dodds and Biggs 2002). Periphytic algal taxa benefited from increased nutrients (Scrimgeour et al. 1988, Allan et al. 2007) and relatively low water velocities during the extended flood. Hosseini and van der Valk (1989) suggested increases in algal biomass after extended summer flooding in a freshwater marsh were likely the result of nutrient release from plant decomposition. Decomposition of accumulated macrophyte detritus from the extended ARB inundation event would also have provided essential nutrients to resident algae to uptake (Battle and Mihuc 2000) and this, too, could have contributed to the higher algal abundance recorded in 2019 compared to 2017.

Low DO levels from decomposition also likely impacted ARB algal abundance and assemblage composition, as it does in other floodplain systems such as in the Pinang River Basin, Malaysia (Wan Maznah and Mansor 2002) and Acarlar floodplain, Turkey (Tunc et al. 2014). Summer hypoxia from organic decomposition in the ARB is widespread (Pasco et al. 2016), particularly below the littoral macrophyte canopy (Colon-Gaud et al. 2004). Reduced DO, along with nutrient release from decomposition would likely encourage the growth of low DO-tolerant species, such as euglenoids and xanthophytes, over more nutritious taxa such as diatoms (Oliveria and Calheiros 2000, Cook et al. 2010, Mihaljevic et al. 2013). With the increase of macrophyte coverage in freshwater littoral habitats (Strayer 2010), along with the threat of rising water temperatures from climate change, future ARB periphytic assemblages could be skewed to nutritionally low-quality taxa during the extended summers when hypoxia is prevalent (Torres-Ruiz et al. 2007, Abedi and Sahair 2014, Guo et al. 2016).

In addition to increased algal abundance relative to 2017, the extended 2019 ARB flood also resulted in substantial changes in taxonomic composition of periphytic assemblages. In the floodplain lakes of the Lower Rhine and Meuse Rivers, large floods favored cyanobacteria and chlorophytes and reduced overall diatom abundance (van den Brink et al. 1994). Similar to our study, Gottlieb et al. (2005) reported total diatom abundance in the Everglades increased with longer flood events, and in Moreton Bay, Australia, the post-flood (1:100-year flood) planktonic algal assemblage was also dominated by diatoms, particularly larger taxa such as *Chaetoceros* spp., *Asterionellopsis glacialis*, and *Skeletonema* spp. (Clementson et al. 2021). Larger diatoms, such as *Achnanthese*, *Achnanthidium*, *Pinnularia*, or *Fragilaria*, were also observed to dominate algal assemblages in the Kowie River, South Africa, after a large flood event (Dalu et al. 2014), most likely due to rapid settlement after removal by flood waters, given their larger size (Stevenson 1990, Krajil et al. 2006, Dalu et al. 2014). Disturbances, such as floods, can give diatoms advantages over other taxa because of their ability to rapidly uptake newly available nutrients. However, because they are considered poor resource competitors, diatom abundance typically declines as nutrients are used up, with an assemblage shift to taxa more capable of dealing with resource limitation, such as chlorophytes or cyanobacteria (Reynolds 2002). Continued nutrient inputs likely explain the dominance of diatoms in the ARB during the extended 2019 flood.

Size distribution in algal communities is an important component of energy transfer and nutrient cycling (Maranon 2014). Smaller algal species with a higher surface area to volume ratio tend to fare better in low-nutrient and low-light environments (Chetelat et al. 2006, Maranon 2014) and tend to be favored during low-water periods in other floodplain systems (Chaparro et al. 2011). This is consistent with the dominance of smaller-sized periphytic algal taxa observed during the summer of 2017 in the ARB. In 2019, however, ARB periphyton was dominated by intermediate-size algal pennate diatoms. Intermediate-sized algae have superior abilities to exploit higher nutrient concentrations because of metabolic tradeoffs (Finkel et al. 2004, Maranon 2014). Although I did not measure water column nutrient concentrations in the present study, inundation of the ARB floodplain imports river-borne nutrients into the water column and improves water quality (Kaller et al. 2011, Baustian et al. 2019), and it is likely that increased nutrient concentrations contributed to the increase of intermediate-size algae in 2019. In addition, because diatoms typically have a wider range of maximum growth potential compared to other groups such as chlorophytes, they may be particularly well adapted for rapid colonization directly after flood events (Chan and Hamilton 2001).

Trophic Web Implications

In addition to providing nutrients and influencing water quality, extended flooding can also impact periphyton biomass (Liston et al. 2008, Chessman et al. 2009, Graca et al. 2018, do Nascimento Filho and do Nascimento Moura 2021) and species composition (Hillebrand et al. 2003, de Oliveira Macado et al. 2017, Silva et al. 2019) by modifying periphyton-grazer interactions. Macroinvertebrate consumers can be positively affected by prolonged floodplain inundation because of increased in available habitat and improved water quality (Bonvillian et al. 2013). However, as temperatures rise and floodwaters stagnate on the floodplain, BOD increases, driving water quality and invertebrate abundance down (Sabo et al. 1999; Kaller et al. 2011). Predation from floodplain fishes will also impact macroinvertebrate-periphyton interactions (Fontenot et al. 2001, Alford and Walker 2013). Because the density, diversity, and recruitment of floodplain fishes are impacted by inundation duration (Janac et al. 2010, Rolls and Wilson 2010), the extended flood pulse in 2019 likely impacted both primary and secondary production (e.g., Rees et al. 2020; Sommer et al. 2004; Death 2002, Tonkin and Death 2013, Eckert 2020).

Extreme flood events can also trigger bottom-up effects on macroinvertebrate communities by altering basal resources (Death 2002, Tonkin and Death 2013, Eckert 2020). Algae are superior food sources compared to fungus, bacteria, and leaf litter and are preferentially eaten by primary consumers (Kuhmayer et al. 2020). Changes to algal biomass and composition, therefore, could impact grazer assemblage composition and, potentially, production at higher trophic levels. For example, invertebrate taxonomic richness in a New Zealand river responded positively to intermediate levels of periphyton biomass, although the percentage of Ephemeroptera, Plecoptera, and Trichoptera (%EPT), which serve as indicators of ecosystem condition, was negatively related to periphyton biomass (Tonkin et al. 2009). Macroinvertebrate growth rate and diversity can also be impacted by periphyton species composition (Feminella and Resh 1991, Koksvik and Reinertsen 2008, Tonkin et al. 2014). Although periphytic algae are considered a high-quality food source (Guo et al. 2018, Kuhmayer et al. 2020, Ebm et al. 2021), nutritional quality can differ among algal groups. For example, diatoms and euglenoids tend to be high in essential long-chain polyunsaturated fatty acids (LC-PUFA; > 18 carbon molecules; Torres-Ruiz et al. 2007, Abedi and Sahair 2014, Guo et al. 2016) and are considered a high-quality food source for consumers. Differential nutritional quality between algal taxa can be further amplified by intracellular responses to environmental and physicochemical changes caused by flooding. LC-PUFA, like eicosapentaenoic acid (EPA) and docosahexanoic acid (DHA), are sensitive to shifts in nutrients, temperature, and light, which can lead to changes in the ratio of EPA and DHA (Hill et al. 2011, Cashman et al. 2013, Guo et al. 2016, Guo et al. 2021). Thus, extended flood events that influence water physicochemistry have the potential to alter not only the proportion of high- and low-quality food sources by impacting periphyton taxonomic composition, but also the intracellular carbon content of resident algal taxa. These basal-level changes can have significant implications for primary and secondary consumers, which suggests a complex interaction of flood duration and timing, nutrient availability, and water quality (particularly turbidity; Molinari et al. 2021) ultimately determines trophic web productivity on inundated floodplain environments.

CONCLUSION

Periphytic algae respond in a similar fashion to planktonic taxa regarding changing environmental conditions, such as temperature, nutrient concentrations, and flow velocity (Marberly et al. 2002, Kniffin et al. 2009). In floodplain systems, there is additional variability in environmental drivers of algal composition related to annual changes in the magnitude and duration of the flood pulse (Agostinho et al. 2004, Davies et al. 2008, Agostinho et al. 2008, Fuller et al. 2011). For periphyton, this variability is reflected in the highly dynamic composition of periphytic algal assemblages, as seen in the ARB and elsewhere (Robertson et al. 2001, Dunck et al. 2013, Santos et al. 2018). In this study, I saw changes in periphytic algal assemblages in response to extended flood conditions in the ARB in 2019, specifically the increase of pennate and centric diatoms. Historically, floodplain flora and fauna were adapted to natural variability in annual flood regimes (Junk et al. 1989), but alterations to hydrologic patterns caused by dams and levees, particularly reductions in flow variability (Moyle and Mount 2007, Remo et al. 2018), can seriously impact floodplain productivity (Ahn et al. 2006, see review by Opperman et al. 2010, Leauthaud et al. 2018) by blocking migration routes and reducing habitat heterogeneity (Liu and Wang 2010, Jiang et al. 2020). In addition, changes in watershed runoff related to climate change and river/floodplain alterations have the potential to increase the frequency of large flooding events, which may become an important driver of periphytic algal assemblage composition and productivity in floodplain river systems in the 21st century (Piggott et al. 2015, Cao et al. 2017).

CHAPTER V. SUMMARY

Several factors emerged as important drivers of ARB periphytic algal assemblage composition and abundance, but the effects appeared to vary depending on the magnitude of the ARB flood pulse. For example, periphytic algae showed variable spatial trends along a longitudinal gradient moving away from source water. Samples collected during 2017 and 2018 showed that most algal groups, except for chrysophytes and chlorophytes, increased with distance from the GIWW, with chlorophytes decreasing with distance. Samples collected in 2019, however, showed that diatoms tended to be found nearer to river water sources and chlorophytes favored more distant sites (Chapter 3). It is likely this difference is related to higher nitrogen inputs further into the floodplain. Even though extensive flooding would have transported nutrients deeper into the floodplain, water quality and dissolved nutrients showed spatial gradients relative to the GIWW, with both nitrogen and phosphorus declining with distance from river source. Chlorophytes are superior competitors in resource-limiting environments; thus, the spatial gradient in dissolved nutrient concentration would have facilitated a differential taxonomic response (Reynolds et al. 2002, Kiss et al. 2012). Water velocity was also much higher at near-source sites, favoring diatoms with firm surface attachments over smaller, flagellated chlorophytes. Macrophyte distribution also changes with distance from source water, with sites located deeper in the floodplain tending to have higher macrophyte abundance than sites nearer to river sources.

Macrophytes also emerged as an influential factor on periphytic algal assemblages. Most of the floating macrophytes observed were water hyacinth (*Eichhornia crassipes*) and *Salvinia* spp., both invasive species in the ARB. Aquatic macrophytes can have positive impacts on algal assemblages that increase periphytic growth (Liboriussen and Jeppesen 2006), e.g., waterthyme (*Hydrilla verticillate*) was found to promote photosynthetic activity of the cyanobacteria *Oscillatoria* (Zhang et al. 2020). Macrophyte impacts on water quality (Kaller et al. 2011, Pasco et al. 2016) can also influence periphytic algal abundance and composition (Santos and Ferragut 2018, Ward et al. 2016, Silva et al. 2020) and can promote variability of metabolic strategies among periphytic algal taxa. For example, mixotrophic strategies, as commonly seen in euglenoids, xanthophytes, and chrysophytes, are often observed in algal assemblages near macrophyte areas, where competition for light and nutrients are high (Tunca et al. 2014, Wehr et al. 2015, Cao et al. 2018, Pribyl and Cepak 2019). Regions with dense macrophyte stands can also exhibit increases in diatom populations and reductions in chlorophyte and chrysophyte numbers (Santos and Ferragut 2018), in contrast to observations in the ARB. This relationship likely continues to impact ARB periphyton assemblages, as waterways continue to support dense stands of invasive water hyacinth, salvinia, and hydrilla.

Negative macrophyte-algae interactions have also been reported and have the potential to impact periphytic assemblage composition in the ARB. Resource competition is a major issue for primary producers, particularly when these resources are severely limited, such as the late flood stage when most dissolved nutrients have been removed (Souza et al. 2015, Santos and Ferragut 2018). Light availability is another contested resource, with periphytic biofilms blocking sunlight availability to their macrophyte substrate, which can reduce growth of the macrophyte host (Roberts et al.

2003, Perillon and Hilt 2019, Zhang et al. 2020), e.g., periphytic algae such as *Oscillatoria* filaments on the leaves of submerged aquatic plants can monopolize incoming sunlight (Zhang et al. 2020).

Allelopathy is also an important macrophyte-algae interaction. Some algae have evolved toxins that can reduce plant growth by altering photosynthetic rates and interfering with enzyme and pigment production (Carmichael 2001, Pflugmacher 2002). However, macrophytes also produce allelopathic substances to rid their leaves and stems of unwanted algal growth. Although these allelopathic chemicals reduce overall algal growth, some macrophyte exudates target specific algal taxa, e.g., the invasive floating-macrophyte *E. crassipes* can inhibit chlorophyte growth while leaving other algae unaffected (Almeida et al. 2006). *Myrophyllum spicatum* has also been observed to alter algal taxonomic assemblages, shifting the assemblage away from large, nutritious diatoms to taxa with less nutritional value for consumers (i.e., cryptomonads and chlorophytes; Khuantrairong and Traichaiyaporn 2011, Ortiz *et al*. 2019). *Ludwigia hexapetala* can also stimulate *Scenedesmus communis* and toxic strains of *Microcystis aeruginosa*, while inhibiting non-toxic strains (Santonja et al. 2018). Clearly these interactions have the potential to significantly affect periphytic assemblage composition in the ARB, although their importance relative to physicochemical changes throughout the flood pulse, as well as grazing impacts from ARB invertebrates, is unknown.

Another aspect of the macrophyte-periphyton relationship is the role of aquatic plants as habitat for macroinvertebrate grazers, which also affect algal abundance and assemblage composition via preferential grazing. Some algae are toxic, such as certain strains of *Microcystis*, and are strongly avoided by grazers (Rangel et al. 2020). Large algal cells, such as nutritious diatoms, are a superior food source, but have long handling times (Troch et al. 2005) and are only available to larger macroinvertebrates. Smaller algal cells are more susceptible to grazing (Sunda and Hardison 2010), however, smaller algal cells are more efficient at nutrient uptake. Thus, while these small cells have an advantage in certain environments, such as macrophyte beds where nutrient resources are limited, there is a substantial tradeoff between growth potential and susceptibility to herbivores (Jiang et al. 2005). Macrophytes also provide habitat for predatory invertebrates (Fisher et al. 2012) and invertivorous floodplain fishes (Rutherford et al. 2001) that can further influence periphytic algal assemblages through predation on periphyton grazers.

Although periphytic biofilms are comprised of bacteria, fungi, and algae, algae are a far superior food source for aquatic grazers (Kuhmayer et al. 2020), and the nutritional quality of periphytic algae can affect both macroinvertebrate grazers and their predators. There is also variability between algal groups in nutritional quality. For example, diatoms and euglenoids tend to have higher carbon and nitrogen content compared to other algal groups, such as cyanobacteria and chlorophytes (Abedi and Sahair 2014, Guo et al. 2016). In addition, physicochemical changes in dissolved nutrients, water temperature, and light intensity can also alter algal nutritional content (Hill et al. 2011, Cashman et al. 2013, Guo et al. 2016, Guo et al. 2021) and could have complex and substantial effects on littoral food webs in the ARB, particularly given the seasonal and annual variability in floodplain hydrology.

One of the goals of this dissertation was to better understand the role flooding plays in periphytic algal assemblages in the ARB. During the three years of the study, the timing, duration, and magnitude of the ARB flood pulse varied substantially, particularly during the historic flood event in 2019, when the AR stayed in flood stage for nearly an entire year (Chapter 4; Price and Berkowitz 2020). This fortuitous event provided a unique opportunity to observe how periphytic algal communities responded to high-magnitude flooding, which may be increasingly relevant in future decades. Typically, large floods, accompanied by high water velocities, reduce algal biomass and species richness (Izagirre and Elosegi 2005, Tsai et al. 2014, Schneider and Petrin 2017, Townsend et al. 2017), while small floods tend to increase algal growth (Weilhoefer et al. 2008). However, this is not what we observed in the ARB. During the 2019 flood, there was a substantial increase in algal abundance, rather than a decrease. One reason why there was not a sharp decline in algal abundance is partly due to floodplain water velocities; other than in the main channels, water velocities in the floodplain are typically not high enough to induce scouring. Secondly, there was likely a much higher than normal spike in dissolved nutrient availability further onto the inundated floodplain, which facilitated the fast growth of taxa with high-nutrient requirements (i.e., diatoms). In addition to inundation, there would have been substantial nutrient release from plant decomposition that occurs during hot summer months, which would have also contributed to algal production (Hosseini and van der Valk 1989). However, this decomposition would also have driven down DO levels (Colon-Gaud and Kelso 2004) which could have negatively impacted algal growth and species composition (Maznah and Mansor 2002, Oliverira et al. 2000, Cook et al. 2010, Mihalijevic et al. 2013). In the ARB, extended summer flooding not only led to an increase in total algal abundance, but also resulted in an increase in high nutrient-seeking taxa, mainly diatoms (Reynolds et al. 2002). These results are similar to large flood events seen in other aquatic systems (Gottlieb et al. 2005, Dalu et al. 2014, Clementson et al. 2021) and emphasize the dynamic nature of periphyton production is likely resulting in an equally complex and dynamic littoral food web.

In conclusion, periphytic algae play an important role in aquatic ecosystems by contributing to primary production and nutrient cycling. In the hydrologically variable ARB floodplain, periphytic algal assemblages shifted in response to water quality, nutrient input, floodplain inundation, macrophyte presence, and distance from the river source. Alterations to hydrologic regimes, particularly dam and levee construction, can have serious trophic web implications in floodplain ecosystems by causing shifts in periphytic algal assemblages. Large flood events, such as the historic 2019 flood, further have the potential to impact floodplain ecosystems by altering algal assemblages (Talbot et al. 2018), and importantly may increase the abundance of toxic algal species (Trainer et al. 2020). The effects of climate change, which threatens to increase the frequency and magnitude of extreme weather events, including river flooding (Muzik 2002, Hirabayashi et al. 2008), are further compounded by the projected rise in world population, which will undoubtedly increase agriculture and urbanization, floodplain alterations, and nutrient runoff from farming (Devline et al. 2012, D’Sa et al. 2019, Clemenston et al. 2021). This portends significant changes in pelagic and periphytic algal assemblages (Francoeur and Biggs 2006, Hintz and Willnitz 2013, Tang et al. 2013), as well as higher trophic levels (Mihalijevic et al. 2013, Bondar-Kunze et al. 2016, Algarte et al. 2016), in the coming decades. Understanding basal-level responses in floodplain ecosystems are critical to mitigating future problems and preserving biodiversity. Future work should include whole community analysis, particularly how changes to floodplain ecosystems impact energy transfer from periphytic algae to higher trophic levels.

APPENDIX A. SUPPLEMENTARY MATERIAL FOR CHAPTER II

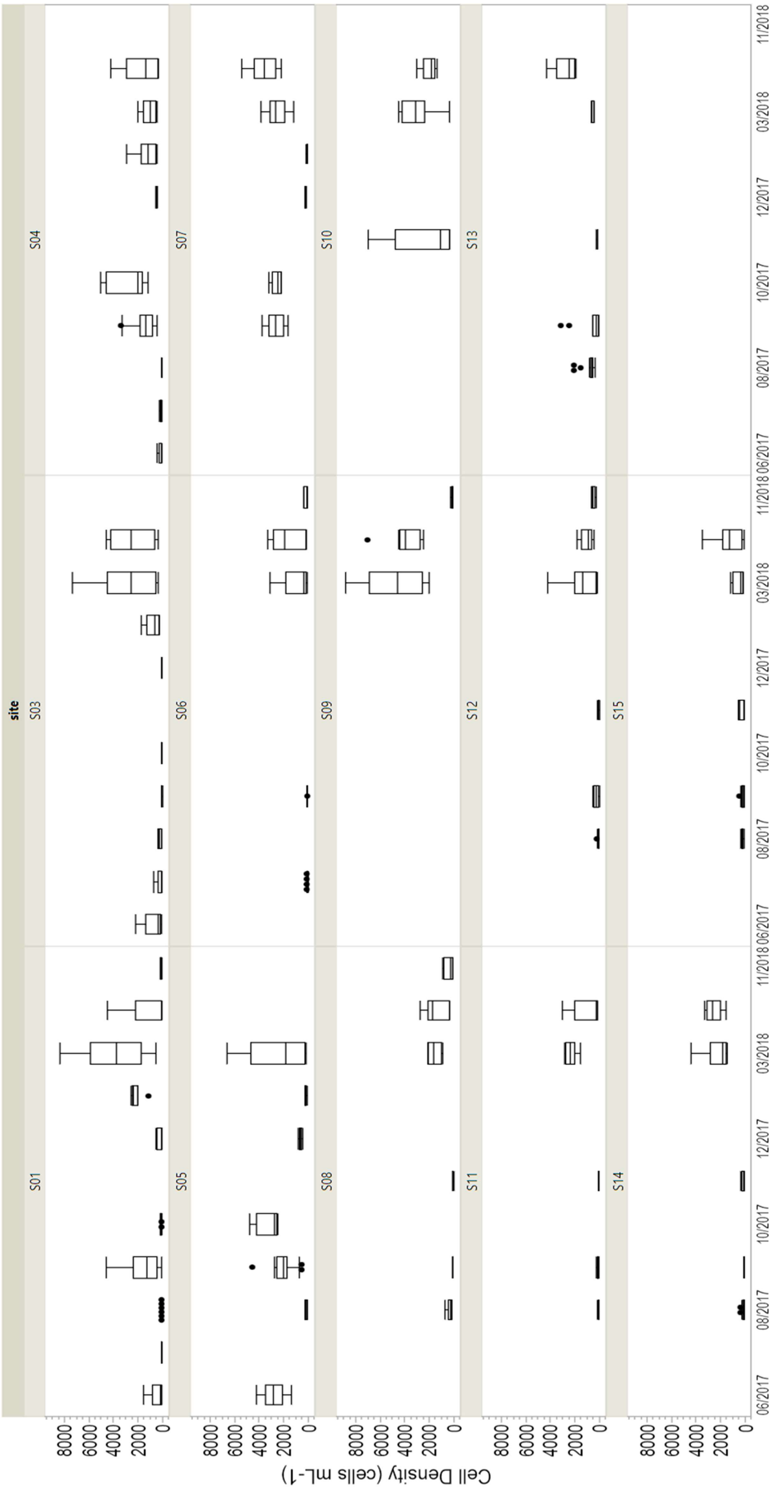

Figure A.1. Box plots (mean, 25th and 75th quartiles, and range) of dissolved oxygen, turbidity, water temperature, pH and river stage measurements for all sites sampled in 2017-2018 for each site.

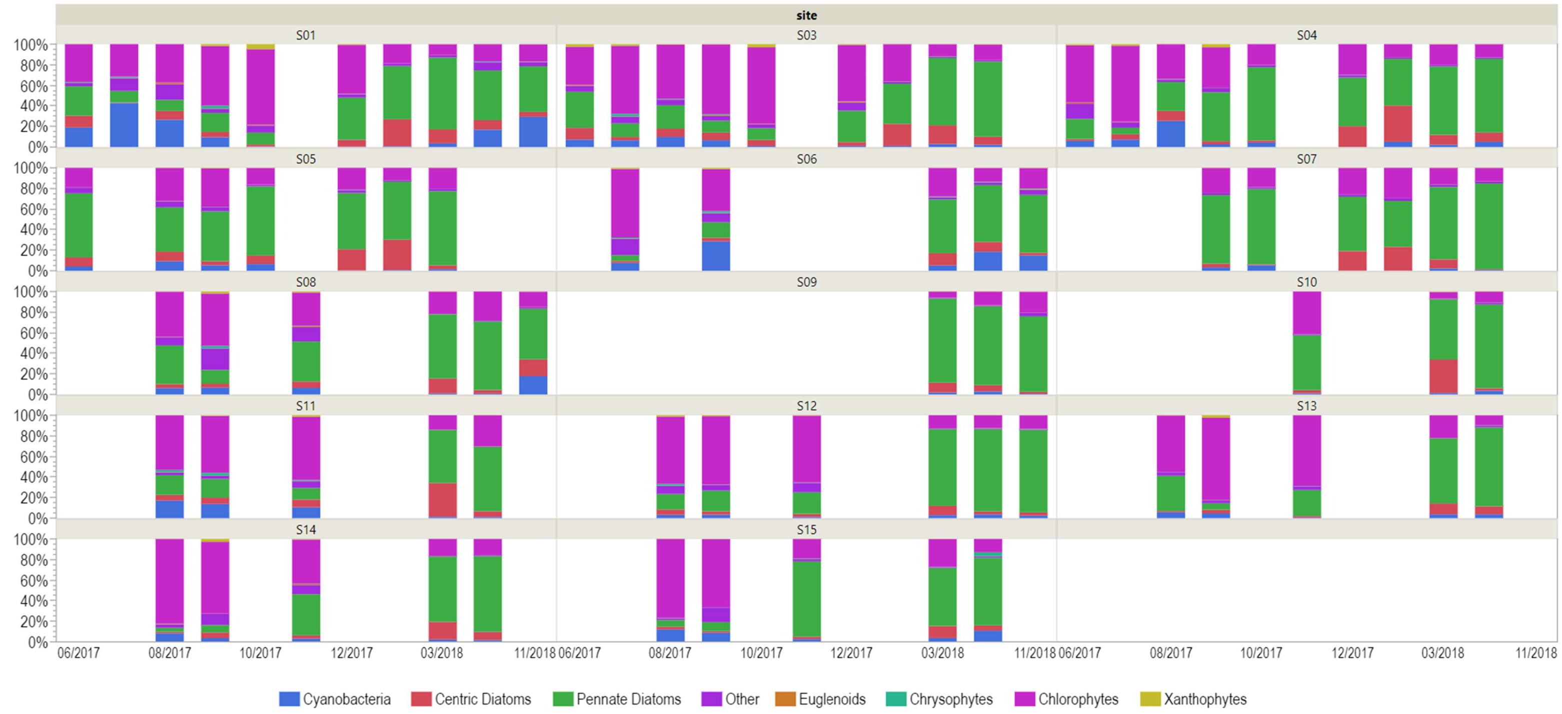

Figure A.2 Composition (percentage of total cell count) of periphyton assemblages by algal group during the 2017-2018 sampling period for all sites.

APPENDIX B. SUPLIMENTARY MATERIAL FOR CHAPTER III

Table B.1. General linear models from the ARB CCA for each algal group chrysophytes, centric diatoms, pennate diatoms, euglenoids, chlorophytes, cyanobacteria, xanthophytes.

Chrysophytes	Estimate	Std. Error	z value	Pr(>|z|)	
(Intercept)	-44.10	106.10	-0.42	0.68	
Date^1	-89.89	16.17	-5.56	<0.01	*
Date^2	-0.65	5.09	-0.13	0.90	
SiteS06	9.15	32.69	0.28	0.78	
SiteS08	14.36	59.49	0.24	0.81	
SiteS09	19.30	78.80	0.25	0.81	
SiteS12	-50.12	232.20	-0.22	0.83	
Distance	3.79	17.40	0.22	0.83	
DO	-1.32	0.21	-6.34	<0.01	*
pH	0.57	0.74	0.77	0.44	
Turbidity	0.03	0.02	1.97	0.05	*
Specific Conductance	51.65	8.50	6.08	<0.01	*
CFU	0.00	0.00	13.73	<0.01	*
Water Velocity	8.72	3.91	2.23	0.03	*
BOD	-0.05	0.11	-0.48	0.63	
Nitrate	-7.54	4.91	-1.54	0.12	
Nitrite	-35.36	27.01	-1.31	0.19	
Phosphorus	-0.44	1.07	-0.41	0.68	
Ammonium	27.36	4.32	6.34	<0.01	*
PC	0.28	0.05	5.37	<0.01	*
TC	0.18	0.18	1.01	0.31	
C:N	0.19	0.09	2.12	0.03	*
Centric Diatoms	Estimate	Std. Error	z value	Pr(>|z|)	
(Intercept)	1057.00	49.49	21.36	<0.01	*
Date^1	-143.20	2.41	-59.36	<0.01	*
Date^2	-61.92	0.87	-70.78	<0.01	*
SiteS06	-321.40	15.23	-21.10	<0.01	*
SiteS08	-585.50	27.72	-21.13	<0.01	*
SiteS09	-775.00	36.72	-21.11	<0.01	*
SiteS12	2263.00	108.20	20.92	<0.01	*
Distance	-170.10	8.11	-20.99	<0.01	*
DO	-0.11	0.03	-4.23	<0.01	*
pH	-6.25	0.22	-27.96	<0.01	*
Turbidity	0.09	0.00	25.16	<0.01	*
Specific Conductance	87.99	1.47	59.85	<0.01	*
CFU	0.00	0.00	105.76	<0.01	*

Water Velocity	-36.38	0.50	-73.50	<0.01	*
BOD	0.04	0.01	4.47	<0.01	*
Nitrate	2.33	0.66	3.54	<0.01	*
Nitrite	188.60	3.02	62.43	<0.01	*
Phosphorus	-3.34	0.18	-18.81	<0.01	*
Ammonium	-12.55	0.76	-16.50	<0.01	*
PC	0.26	0.00	53.43	<0.01	*
TC	2.65	0.03	98.60	<0.01	*
C:N	0.18	0.01	29.47	<0.01	*

Pennate Diatoms	Estimate	Std. Error	z value	Pr(>|z|)	
(Intercept)	118.20	5.48	21.55	<0.01	*
Date^1	55.35	0.64	86.78	<0.01	*
Date^2	11.64	0.18	64.98	<0.01	*
SiteS06	-26.38	1.69	-15.60	<0.01	*
SiteS08	-48.61	3.08	-15.80	<0.01	*
SiteS09	-63.52	4.08	-15.59	<0.01	*
SiteS12	184.40	12.01	15.36	<0.01	*
Distance	-13.88	0.90	-15.42	<0.01	*
DO	0.30	0.01	37.17	<0.01	*
pH	-2.43	0.04	-53.99	<0.01	*
Turbidity	-0.06	0.00	-68.07	<0.01	*
Specific Conductance	-33.60	0.33	-100.99	<0.01	*
CFU	0.00	0.00	50.00	<0.01	*
Water Velocity	-2.25	0.15	-14.92	<0.01	*
BOD	0.06	0.00	17.91	<0.01	*
Nitrate	13.81	0.19	74.20	<0.01	*
Nitrite	193.70	0.93	209.02	<0.01	*
Phosphorus	-8.65	0.05	-167.94	<0.01	*
Ammonium	-14.53	0.19	-77.27	<0.01	*
PC	-0.11	0.00	-67.02	<0.01	*
TC	1.57	0.01	203.27	<0.01	*
C:N	0.28	0.00	74.72	<0.01	*

Euglenoids	Estimate	Std. Error	z value	Pr(>|z|)	
(Intercept)	5706.00	317700.00	0.02	0.99	
Date^1	-91.66	24.07	-3.81	<0.01	*
Date^2	-7.68	4.04	-1.90	0.06	
SiteS06	-1763.00	97920.00	-0.02	0.99	
SiteS08	-3205.00	178100.00	-0.02	0.99	
SiteS09	-4248.00	235900.00	-0.02	0.99	
SiteS12	12500.00	694800.00	0.02	0.99	
Distance	-937.10	52080.00	-0.02	0.99	
DO	-0.61	0.24	-2.50	0.01	*
pH	-0.35	0.58	-0.59	0.55	
Turbidity	0.04	0.03	1.43	0.15	
Specific Conductance	55.91	12.50	4.47	<0.01	*
CFU	0.00	0.00	-2.60	<0.01	*

Water Velocity	-83.93	13.03	-6.44	<0.01	*
BOD	-0.59	0.15	-3.89	<0.01	*
Nitrate	-19.28	9.03	-2.14	0.03	*
Nitrite	-5.59	32.20	-0.17	0.86	
Phosphorus	-0.56	1.78	-0.31	0.75	
Ammonium	5.50	5.58	0.99	0.32	
PC	1.37	0.21	6.53	<0.01	*
TC	2.96	0.33	8.99	<0.01	*
C:N	-0.13	0.12	-1.11	0.27	

Chlorophytes	Estimate	Std. Error	z value	Pr(>|z|)	
(Intercept)	47.94	8.97	5.34	<0.01	*
Date[1]	17.52	0.71	24.82	<0.01	*
Date[2]	1.91	0.20	9.74	<0.01	*
SiteS06	-9.14	2.77	-3.30	<0.01	*
SiteS08	-16.77	5.04	-3.33	<0.01	*
SiteS09	-21.64	6.67	-3.24	<0.01	*
SiteS12	65.01	19.66	3.31	<0.01	*
Distance	-4.83	1.47	-3.28	<0.01	*
DO	-0.28	0.01	-31.91	<0.01	*
pH	-0.76	0.04	-20.43	<0.01	*
Turbidity	0.03	0.00	31.49	<0.01	*
Specific Conductance	-22.04	0.35	-62.87	<0.01	*
CFU	0.00	0.00	117.43	<0.01	*
Water Velocity	-5.22	0.21	-25.03	<0.01	*
BOD	-0.13	0.00	-39.40	<0.01	*
Nitrate	-4.91	0.24	-20.29	<0.01	*
Nitrite	77.11	1.03	74.81	<0.01	*
Phosphorus	-5.40	0.06	-93.63	<0.01	*
Ammonium	-6.94	0.19	-36.88	<0.01	*
PC	-0.04	0.00	-19.51	<0.01	*
TC	1.66	0.01	173.77	<0.01	*
C:N	0.29	0.00	66.49	<0.01	*

Cyanobacteria	Estimate	Std. Error	z value	Pr(>|z|)	
(Intercept)	39.35	6.46	6.09	<0.01	*
Date[1]	110.30	2.03	54.28	<0.01	*
Date[2]	7.95	0.43	18.42	<0.01	*
SiteS06	-5.08	1.97	-2.57	0.01	*
SiteS08	-8.96	3.59	-2.50	0.01	*
SiteS09	-11.90	4.76	-2.50	0.01	*
SiteS12	35.12	14.01	2.51	0.01	*
Distance	-2.60	1.05	-2.47	0.01	*
DO	0.51	0.03	20.07	<0.01	*
pH	-0.84	0.14	-6.03	<0.01	*
Turbidity	-0.09	0.00	-42.67	<0.01	*
Specific Conductance	-53.36	1.02	-52.33	<0.01	*
CFU	0.00	0.00	20.17	<0.01	*

Water Velocity	5.45	0.40	13.56	<0.01	*
BOD	-0.26	0.01	-23.58	<0.01	*
Nitrate	12.84	0.57	22.47	<0.01	*
Nitrite	248.70	2.23	111.71	<0.01	*
Phosphorus	-6.94	0.14	-49.69	<0.01	*
Ammonium	-0.94	0.47	-1.99	0.05	*
PC	-0.10	0.01	-19.39	<0.01	*
TC	1.31	0.01	91.26	<0.01	*
C:N	0.65	0.01	58.16	<0.01	*

Xanthophytes	Estimate	Std. Error	z value	Pr(>|z|)	
(Intercept)	-19.94	65.06	-0.31	0.76	
Date[1]	-4.08	12.58	-0.32	0.75	
Date[2]	22.83	4.90	4.66	<0.01	*
SiteS06	7.69	20.04	0.38	0.70	
SiteS08	9.85	36.45	0.27	0.79	
SiteS09	13.91	48.29	0.29	0.77	
SiteS12	-34.87	142.30	-0.25	0.81	
Distance	2.64	10.66	0.25	0.80	
DO	-0.79	0.16	-5.08	<0.01	*
pH	2.09	0.41	5.11	<0.01	*
Turbidity	0.09	0.02	4.08	<0.01	*
Specific Conductance	-12.57	6.72	-1.87	0.06	
CFU	0.00	0.00	-3.22	<0.01	*
Water Velocity	4.03	4.55	0.89	0.38	
BOD	0.34	0.09	3.73	<0.01	*
Nitrate	-13.63	5.54	-2.46	0.01	*
Nitrite	173.70	27.58	6.30	<0.01	*
Phosphorus	-12.33	1.61	-7.64	<0.01	*
Ammonium	-47.20	5.92	-7.97	<0.01	*
PC	-0.74	0.13	-5.72	<0.01	*
TC	3.76	0.31	12.10	<0.01	*
C:N	-0.82	0.12	-7.01	<0.01	*

Table B.2. General linear models from the LV CCA for each algal group chrysophytes, centric diatoms, pennate diatoms, euglenoids, chlorophytes, cyanobacteria, xanthophytes.

Chrysophytes	Estimate	Std. Error	z value	Pr(>|z|)	
(Intercept)	5.38	1.26	4.29	<0.01	*
Date^{1}	4.82	3.54	1.36	0.17	
Date^{2}	1.40	2.56	0.55	0.59	
SiteV02	0.13	0.26	0.48	0.63	
SiteV03	-1.37	0.32	-4.26	<0.01	*
SiteV04	-3.00	0.53	-5.70	<0.01	*
SiteV05	0.02	0.46	0.04	0.97	
Dissolved Oxygen	-0.06	0.10	-0.61	0.55	
pH	-0.59	0.11	-5.22	<0.01	*
Turbidity	-0.05	0.01	-3.49	<0.01	*
Specific Conductance	15.46	2.81	5.50	<0.01	*
CFU	0.00	0.00	-1.74	0.08	
Water Velocity	10.14	2.34	4.33	<0.01	*
BOD	0.08	0.03	2.55	0.01	*
Phosphorus	-3.13	0.70	-4.48	<0.01	*
Ammonium	1.69	1.30	1.30	0.19	
CHL	0.00	0.00	0.00	1.00	
TN	-13.92	3.19	-4.36	<0.01	*
TC	2.84	0.63	4.50	<0.01	*
Tree Cover	-0.53	0.13	-4.14	<0.01	*
Macrophyte	0.00	0.00	1.10	0.27	

Centric Diatoms	Estimate	Std. Error	z value	Pr(>|z|)	
(Intercept)	-1.96	0.57	-3.462	<0.01	*
Date^{1}	-1.96	0.97	-2.022	0.04	*
Date^{2}	-3.44	0.68	-5.052	<0.01	*
SiteV02	0.48	0.10	4.9	<0.01	*
SiteV03	-0.65	0.10	-6.609	<0.01	*
SiteV04	0.52	0.16	3.185	<0.01	*
SiteV05	-1.43	0.19	-7.615	<0.01	*
Dissolved Oxygen	0.17	0.03	5.187	<0.01	*
pH	0.45	0.06	7.463	<0.01	*
Turbidity	0.01	0.00	2.74	<0.01	*
Specific Conductance	-4.35	1.01	-4.292	<0.01	*
CFU	0.00	0.00	-2.52	0.01	*
Water Velocity	7.11	0.86	8.236	<0.01	*
BOD	-0.33	0.01	-30.581	<0.01	*
Phosphorus	1.17	0.18	6.526	<0.01	*
Ammonium	-0.72	0.41	-1.76	0.08	
CHL	0.00	0.00	-1.875	0.06	
TN	-15.65	1.04	-15.122	<0.01	*

TC	4.13	0.21	19.902	<0.01	*
Tree Cover	0.73	0.04	18.211	<0.01	*
Macrophyte	0.00	0.00	-4.851	<0.01	*

Pennate Diatoms	Estimate	Std. Error	z value	Pr(>|z|)	
(Intercept)	6.81	0.10	67.088	<0.01	*
Date^1	0.07	0.20	0.331	0.74	
Date^2	-1.43	0.13	-11.096	<0.01	*
SiteV02	0.41	0.02	17.469	<0.01	*
SiteV03	1.03	0.02	46.818	<0.01	*
SiteV04	-0.59	0.04	-14.081	<0.01	*
SiteV05	0.56	0.03	19.345	<0.01	*
Dissolved Oxygen	0.18	0.01	24.912	<0.01	*
pH	-0.12	0.01	-11.286	<0.01	*
Turbidity	-0.01	0.00	-21.234	<0.01	*
Specific Conductance	-8.53	0.17	-49.079	<0.01	*
CFU	0.00	0.00	-16.579	<0.01	*
Water Velocity	-5.79	0.16	-36.772	<0.01	*
BOD	-0.11	0.00	-66.332	<0.01	*
Phosphorus	1.13	0.04	28.692	<0.01	*
Ammonium	-0.56	0.09	-6.138	<0.01	*
CHL	0.00	0.00	43.505	<0.01	*
TN	-16.14	0.22	-72.089	<0.01	*
TC	3.48	0.05	74.028	<0.01	*
Tree Cover	0.31	0.01	51.158	<0.01	*
Macrophyte	-0.02	0.00	-78.497	<0.01	*

Euglenoids	Estimate	Std. Error	z value	Pr(>|z|)	
(Intercept)	7.59	1.31	5.793	<0.01	*
Date^1	5.70	2.77	2.053	0.04	*
Date^2	0.28	2.17	0.127	0.90	
SiteV02	-1.37	0.27	-5.069	<0.01	*
SiteV03	-1.69	0.29	-5.88	<0.01	*
SiteV04	-2.26	0.44	-5.093	<0.01	*
SiteV05	-1.76	0.60	-2.951	<0.01	*
Dissolved Oxygen	-0.18	0.08	-2.093	0.04	*
pH	-0.04	0.12	-0.353	0.72	
Turbidity	-0.04	0.01	-3.204	<0.01	*
Specific Conductance	-14.32	4.05	-3.535	<0.01	*
CFU	0.00	0.00	0.991	0.32	
Water Velocity	4.00	2.66	1.505	0.13	
BOD	0.04	0.03	1.301	0.19	
Phosphorus	-0.46	0.45	-1.03	0.30	
Ammonium	2.54	1.40	1.819	0.07	
CHL	0.00	0.00	8.691	<0.01	*
TN	-13.08	2.66	-4.915	<0.01	*
TC	2.92	0.55	5.279	<0.01	*
Tree Cover	-0.67	0.11	-6.273	<0.01	*

Macrophyte	0.00	0.00	-1.869	0.06	
Chlorophytes	Estimate	Std. Error	z value	Pr(>|z|)	
(Intercept)	4.46	0.09	52.248	<0.01	*
Date^1	6.10	0.19	32.26	<0.01	*
Date^2	-6.43	0.13	-48.813	<0.01	*
SiteV02	0.99	0.02	51.326	<0.01	*
SiteV03	0.60	0.02	29.47	<0.01	*
SiteV04	1.03	0.03	30.783	<0.01	*
SiteV05	0.55	0.03	20.368	<0.01	*
Dissolved Oxygen	0.08	0.01	11.888	<0.01	*
pH	0.07	0.01	7.15	<0.01	*
Turbidity	-0.02	0.00	-35.018	<0.01	*
Specific Conductance	-0.37	0.16	-2.342	0.02	*
CFU	0.00	0.00	19.532	<0.01	*
Water Velocity	2.28	0.12	18.93	<0.01	*
BOD	-0.06	0.00	-34.402	<0.01	*
Phosphorus	1.53	0.03	50.663	<0.01	*
Ammonium	-2.29	0.07	-32.023	<0.01	*
CHL	0.00	0.00	7.359	<0.01	*
TN	-2.63	0.17	-15.73	<0.01	*
TC	0.70	0.03	20.175	<0.01	*
Tree Cover	0.06	0.01	9.724	<0.01	*
Macrophyte	-0.01	0.00	-66.007	<0.01	*
Cyanobacteria	Estimate	Std. Error	z value	Pr(>|z|)	
(Intercept)	3.75	0.16	22.927	<0.01	*
Date^1	15.90	0.58	27.233	<0.01	*
Date^2	-18.11	0.40	-45.258	<0.01	*
SiteV02	0.87	0.04	22.215	<0.01	*
SiteV03	0.79	0.05	16.752	<0.01	*
SiteV04	0.44	0.07	6.285	<0.01	*
SiteV05	1.45	0.06	24.006	<0.01	*
Dissolved Oxygen	-0.16	0.02	-10.344	<0.01	*
pH	0.22	0.02	10.258	<0.01	*
Turbidity	0.03	0.00	19.166	<0.01	*
Specific Conductance	-1.94	0.30	-6.411	<0.01	*
CFU	0.00	0.00	16.125	<0.01	*
Water Velocity	2.38	0.22	10.848	<0.01	*
BOD	-0.10	0.00	-23.463	<0.01	*
Phosphorus	-0.76	0.07	-11.506	<0.01	*
Ammonium	-3.07	0.15	-21.045	<0.01	*
CHL	0.00	0.00	-1.093	0.27	
TN	-0.86	0.28	-3.071	<0.01	*
TC	0.58	0.06	9.722	<0.01	*
Tree Cover	0.00	0.01	-0.107	0.91	
Macrophyte	-0.01	0.00	-22.123	<0.01	*
Xanthophytes	Estimate	Std. Error	z value	Pr(>|z|)	

(Intercept)	0.84	0.97	0.866	0.39	
Date^{1}	14.77	2.96	4.996	<0.01	*
Date^{2}	0.72	1.89	0.381	0.70	
SiteV02	-0.53	0.27	-1.924	0.05	*
SiteV03	0.44	0.27	1.632	0.10	
SiteV04	2.13	0.49	4.347	<0.01	*
SiteV05	1.21	0.36	3.376	<0.01	*
Dissolved Oxygen	0.69	0.10	6.72	<0.01	*
pH	-0.18	0.11	-1.587	0.11	
Turbidity	-0.05	0.01	-6.422	<0.01	*
Specific Conductance	-24.57	3.08	-7.988	<0.01	*
CFU	0.00	0.00	12.594	<0.01	*
Water Velocity	-3.87	1.42	-2.728	<0.01	*
BOD	-0.07	0.02	-2.786	<0.01	*
Phosphorus	3.25	0.53	6.152	<0.01	*
Ammonium	1.10	0.81	1.359	0.17	
CHL	0.00	0.00	5.641	<0.01	*
TN	6.12	1.98	3.089	<0.01	*
TC	0.22	0.42	0.517	0.61	
Tree Cover	0.14	0.09	1.58	0.11	
Macrophyte	0.00	0.00	1.991	0.05	*

REFERENCES

Abedi, E. and M. A. Sahari. 2014. Long-chain polyunsaturated fatty acid sources and evaluation of their nutritional and functional properties. Food Science and Nutrition 2:443-463.

Adame, K. L., B. Dunck, and L. Rodrigues. 2018. Periphytic algal community in lentic environments of the Upper Parana River floodplain: seasonal and spatial variation. Acta Limnologica Brasiliensia 30.e205.

Adame, M. F., N. E. Pettit, D. Valdez, D. Ward, M. A. Burford, and S. E. Bunn. 2017. The contribution of epiphyton to the primary production of tropical floodplain wetlands. Biotrophica 49:461-471.

Agostinho, A. A., F. M. Pelicice, and L. C. Gomes. 2008. Dams and fish fauna of the Neotropical region: impacts and management related to diversity and fisheries. Brazilian Journal of Biology 68:1119-1132.

Agostinho, A. A., L. C. Gomes, S. Verissimo, and E. K. Okada. 2004. Flood regime, dam regulation and fish in the Upper Parana River: effects on assemblage attributes, reproduction and recruitment. Reviews in Fish Biology and Fisheries 14:11-19.

Ahearn, D. S., J. H. Viers, J. F. Mount, and R. A. Dahlgren. 2006. Priming the productivity pump: flood pulse driven trends in suspended algal biomass distribution across a restored floodplain. Freshwater Biology 51:1417-1433.

Ahn, C., D. M. Johnston, R. E. Sparks, and D. C. White. 2006. Analysis of naturalization alternatives for the recovery of moist-soil plants in the floodplain of the Illinois River. Hydrobiologia 565:217-228.

Alford, J. B. and M. R. Walker. 2013. Managing the flood pulse for optimal fisheries production in the Atchafalaya River Basin, Louisiana (USA). River Research and Application 29:279-296.

Algarte, V. M., B. Dunck, J. A. Leandrini, and L. Rodrigues. 2016. Periphytic diatom ecological guilds in floodplain: Ten years after dam. Ecological Indicators 69:407-414.

Algarte, V. M., N. S. Siqueira, E. A. Murakami, and L. Rodrigues. 2009. Effects of hydrological regime and connectivity on the interannual variation in taxonomic similarity of periphytic algae. Brazilian Journal of Biology 69:609-616.

Allan, J. D., M. M. Castillo, and K. A. Capps. 2007. Stream Ecology: structure and function of running water, 2nd Ed. Springer Nature, Cham, Switzerland.

Allen, Y. C., G. C. Constant, and B. R. Couvillion. 2008. Preliminary classification of water areas within the Atchafalaya Basin Floodway system by using Landsat imagery. U.S. Geological Survey Open-File Report 1320:1-21.

Almeida, A. S., A. M. Goncalves, J. L. Pereira, and F. Goncalves. 2006. The impacts of Eichhornia crassipes on green algae and cladocerans. Fresenius Environmental Bulletin 15:1531-1538.

AMHA. American Public Health Association. 2018. Standard methods for the examination of water and wastewater, 20th ed. Am. Publ. Hlth. Ass., New York.

Andersen, I. M., T. J. Williamson, M. J. Gonzalez, and M. J. Vanni. 2020. Nitrate, ammonium, and phosphorus drive seasonal nutrient limitation of chlorophytes, cyanobacteria, and diatoms in a hyper-eutrophic reservoir. Limnology and Oceanography 65:962-978.

Andersen, R. A. 2005. Algal culturing techniques. Elsevier Academic Press, Burlington, MA.

APHA. American Public Health Association. 2018. Standard methods for the examination of water and wastewater, 20th ed. American Public Health Association, New York.

Bates, D., M. Maechler, B. Bolker, R. H. B. Christensen, H. Singmann, B. Dai, F. Scheipl, and G. Grothenkieck. “Package ‘lme4’.” Linear mixed-effects modeling using S4 classes. R package version 1.6.

Battin, T. J., K. Besemer, M. M. Bengtsson, A. M. Romani, and A. I. Packmann. 2016. Nature Reviews Microbiology 14:251.

Battin, T.J., K. Besemer, M. M. Bengtsson, A. M. Romani, and A. I. Packmann. 2016. The ecology and biogeochemistry of stream biofilms. Nature Reviews Microbiology 14:251-263.

Battle, J. M., and T. B. Mihuc. 2000. Decomposition dynamics of aquatic macrophytes in the lower Atchafalaya, a large floodplain river. Hydrobiologia 418:123-136.

Batzer, D. P., G. B. Noe, L. Lee, and M. Galatowitsch. 2018. A floodplain continuum for Atlantic Coast Rivers of the Southeastern US: Predictable changes in floodplain biota along a river’s length. Wetlands 38:1-13.

Baustian, J. J., B. P. Piazza, and J. F. Bergan. 2019. Hydrologic connectivity and backswamp water quality during a flood in the Atchafalaya Basin, USA. River Research and Applications 35:430-435.

Bayley, P. B., L. Castello, V. S. Batista, and N. N. Fabre. 2018. Response of

Prochilodus nigricans to flood pulse variation in the central Amazon. Royal Society open science 5:172232.

Beaulieu, M., F. Pick, and I. Gregory-Eaves. 2013. Nutrients and water temperature are significant predictors of cyanobacterial biomass in a 1147 lakes data set. Limnological Oceanography 58:1736-1746.

Beisner, B. E., P. R. Peres-Neto, E. S. Lindstrom, A. Barnett, and M. L. Longhi. 2006. The role of environmental and spatial processes in structuring lake communities from bacteria to fish. Ecology 87:2985-2991.

Bellinger, E. G. and D. C. Sigee. 2015. Freshwater Algae: Identification, enumeration, and use as bioindicators. Wiley-Blackwell, Hoboken, NJ.

Biggs, B. J. F. and H. A. Thomsen. 1995. Disturbance of stream periphyton by perturbations in shear stress: time to structural failure and differences in community resistance. Journal of Phycology 31:233-241.

Bondar-Kunze, E., S. Maier, D. Schonauer, N. Bahl, and T. Hein. 2016. Antagonistic and synergistic effects on a stream periphyton community under the influence of pulsed flow velocity increase and nutrient enrichment. Science of the Total Environment 573:594-602.

Bonvillian, C. P., D. A. Rutherford, W. E. Kelso, and C. E. Murphy. 2013. Biotic and abiotic influences on population characteristics of *Procambarus clarkia* in the Atchafalaya River Basin, Louisiana. Freshwater Crayfish 19:125-136.

Borics, G., B. Tothmeresz, I. Grigorszky, J. Padisak, G. Varbiro, and S. Szabo. 2003. Algal assemblage types of bog-lakes in Hungary and their relation to water chemistry, hydrological conditions and habitat diversity. Hydrobiologia 502:145-155.

Bortolini, J. C., S. Train, and L. C. Rodrigues. 2016. Extreme hydrological periods: effects on phytoplankton variability and persistence in a subtropical floodplain. Hydrobiologia 763:223-236.

Bottino, F., S. R. Vargas, A. C. P. Miwa, M. D. C. Calijuri, I. Bianchini Jr. D. G. F. Cunha. 2018. Effects of macrophyte leachate on *Anabaena* sp. And *Chlamydomonas moewusii* growth in freshwater tropical ecosystems. Limnology 16:171-176.

Brett, M. T., M. J. Kainz, S. J. Taipale, and H. Seshan. 2009. Phytoplankton, not allochthonous carbon, sustains herbivorous zooplankton production. Proceedings of the National Academy of Sciences 106:21197-21201.

Brinson, M. M. and A. I. Malvarez. 2002. Temperate freshwater wetlands: types, statues, and threats. Environmental Conservation 29:115-133.

Bryan, D. F., F. M. Truesdale, and D. S. Sabins. 1975. A limnological survey of the Atchafalaya Basin, annual report. Louisiana Coop. Fish. Res. Unit, Baton Rouge.

BryantMason, A., Y. J. Xu, and M. A. Altabet. 2013. Limited capacity of river corridor wetlands to remove nitrate: A case study on the Atchafalaya River Basin during the 2011 Mississippi River Flooding. Water Resources Research 49:283-290.

Calapez, A. R., C. L. Elias, S. F. P. Almeida, A. G. Brito, and M. J. Feio. 2019. Sewage contamination under water scarcity effects on stream biota: biofilm, grazers, and their interaction. Environmental Science and Pollution Research 26:26636-26645.

Campos-Silva, J. V., C. A. Peres, J. H. F. Amaral, H. Sarmento, B. Forsberg, and C. R. Fonseca. 2020. Fisheries management influences phytoplankton biomass of Amazonian floodplain lakes. Journal of Applied Ecology 58:731-743.

Cao, Y., N. Zhang, J. Sun, and W. Li. 2018. Responses of periphyton on non-plant substrates to different macrophytes under various nitrogen concentrations: A mesocosm study. Aquatic Botany 154:53-59.

Cao, Y., S. Olsen, M. F. Gutierrez, S. Brucet, T. H. Davidson, W. Li, T. L. Lauridsen, M. Sondergaard, and E. Jeppsen. 2017. Temperature effects on periphyton, epiphyton and epipelon under a nitrogen pulse in low-nutrient experimental freshwater lakes. Hydrobiologia 795:267-279.

Caraco, N. F. and J. J. Cole. 2002. Contrasting impacts of native and alien macrophyte on dissolved oxygen in a large river. Ecological Applications 12:1496-1509.

Carmichael, W. W. 2001. Health effects of toxin-producing cyanobacteria: “The CyanoHABs.” Human and Ecological Risk Assessment 7:1393-1407.

Cashman, M. J., J. D. Wehr, and K. Truhn. 2013. Elevated light and nutrients and alter the nutritional quality of stream periphyton. Freshwater Biology 58:1447-1457.

Cazzanelli, M. M. Soria-Barreto, M. M. Castillo, and R. Rodiles-Hernandez. 2021. Seasonal variations in food web dynamics of floodplain lakes with contrasting hydrological connectivity in the Southern Gulf of Mexico. Hydrobiologia 848:773-797.

Chakdar, J. and S. Pabbi. 2016. Cyanobactrial phycobilins: production, purification, and regulation. Pages 45-69 in P. Shukla, editor. Frontier Discoveries and Innovations in Interdisciplinary Microbiology. Springer, New Delhi.

Chan, T. U., and D. P. Hamilton. 2001. Effects of freshwater flow on the succession and biomass of phytoplankton in a seasonal estuary. Marine and Freshwater Research 52:869-84.

Chaparro, G., M. C. Marinone, R. J. Lombardo, M. R. Schiaffino, A. de Souza Guimaraes, and I. O'Farrel. 2011. Zooplankton succession during extraordinary drought-flood cycles: a case study in a South American floodplain lake. Limnologica 41:371-381.

Chessman, B. C., D. P. Westhorpe, S. M. Mitrovic, and L. Hardwick. 2009. Trophic linkages between periphyton and grazing macroinvertebrates in rivers with different levels of catchment development. Hydrobiologia 625:135-150.

Chetelat, J., F. R. Pick, and P. B. Hamilton. 2006. Potamoplankton size structure and taxonomic composition: influence of river size and nutrient concentrations. Limnology and Oceanography 51:681-689.

Clementson, L. A, A. J. Richardson, W. A. Rochester, K. Oubelkheir, B. Liu, E. J. D'Sa, L. F. M. Gusmao, P. Ajani, T. Schroeder, P. W. Ford, M. A. Burford, E. Saeck, and A. D. L. Steven. 2021. Effect of a once in 100-year flood on a subtropical coastal phytoplankton community. Frontiers in Marine Science 8:580516.

Colon-Gaud, J., W. E. Kelso, and D. A. Rutherford. 2004. Spatial distribution of macroinvertebrates inhabiting hydrilla and coontail beds in the Atchafalaya Basin, Louisiana. Journal of Aquatic Plant Management 42:85-91.

Cook, P. L. M., D. P. Holland, and A. R. Longmore. 2010. Effect of a flood event on the dynamics of phytoplankton and biogeochemistry in a large temperate Australian lagoon. Limnology and Oceanography 55:1123-1133.

Costa, A. P. T., L. O. Crossetti, S. M. Hartz, F. G. Becker, L. U. Hepp, J. E. Bohnenberger, M. S. Lima, T. Guimaraes, and F. Schneck. 2020. Land cover is the main correlate of phytoplankton beta diversity in subtropical coastal shallow lakes. Aquatic Ecology 54:1015-1025.

Costanza, R., R. D. Groot, P. Sutton, S. V. D. Ploeg, S. J. Anderson, I. Kubiszewski, S. Farber, and R. K. Turner. 2014. Changes in the global values of ecosystem services. Global Environmental Change 26:152-158.

Crook, D. A., D. J. Buckle, J. R. Morrongiello, Q. A. Allsop, W. Baldwin, T. M. Saunders, and M. M. Douglas. 2019. Tracking the resources pulse: Movement responses of fish to dynamic floodplain habitat in a tropical river. Journal of Animal Ecology 89:795-807.

D'Sa, E. J., I. D. Joshi, B. Liu, D. S. Ko, C. L. Osburn, and T. S. Bianchi. 2019.

Biogeochemical response of Apalachicola Bay and the shelf waters to Hurricane Michael using ocean color semi-analytic/inversion and hydrodynamic models. Frontiers in Marine Science 6:523.

Dai, G., J. Shang, and B. Qiu. 2012. Ammonia may play an important role in the succession of cyanobacterial blooms and the distribution of common algal species in shallow freshwater lakes. Global Change Biology 18:1571-1581.

Dalu, T., P. W. Froneman, L. D. Chari, and N. B. Richoux. 2014. Colonisation and community structure of benthic diatoms on artificial substrates following a major flood event. A case of the Kowie River (Eastern Cape, South Africa). Water SA 40:471-480.

Davies, G. M. and A. Gray. 2015. Don’t let spurious accusations of pseudoreplication limit our ability to learn from natural experiments (and other messy kinds of ecological monitoring). Ecology and Evolution 5:5295-5304.

Davies, P. M., S. E. Bunn, and S. K. Hamilton. 2008. Primary production in tropical streams and rivers. Pages 23-42 in D. Dudgeon, editor. Tropical Stream Ecology. Academic Press, Amsterdam.

Death, R. G. 2002. Predicting invertebrate diversity from disturbance regimes in forest streams. Oikos 97:18-30.

Devlin, M. J., L. W. McKinna, J. G. Alvarez-Romero, C. Petus, B. Abott, P. Harkness, and J. Brodie. 2012. Mapping the pollutants in surface riverine flood plume waters in the Great Barrier Reef, Australia. Marine Pollution Bulletin 65: 224–235.

do Nascimento Filho, S. L. and A. do Nascimento Moura. 2021. Strong top-down effects of omnivorous fish and macroinvertebrates on periphytic algae and macrophytes in a tropical reservoir. Aquatic Ecology 55:667-680.

do Nascimento Filho, S. L., W. A. Gama, and A. do Nascimento Moura. 2021. Effects of the structural complexity of aquatic macrophytes on epiphytic algal, macroinvertebrates, and their interspecific relationships. Aquatic Sciences 83:1-14.

Dodds, W. K. and B. J. Biggs. 2002. Water velocity attenuation by stream periphyton and macrophytes in relation to growth form and architecture. Journal of the North American Benthological Society 21:2-15.

Dodds, W. K. and E. B. Welch. 2000. Establishing nutrient criteria in streams. Journal of the North American Benthological Society 19:186-196.

Doi, H. 2008. Spatial patterns of autochthonous and allochthonous resources in aquatic food webs. Population Ecology 51:57-64.

Dokulil, M. T. and J. Padisak. 1994. Long-term compositional response of phytoplankton in shallow, turbid environment, Neusiedlersee (Austria/Hungary). Hydrobiologia 276:125-137.

Dudgeon, D. 1992. Endangered ecosystems: a review of the conservation status of tropical Asian rivers. Hydrobiologia 248:167-191.

Dunck, B., J. C. Bortolini, L. Rodrigues, L. C. Rodrigues, S. Jati, and S. Train. 2013. Functional diversity and adaptive strategies of planktonic and periphytic algae in isolated tropical floodplain lakes. Brazilian Journal of Botany 36:257-266.

Eckert, R. A. 2020. Leaf-associated periphyton in heterotrophic streams: effect on macroinvertebrate assemblages and growth. Dissertation. University of Maryland, College Park, MD.

Emb, N., F. Guo, M. T. Brett, S. E. Bunn, M. J. Kainz. 2021. Polyunsaturated fatty acids in fish tissues more closely resemble algal than terrestrial diet sources. Hydrobiologia 848:371-383.

Feminella, J. W. and V. H. Resh. 1991. Herbivorous caddisflies, macroalgae, and epilithc microalgae: dynamic interactions in a stream grazing system. Oecologia 87:247-256.

Fernandes, R., A. A. Agostinho, E. A. Ferreira, C. S. Pavanelli, H. I. Suzuki, D. P. Lima, and L. C. Gomes. 2009. Effects of hydrological regime on the ichthyofauna of riverine environments of the Upper Parana River floodplain. Brazilian Journal of Biology 69:669-680.

Fernandes, U. L., E. C. C. de Oliverira, and S. R. Lacerda. 2016. Role of macrophyte life forms in driving periphytic microalgae assemblages in a Brazilian reservoir. Journal of Limnology 75:44-51.

Findlay, D. L., M. J. Paterson, L. L. Hendzel, and H. J. King. 2005. Factors influencing *Gonyostomum semen* blooms in a small boreal reservoir lake. Hydrobiologia 533:243-252.

Finkel, Z. V., A. J. Irwin, and O. Schofield. 2004. Resource limitation alters the ¾ size scaling of metabolic rates in phytoplankton. Marine Ecology Progress Series 273:269-279.

Finkel, Z. V., J. Beardall, K. J. Flynn, A. Quigg, T. A. V. Rees, and J. A. Raven. 2010. Phytoplankton in a changing world: cell size and elemental stoichiometry. Journal of Plankton Research 32:119-137.

Finlay, B. J., E. B. Monaghan, and S. C. Maberly. 2002. Hypothesis: The rate of scale of dispersal of freshwater diatom species is a function of their global abundance. Protist 153:261-273.

Fisher, J. C., W. E. Kelso, and D. A. Rutherford. 2012. Macrophyte mediated predation on hydrilla-dwelling macroinvertebrates. Fundamental Applied Limnology 181:25-38.

Flemming, H. C. 1993. Biofilms and environmental protection. Water Science and Technology 27:1-10.

Fontenot, Q. C., D. A. Rutherford, and W. E. Kelso. 2001. Effects of environmental hypoxia associated with the annual flood pulse on the distribution of larval sunfish and shad in the Atchafalaya River Basin, Louisiana. Transactions of the American Fisheries Society 130:107-116.

Ford, M. and J. A. Nyman. 2011. Preface: an overview of the Atchafalaya River. Hydrobiologia 658:1-5.

Foundation for Statistical Computing, Vienna, Austria. URL https://www.R-project.org/. Franca, R. C. S, M. R. M. Lopes, and C. Ferragut. 2011. Structural and successional variability of periphytic algal community in a Amazonian lake during the dry and rainy season (Rio Branco, Acre). Acta Amazonica 41:257-266.

Francoeur, S. N. and B. J. F. Biggs. 2006. Short-term effects of elevated velocity and sediment abrasion on benthic algal communities. Hydrobiologia 56:59-69.

Fuller, R. L., S. Doyle, L. Levy, J. Owens, E. Shope, L. Vo, E. Wolyniak, M. J. Small, and M. W. Doyle. 2011. Impact of regulated releases on periphyton and macroinvertebrate communities: the dynamic relationship between hydrology and geomorphology in frequently flooded rivers. River Research and Applications 27:630-645.

Gabyshev, V. A. and O. I. Gabysheva. 2010. Water quality of the Anabar River indicated by phytoplankton structure and hydrochemical characteristics. Contemporary Problems of Ecology 3:395-400.

Gargas, E., I. Hare, P. Martens, and L. Edler. 1979. Diel changes in phytoplankton photosynthetic efficiency in brackish waters. Marine Biology 52:113-122.

Gillett, N. D., Y. Pan, J. E. Asarian, and J. Kann. 2016. Spatial and temporal variability of river periphyton below a hypereutrophic lake and series of dams. Science of the Total Environment 541:1382-1392.

Gomes, L. C. and A. A. Agostinho. 1997. Influence of the flooding regime on the nutritional state and juvenile recruitment of the curimba, *Prochilodus scrofa*, Steindachner, in upper Parana River, Brazil. Fisheries Management and Ecology 4:263-274.

Gottlieb, A. D., J. Richards, and E. Gaiser. 2005. Effects of desiccation duration on the community structure and nutrient retention of short and long-hydroperiod Everglades periphyton mats. Aquatic Botany 82:99-112.

Graca, M. A. S., M. Callisto, J. E. L. Barbosa, K. R. Firmiano, J. Franca, and J. F. Goncalves, Jr. 2018.Top-down and bottom-up control of epilithic periphyton in a tropical stream. Freshwater Science 37:857-869.

Guo, F., M. J. Kainz, F. Sheldon, and S. E. Bunn. 2016. Effects of light and nutrients on periphyton and the fatty acid composition and somatic growth of invertebrate grazers in subtropical streams. Oecologia 181:449-462.

Guo, F., S. E. Bunn, M. T. Brett, B. Fry, H. Hager, X. Ouyang, M. J. Kainz. 2018. Feeding strategies for the acquisition of high-quality food sources in stream macroinvertebrates: Collecting, integrating, and mixed feeding. Limnology and Oceanography 63:1964-1978.

Guo, F., S. E. Bunn, M. T. Brett, H. Hager, M. J. Kainz. 2021. The dark side of rocks: an underestimated high-quality food source in river ecosystems. Journal of Ecology 109:2395-2404.

Hart, D. D., B. J. F Biggs, V. I. Nikora, and C. A. Flinders. 2013. Flow effects on periphyton patches and their ecological consequences in a New Zealand river. Freshwater Biology 58:1588-1602.

Hay, M. B., N. Michelutti, and J. P. Smol. 2000. Ecological patterns of diatom assemblages from Mackenzie Delta lakes, Northwest Territories, Canada. Canadian Journal of Botany 78: 19-33.

Hern, S. C. 1978. Distribution and importance of phytoplankton in the Atchafalaya Basin. Environmental Protection Agency. Office of Research and Development. Environmental Monitoring and Support Laboratory.

Hill, W. R., J. Rinchard, and S. Czesny. 2011. Light, nutrients, and the fatty acid composition of stream periphyton. Freshwater Biology 56:1825-1836.

Hillebrand, H. 2003. Opposing effects of grazing and nutrients on diversity. OIKOS 100:592-600.

Hillebrand, H. and U. Sommer. 1999. The nutrient stoichiometry of benthic microalgae growth: Redfield proportions are optimal. Limnology and Oceanography 44:440-446.

Hintz, W. D. and T. Wellnitz. 2013. Current velocity influences the facilitation and removal of algae by stream grazers. Aquatic Ecology 47:235-244.

Hirabayashi, Y., K. Shinjiro, S. Emori, T. Oki, and M. Kimoto. 2010. Global projections of changing risks of floods and droughts in a changing climate. Hydrological Sciences Journal 53:754-772.

Holmes, N. T. H. and B. A. Whitton. 1977. The macrophytic vegetation of the River Tees in 1975: observed and predicted changes. Freshwater Biology 7:43-60.

Hosseini, S. M. and A. G. van der Valk. 1989. The impact of prolonged, above-normal flooding on metaphyton in a freshwater marsh. Iowa State University, Ames, IA.

Hoyle, G. M., C. Holderman, P. J. Anders, B. Shaffi, and K. I. Ashley. 2014. Water quality, chlorophyll, and periphyton responses to nutrient addition in the Kootenai River, Idaho. The Society for Freshwater Science 33:1024-1029.

Hupp, C. R., C. R. Dema, D. E. Kroes, R. H. Day, and T. W. Doyle. 2008. Recent sedimentation patterns within the central Atchafalaya Basin, Louisiana. Wetlands 28:125-140.

Hupp, C. R., D. E. Kroes, G. B. Noe, E. R. Schenk, and R. H. Day. 2019. Sediment trapping and carbon sequestration in floodplains of the lower Atchafalaya Basin, LA: allochthonous versus autochthonous carbon sources. Journal of Geophysical Research: Biogeosciences 124:663-677.

Hurlbert, S. H. 1984. Pseudoreplication and the design of ecological field experiments. Ecological Monographs 54:187-211.

Izagirre, O. and A. Elosegi. 2005. Environmental control of seasonal and inter-annual variations of periphytic biomass in a North Iberian stream. International Journal of Limnology 41:35-46.

Janac, M., M. Ondrackova, P. Jurajda, Z. Valova, and M. Reichard. 2010. Flood duration determines the reproduction success of fish in artificial oxbows in a floodplain of a potamal river. Ecology of Freshwater Fish 19:644-655.

Jardine, T. D., N. E. Pettit, D. M. Warfe, B. J. Pusey, D. P. Ward, M. M. Douglas, P. M. Davies, and S. E. Bunn. 2012. Consumer-resource coupling in wet-dry tropical rivers. Journal of Animal Ecology 81:310-322.

Jardine, T. D., N. R. Bond, M. A. Burford, M. J. Kennard, D. P. Ward, P. Bayliss, P. M. Davies, M. M. Douglas, S. K. Hamilton, J. M. Melack, R. J. Naiman, N. E. Pettit, B. J. Pusey, D. M. Warfe, and S. E. Bunn. 2015. Does flood rhythm drive ecosystem response in tropical riverscape Ecology. 96:684-692.

Jiang, L., O. M. E. Schofield, and P. G. Falkowski. 2005. Adaptive evolution of phytoplankton cell size. The American Naturalist 166:496-505.

Jiang, X., B. Pan, Z. Sun, L. Cao, and Y. Lu. 2020. Application of taxonomic distinctness indices of fish assemblages for assessing effects of river-lake disconnection and eutrophication in floodplain lakes. Ecological Indicators 110:105955.

Jones, J. I. and C. D. Sayer. 2003. Does the fish-invertebrate-periphyton cascade precipitate plant loss in shallow lakes? Ecology 84:2155-2167.

Julian, J. P., E. H. Stanley, and M. W. Doyle. 2008. Basin-scale consequences of agricultural land use on benthic light and availability and primary production along a sixth-order temperate river. Ecosystems 11:1091-1105.

Junk, W. J. 2005. Flood pulsing and the linkages between terrestrial, aquatic, and wetland systems. Internationale Vereinigung fur theoretische und angewandte Limnologie: Verhandlungen 29:11-38.

Junk, W. J., P. B. Bayley, and R. E. Sparks. 1989. The Flood Pulse Concept in River Floodplain Systems. Canadian Special Publication of Fisheries and Aquatic Sciences 106:110-127.

Kalff, J. 2002. The Phytoplankton. Pages 309-348 in: Limnology: Inland Water Ecosystems. Bibliogenica, LLC, Duluth, MN.

Kaller, M. D., R. F. Keim, B. L. Edwards, A. R. Harlan, T. E. Pasco, W. E. Kelso, and D. A. Rutherford. 2015. Aquatic vegetation mediates the relationship between hydrologic connectivity and water quality in a managed floodplain. Hydrobiologia 760:29-41.

Kaller, M. D., W. E. Kelso, B. T. Halloran, and D. A. Rutherford. 2011. Effects of spatial scale on the assessment of dissolved oxygen dynamics in the Atchafalaya River Basin, Louisiana. Hydrobiologia 658:7-15.

Keizer, F. M., P. P. Schot, T. Okruszko, J. Chormanski, I. Kardel, and M. J. Wassen. 2014. A new look at the Flood Pulse Concept: the (ir)relevance of the moving littoral in temperate zone rivers. Ecological Engineering 64:85-99.

Khuantrairong, T. and S. Traichaiyaporn. 2011. The nutritional values of edible freshwater algae Cladophora sp. (Chlorophyta) grown under different phosphorus concentrations. International Journal of Agriculture and Biology 13:297-300.

Kiss, K. T., R. Klee, L. Ector, and E. Acs. 2012. Centric diatoms of large rivers and distributaries in Hungary: morphology and biogeographic distribution. Acta Botanica Croatica 71:311-363.

Kniffin, M., C. Neill, R. McHorney, and G. Gregory. 2009. Nutrient limitation of periphyton and phytoplankton in Cape Cod Coastal plain ponds. Northeastern Naturalist 16:395-408.

Koksvik, J. I. and H. Reinertsen. 2008. Changes in macroalgae and bottom fauna in the winter period in the regulated Alta river in Northern Norway. River Research and Applications 24:720-731.

Kralj, K., A. Plenkovic-Moraj, M. Gligora, B. Primc-Habdija, and L. Sipos. 2006. Structure of periphytic community on artificial substrate: influence of depth, slide orientation, and colonization tie in karstic Lake Visovacko, Croatia. Hydrobiologia 560:249-258.

Kroes, D. E., R. Day, C. Demas, Y. Allen, and S. Roberts. 2019. Channel modification and evolution alter hydraulic connectivity in the Atchafalaya River basin increasing vulnerability to sea-level rise. SEDHYD 2019 Conference.

Kuhmayer, T., F. Guo, N. Ebm, T. J. Battin, M. T. Brett, S. E. Bunn, B. Fry, and M. J. Kainz. 2020. Preferential retention of algal carbon in benthic invertebrates: stable isotope and fatty acid evidence from an outdoor flume experiment. Freshwater Biology 65:1200-1209.

Lambou, V. W. 2020. Importance of bottomland hardwood forest zones to fishes and fisheries: the Atchafalaya Basin, a case history. Pages 125-193 in: Lambou, V. W (editor). Ecological Processes and Cumulative Impacts. CRC Press, Boca Raton.

Lansac-Toha, F. M., B. R. Meira, B. T. Segovia, F. A. Lansac-Toha, and L. F. M. Velho. 2016. Hydrological connectivity determining metacommunity structure of plankton heterotrophic flagellates. Hydrobologia 78:81-94.

Leauthaud, C., L. Kergoat, P. Hiernaux, M. Grippa, W. Musila, S. Duvail, and J. Albergel. 2018. Modelling the growth of floodplain grasslands to explore the impact of changing hydrological conditions on vegetation productivity. Ecological Modelling 387:220-237.

Lemes-da-Silva, N. M., L. H. Z. Branco, and O. Necchi-Junior. 2010. Corticolous green algae from tropical forest remnants in the northwest region of Sao Paulo State, Brazil. Brazilian Journal of Botany 33:215-226.

Leveque, C. 1995. River and stream ecosystems of northwest Africa. Ecosystems of the World 519-536.

Lewis, W. M., S. K. Hamilton, M. A. Lasi, and M. Rodriguez. 2000. Ecological determinism on the Orinoco Floodplain: A 15-year study of the Orinoco floodplain shows that this productive and biotically diverse ecosystem is functionally less complex than it appears. Hydrographic and geomorphic controls induce a high degree of determinism in biogeochemical and biotic processes. BioScience 50:681-692.

Li, C., W. Feng, H. Chen, X. Li, F. Song, W. Guo, J. P. Giesy, and F. Sun. 2019. Temporal variation in zooplankton and phytoplankton, community species composition and the affecting factors in Lake Taihu - a large freshwater lake in China. Environmental Pollution 245:1050-1057.

Liboriussen, L. and D. Jeppesen. 2006. Structure, biomass, production, and depth distribution of periphyton on artificial substratum in shallow lakes with contrasting nutrient concentration. Freshwater Biology 51:95-109.

Liston, S. E., S. Newman, and J. C. Trexler. 2008. Macroinvertebrate community response to eutrophication in an oligotrophic wetland: an in situ mesocosm experiment. Wetlands 28:686-694.

Litchman, E., C. A. Klausmeier, and K. Yoshiyama. 2009. Contrasting size evolution in marine and freshwater diatoms. Proceedings of the National Academy of Sciences 106:2665-2670.

Liu, X. and H. Wang. 2010. Estimation of minimum area requirement of river-connected lakes for fish diversity conservation in the Yangtze River floodplain. Diversity and Distributions 16:932-940.

Louisiana Department of Natural Resources. 2010. Atchafalaya Basin. FY 2010 annual plan.

Maberly, S. C., K. M. Dent, R. I. Jones, and C. E. Gibson. 2002. Nutrient limitation of phytoplankton and periphyton growth in upland lakes. Freshwater Biology 47:2136-2152.

Maranon, E. 2014. Cell size as a key determinant of phytoplankton metabolism and community structure. Annual Review of Marine Science 7:241-264.

Marrase, C., C. M. Duarte, and D. Vaque. 1989. Succession patterns of phytoplankton blooms: directionality and influence of algal cell size. Marine Biology 102:43-48.

Matejovic, I. 2008. Determination of carbon, hydrogen, and nitrogen in soils by automated elemental analysis (dry combustion method). Communications in Soil Science and Plant Analysis 24:17-18.

Maznah, W. O. W and M. Mansor. 2002. Aquatic pollution assessment based on attached diatom communities in the Pinang River Basin, Malaysia. Hydrobiologia 487:229-241.

Mihalijevic, M. and T. Z. Pfeiffer. 2012. Colonization of periphyton algae in a temperate floodplain lake under a fluctuating spring hydrological regime. Fundamental and Applied Limnology 180:13-25.

Mihaljevic, M. and F. Stevic. 2011. Cyanobacterial blooms in a temperate river floodplain ecosystem: the importance of hydrological extremes. Aquatic Ecology 45:335-349.

Mihaljevic, M., T. Z. Pfeiffer, F. Stevic, and D. S. Maronic. 2013. Dynamics of phytoplankton and periphyton algae in a Danubian floodplain lake: a comparison study under altered hydrological conditions. Fresenius Environmental Bulletin 22:2516-2523.

Molinari, B. B., S. Koster, M. F. Adame, M. D. Campbell, G. McGregor, and C. Schulz. 2021. Relationships between algal primary productivity and environmental variables in tropical floodplain wetlands. Inland Waters 11:180-190.

Morin, J. O. and K. Kimball. 1983. Relationship of macrophyte-mediated changes in the water column to periphyton composition and abundance. Freshwater Biology 13:403-414.

Moulton, T. P., C. L. co-Amorim, C. Y. Sasada-Sato, V. Neres-Lima, and E. Zandona. 2015. Dynamics of algal production and ephemeropteran grazing of periphyton in a tropical stream. International Review of Hydrobiology 100:61-68.

Moyle, P. B. and J. F. Mount. 2007. Homogenous rivers, homogenous faunas. Proceedings of the National Academy of Sciences 104:5711-5712.

Mullin, C. A., C. J. Kirchhoff, G. Wang, and P. Vlahos. 2020. Future projections of water temperature and thermal stratification in Connecticut reservoirs and possible implications for cyanobacteria. Water Resources Research 56:e2020WR027185.

Muzik, I. 2002. A first-order analysis of the climate change effect on flood frequencies in a subalpine watershed by means of a hydrological rainfall-runoff model. Journal of Hydrology 267:65-73.

Necchi, Jr. O. 2004. Light-related photosynthetic characteristics of lotic macroalgae. Hydrobiologia 525:139-155.

NOAA Fisheries: Office of Science and Technology, Annual Commercial Landing Statistics. 2018. NOAA: Silver Springs.

NOAA. National Oceanic and Atmosphere Administration. 2020. U.S. Billion-dollar weather and climate disasters National Centers for Environmental Information (NCEI). https://www.ncdc.noaa.gov/billions/.

O'Farrell, I., A. Vinocur, and P. de Tezanos Pinto. 2015. Long-term study of bloom forming cyanobacteria in a highly fluctuating vegetated floodplain lake: a morpho-functional approach. Hydrobiologia 752:91-102.

Okada, Hisako and Yasunori Watanabe. 2002. Effect of physical factors on the distribution of filamentous green algae in the Tama River. Limnology 3:121-126.

Oksanen, J., F. G. Blanchet, M. Friendly, R. Kindt, P. Legendre, D. McGlinn, P. R. Minchin, R. B. O'Hara, G. L. Simpson, P, Solymos, and M. H. H. Stevens. 2019. Package vegan. R package version 2.5-6.

Oksanen, J., F. G. Blanchet, R. Kindt, P. Legendre, P. R. Minchin, R. B. O'Hara, G. L. Simpson, P. Solymos, M. H. H. Stevens, and H. Wagner. 2014. Vegan: Community Ecology package. R Package Version 2.2-0. http://CRAN.Rproject.org/package=vegan

Oliveira, E. C., K. Alveal, and R. J. Anderson. 2000. Mariculture of the argar-producing Gracilarioid red algae. Reviews in Fisheries Science 8:345-377.

Oliveira, M. and D. F. Calheiros. 2000. Flood pulse influence on phytoplankton communities of the south Pantanal floodplain, Brazil. Hydrobiologia 427:101-112.

Opperman, J. J., R. Luster, B. A. McKenny, M. Roberts, and A. W. Meadows. 2010. Ecologically functional floodplains: Connectivity, flow regime, and scale. Journal of the American Water Resources Association 46.2:211.

Ortiz, J. E., A. M. Marcarelli, K. J. Juneau, and C. J. Huckins. 2019. Aquatic Botany 156:1-9.

Ott, D. W., C. K. Oldham-Ott, N. Rybalka, and T. Friedl. 2015. Xanthophyte, eustigmatophyte, and raphidophyte algae. Pages 485-536 in: Wehr, J. D., S. Sheath, and P. Kociolek, editors. Freshwater Algae of North America. Academic Press, San Diego, CA.

Owens, T. G., P. G. Falkowski, and T. E. Whitledge. 1980. Diel periodicity in cellular chlorophyll content in marine diatoms. Marine Biology 59:71-77.

Pacheco, C. H. A. and I. E. L. Neto. 2017. Effects of artificial circulation on the removal kinetics of cyanobacteria in a hypereutrophic shallow lake. Journal of Environmental Engineering 143:06017010.

Paerl, H. W., K. E. Havens, H. Xu, G. Zhu, M. J. McCarthy, S. E. Newell, J. T. Scott, N.

S. Hall, T. G. Otten, B. Qin. 2020. Mitigating eutrophication and toxic cyanobacterial blooms in large lakes: The evolution of a dual nutrient (N and P) reduction paradigm. Hydrobiologia 847:4359-4375.

Pal, S., T. R. Lee, and N.E. Clark. 2020. The 2019 Mississippi and Missouri river flooding and its impact on atmospheric boundary layer dynamics. Geophysical Research Letters 47.e2019GL086933.

Parra, S. M., V. Sanial, A. D. Boyette, M. K. Cambazoglu, I. M. Soto, A. T. Greer, L. M. Chiaverano, A. Hoover, and M. S. Dinniman. 2020. Bonnet Carre Spillway freshwater transport and corresponding biochemical properties in the Mississippi Bight. Continental Shelf Research 199:104114.

Pasco, T. E., M. D. Kaller, R. Harlan, W. E. Kelso, D. A. Rutherford, and S. Roberts. 2016. Predicting floodplain hypoxia in the Atchafalaya River, Louisiana, USA, a large, regulated southern floodplain river system. River Research and Applications 32:845-855.

Pellegrini, B. G. and C. Ferragut. 2018. Associations between epiphyton species composition and macrophyte diversity in a shallow tropical reservoir. Fundamental and Applied Limnology 191:111-122.

Peres, C. K., A. F. Tonetto, M. V. Garey, and C. C. Z. Branco. 2017. Canopy cover as the key factor for occurrence and species richness of subtropical stream green algae (Chlorophyta). Aquatic Botany 137:24-29.

Perillon, C. and S. Hilt. 2019. Groundwater discharge gives periphyton a competitive advantage over macrophytes. Aquatic Botany 154:72-80.

Pettit, N. E., P. Bayliss, P. M. Davies, S. K. Hamilton, D. M. Warfe, S. E. Bunn, and M. M. Douglass. 2011. Seasonal contrasts in carbon resources and ecological processes on a tropical floodplain. Freshwater Biology 56:1047-1064.

Pettit, N. E., R. J. Naiman, D. M. Warfe, T. D. Jardine, M. M. Douglas, S. E. Bunn, and P. M. Davies. 2017. Productivity and Connectivity in tropical riverscapes of northern Australia: Ecological insights for management. Ecosystems 20:492-514.

Pflugmacher, S. 2002. Possible allelopathic effects of cyanotoxins with references to microcystins-LR, in aquatic ecosystems. Environmental Toxicology 17:407-413.

Philibert, A., P. Gell, P. Newall, B. Chessman, and N. Bate. 2006. Development of diatom-based tools for assessing stream water quality in south-eastern Australia: assessment of environmental transfer functions. Hydrobiologia 572:103-114.

Piazza, B. P. 2014. The Atchafalaya River Basin: history and ecology of an American wetland. No. 26. Texas A&M University Press, College Station, TX.

Piazza, B. P., Y. C. Allen, R. Martin, J. F. Bergan, K. King, and R. Jacob. 2015. Floodplain conservation in the Mississippi River Valley: combining spatial analysis, landowner outreach, and market assessment to enhance land protection for the Atchafalaya River Basin, Louisiana, U.S.A. Restoration Ecology 23:65-74

Piggott, J. J., R. K. Salis, G. Lear, C. R. Townsend, and C. D. Matthaei. 2015. Climate warming and agricultural stressors interact to determine stream periphyton community composition. Global Change Biology 21:206-222.

Prescott, G. W. 1942. The Algae of Louisiana, with descriptions of some new forms and notes on distribution. Transactions of American Microscopical Society 62:109-119.

Pribyl, P. and V. Cepak. 2019. Screening for heterotrophy in microalgae of various taxonomic positions and potential of mixotrophy for production of high-value compounds. Journal of Applied Phycology 31:1555-1564.

Price, J. J. and J.F. Berkowitz. 2020. Wetland functional responses to prolonged inundation in the active Mississippi River Floodplain. Wetlands 40:1949-1956.

Quirino, B. A., N. Carniatto, S. M. Thomaz, and R. Fugi. 2019. Small fish diet in connected and isolated lakes in a Neotropical floodplain. Ecology of Freshwater Fish 28:97-109.

R Core Team (2019). R: A language and environment for statistical computing. R

Rangel, L. M., L. H. S. Silva, E. J. Faassen, M. Lurling, and K. A. Ger. 2020. Copepod prey selection and grazing efficiency mediated by chemical and morphological defensive traits of cyanobacteria. Toxins 12:465.

Raven. J. A. 1994. Why are there no picoplanktonic O_2 evolvers within volumes less than 10-19m^3. Journal of Plankton Research 16:565-580.

Reed, T., L. R. Mason, and C. C. Ekenga. 2020. Adapting to climate change in the Upper Mississippi River Basin: Exploring stakeholder perspectives on river system management and flood risk reduction. Environment and Health 14:1-10.

Rees, G. N., R. A. Cook, N. S. P. Ning, P. J. McInerney, R. T. Petrie, and D. L. Nielsen. 2020. Managed floodplain inundation maintains ecological function in lowland rivers. Science of the Total Environment 727:138469.

Reid, M. A. and R. W. Ogden. 2009. Factors affecting diatom distribution in floodplain lakes of the southeast Murray Basin, Australia and implications for paleolimnological studies. Journal of paleolimnology 41:453-470.

Remo, J. W. F., B. S. Ickes, J. K. Ryherd, R. J. Guida, and M. D. Therrell. 2018. Assessing the impacts of dams and levees on the hydrologic record of the Middle and Lower Mississippi River, USA. Geomorphology 313:88-100.

Report of the Chief of Engineers, U.S. Army. 1941. Annual Reports, War Department. United States Government Printing Office. Washington.

Reynolds, C. S. 1984. The Ecology of Freshwater Plankton. Cambridge University Press, Cambridge, UK.

Reynolds, C. S. 1994. The long, the short and the stalled: on the attributes of phytoplankton selected by physical mixing in lakes and rivers. Hydrobiolgia 289:9-21.

Reynolds, C. S. 2002. Towards a functional classification of the freshwater phytoplankton. Journal of Plankton Research 24:417-428.

Reynolds, C. S., J. P. Descy, and J. Padisak (eds). 1994. Are phytoplankton dynamics in rivers so different from those in shallow lakes? Phytoplankton in Turbid Environments: Rivers and Shallow Lakes. Developments in Hydrobiology 100:1-7.

Reynolds, C. S., V. Huszar, C. Kruk, L. Naselli-Flores, and S. Melo. 2002. Towards a functional classification of the freshwater phytoplankton. Journal of Plankton Research 24:417-428.

Roberts, E., J. Kroker, S. Koner, and A. Nicklisch. 2003. The role of periphyton during the re-colonization of a shallow lake with submerged macrophytes. Hydrobiologia 506:525-530.

Robertson, A. I., P. Bacon, and G. Heagney. 2001. The response of floodplain primary production to flood frequency and timing. Journal of Applied Ecology 38:126-136.

Rodrigues dos Santos, T. and C. Ferragut. 2018. Changes in the taxonomic structure of periphytic algae on a free-floating macrophyte (*Utricularia foliosa* L.) in relation to macrophyte richness over seasons. Acta Botanic Brasilica 32:595-601.

Rolls, J. R. and G. G. Wilson. 2010. Spatial and temporal patterns in fish assemblages following an artificial extended floodplain inundation event, Northern Murray-Darling Basin, Australia. Environmental Assessment 45:822-833.

Rosen, T. and Y. J. Xu. 2015. Estimation of sedimentation rates in the distributary basin of the Mississippi River, the Atchafalaya River Basin, USA. Hydrology Research 46:244-257.

Rutherford, D. A., K. R. Gelwicks, and W. E. Kelso. 2001. Physicochemical effects of the flood pulse on fishes in the Atchafalaya River Basin, Louisiana. Transactions of the American Fisheries Society 130:276-288.

Sabo, M. J., C. F. Bryan, W. E. Kelso, and D. A. Rutherford. 1999. Hydrology and aquatic habitat characteristics of a riverine swamp: II Hydrology and the occurrence of chronic hypoxia. Regulated Rivers: Research and Management: An International Journal Devoted to River Research and Management 15:525-544.

Salmaso, N. 2000. Factors affecting the seasonality and distribution of cyanobacteria and chlorophytes: a case study from the large lakes south of the Alps, with special references to Lake Garda. Hydrobiologia. 438:43-62.

Salmaso, N. and M. Tolotti. 2009. Other phytoflagellates and groups of lesser importance. Pages 174-183 in: Likens, G. E., editor. Encyclopedia of inland waters. Elsevier, Oxford, UK.

Santonja. M., B. L. Rouzic, and G. Thiebaut. 2018. Seasonal dependence and functional implications of macrophyte-phytoplankton allelopathic interactions. Freshwater Biology 63:1161-1172.

Santos, S. A. M., T. R. dos Santos, M. S. R. Furtado, R. Henry, and C. Ferragut. 2018. Periphyton nutrient content, biomass and algal community on artificial substrate: response to experimental nutrient enrichment and the effects of its interruption in a tropical reservoir. Limnology 19:209-218.

Santos, T. R. D. and C. Ferragut. 2018. Changes in the taxonomic structure of periphytic algae on a free-floating macrophyte (*Ultricularia foliosa* L.) in relation to macrophyte richness over seasons. Acta Botanica Brasilica 32:595-601.

Schneider. S. C. and Z. Petrin. 2017. Effects of flow regime on benthic algae and macroinvertebrates – a comparison between regulated and unregulated rivers. Science of the Total Environment 579:1059-1072.

Scott, D. T., R. F. Keim, B. L. Edwards, C. N. Jones, and D. E. Kroes. 2014. Floodplain biogeochemical processing of floodwaters in the Atchafalaya River Basin during the Mississippi River flood of 2011. Journal of Geophysical Research: Biogeosciences 119:537-546.

Scrimgeor, G. J., R. J. Davidson, and J. M. Davidson. 1988. Recovery of benthic macroinvertebrate and epilithic communities following a large flood, in an unstable, braided, New Zealand river. New Zealand Journal of Marine and Freshwater Research 22:337-344.

Sheath, R. G. and J. M. Burkholder. 1983. Morphometry of Batrachospermum populations intermediate between *B. boryanum* and *B. ectocarpu* (Rhodophyta). Journal of Phycology 19:324-331.

Shurin, J. B., K. Cottenie, and H. Hillebrand. 2009. Spatial autocorrelation and dispersal limitation in freshwater organisms. Oecologia 159:151-159.

Silva, I. G. D., F. M. Pelicice, and L. C. Rodrigues. 2020. Loss of phytoplankton functional and taxonomic diversity induced by river regulation in a large tropical river. Hydrobiologia 847:3471-3485.

Silva, T. F., J. M. Melack, and E. M. L. M. Novo. 2013. Responses of aquatic macrophyte cover and productivity to flooding variability on the Amazon floodplain. Global Change Biology 19:3379-3389.

Silvia, J. V. F., M. T. Baumgartner, M. R. Miracle, J. D. Dias, L. C. Rodrigues, and C. C. Bonecker. 2019. Can zooplankton grazing effect the functional features of phytoplankton in subtropical shallow lakes? – Experimental in situ in the south of Brazil. Limnetica 38:773-785.

Siver P. A. and J. S. Hamer. 1992. Seasonal periodicity of chrysophytes and synurophyceae in a small New England Lake: Implications for paleolimnological research. Journal of Phycology 28:186-198.

Siver, P. A. and J. S. Hamer. 1989. Multivariate statistical analysis of the factors controlling the distribution of scaled chrysophytes. Limnology and Oceanography 34:368-381.

Smolar-Žvanut, N. and M. Mikoš. 2014. The impact of flow regulation by hydropower dams on the periphyton community of the Soca River, Slovenia. Hydrological Sciences Journal 59:1032-1045.

Sommer, T. R., W. C. Harrell, A. M. Solger, B. Tom, and W. Kimmerer. 2004. Effects of flow variation on channel and floodplain biota and habitats of the Sacramento River, California, USA. Aquatic Conservation. Marine and Freshwater Ecosystems 14:247-261.

Souza, M. L. D., B. G. Pellegrini, and C. Ferragut. 2015. Periphytic algal community structure in relation to seasonal variation and macrophyte richness in a shallow tropical reservoir. Hydrobiologia 755:183-196.

Stein, J. R. and C. A. Borden. 1979. Checklist of freshwater algae of British Columbia. Syesis 12:3-39.

Stevens, J. P. 2012. Applied multivariate statistics for the social sciences. 5th Ed. Routledge, New York.

Stevenson, R. J. 1990. Benthic algal community dynamics in a stream during and after a spate. Journal of the North American Benthological Society 9:277-288.

Stolte, W. and R. Riegman. 1996. A model approach for size-selective competition of marine phytoplankton for fluctuating nitrate and ammonium. Journal of Phycology 32:732-740.

Stolte, W., T. McCollin, A. A. M. Noordeloos, and R. Riegman. 1994. Effects of nitrogen sources on the size distribution within marine phytoplankton populations. Journal of Experimental Marine Biology and Ecology 184:83-97.

Strayer, D. L. 2010. Alien species in freshwaters: ecological effects, interactions with other stressors, and prospects for the future. Freshwater Biology 55:152-174.

Sunda, W. G. and D. R. Hardison. 2010. Evolutionary tradeoffs among nutrient acquisition, cell size, and grazing defense in marine phytoplankton promote ecosystem stability. Marine Ecology Progress Series 401:63-76.

Svensson, F., J. Norberg, and P. Snoeijs. 2014. Diatom cell size, coloniality and motility: Trad-offs between temperature, salinity and nutrient supply with climate change. PLoS ONE. 9(10): e109993. https://doi.org/10.1371/journal.pone.0109993.

Talbot, C. J., E. M. Bennett, K. Cassell, D. M. Hanes, E. C. Minor, H. Paerl, P. A. Raymond, R. Vargas, P. G. Vidon, W. Wolheim, and M. A. Xenopoulos. 2018. The impact of flooding on aquatic ecosystem services. Biogeochemistry 141:439-461.

Tang, M., Y. J. Xu, W. Xu, B. Wang, and H. Cheng. 2021. Three-decadal erosion and deposition of channel bed in the lower Atchafalaya River, the largest distributary of the Mississippi River. Geomorphology 380:107638.

Tang, T., S. Q. Niu, and D. Dudgeon. 2013. Responses of epibenthic algal assemblages to water abstraction in Hong Kong streams. Hydrobiologia 703:225-237.

Tesolin, G. and G. Tell. 1996. The epiphytic algae on floating macrophytes of a Parana river floodplain lake. Hydrobiologia 33:111-120.

Thomaz, S. M., F. A. Lansac Toha, M. C. Roberto, F. A. Esteves, and A. F. Lima. 1992. Seasonal variation of some limnological factors of lagoa do Guarana: a varzea lake of the High Rio Parana, state of Mato Grosso do Sul, Brazil. Revue d'hydrobiologia tropicale 25:269-276.

Thorp, J. H. and M. D. Delong. 1994. The riverine productivity model: a heuristic view of carbon sources and organic processing in large river ecosystems. Oikos 70:305-308.

Thorp, J. H. and M. D. Delong. 2002. Dominance of autochthonous autotrophic carbon in food webs of heterotrophic rivers. Oikos 96:543-550.

Tillman, D. 1982. Resource Competition and Community Structure. Princeton University Press.

Tonetto, A. F., C. C. Z. Branco, and C. K. Peres. 2012. Effects of irradiance and spectral composition on the establishment of macroalgae in streams in southern Brazil. Annales de Limnologie-International Journal of Limnology 48:363-370.

Tonkin, J. D, R. G. Death, and J. Barquin. 2014. Periphyton control on stream invertebrate diversity: is periphyton architecture more important than biomass? Marine and Freshwater Research 65:818-829.

Tonkin, J. D. and R. G. Death. 2013. Macroinvertebrate drift-benthos trends in a regulated river. Fundamental and Applied Limnology 182:231-245.

Tonkin, J. D., R. G. Death, and J. Barquin. 2014. Periphyton control on stream invertebrate diversity: is periphyton architecture more important than biomass. Marine and Freshwater Research 65:818-829.

Tonkin, J. D., R. G. Death, and M. K. Joy. 2009. Invertebrate drift patterns in a regulated river: dams, periphyton biomass or longitudinal patterns? River Research and Applications 25:1219-1231.

Torres-Ruiz, M., J. D. Wehr, and A. A. Perrone. 2007. Trophic relations in a stream food web: importance of fatty acids for macroinvertebrate consumers. Journal of the North American Benthological Society 26:509-522.

Townsend, S. Jr., J. Schult, M. Douglas, and A. Lautenschlager. 2017. Recovery of benthic producers from flood disturbance and its implications for an altered flow regime in a tropical savannah river (Australia). Aquatic Botany 136:9-20.

Townsend, S., J. Schult, M. Douglas, and A. Lautenschlager. 2017. Recovery of benthic primary producers from flood disturbance and its implications for an altered flow regime in a tropical savanna river (Australia). Aquatic Botany 136:9-20.

Trainer, V. L., S. K. Moore, G. Hallegaeff, R. M. Kudela, A. Clement, J. I. Mardones, and W. P. Cochlan. 2020. Pelagic harmful algal blooms and climate change: Lessons from nature’s experiments with extremes. Harmful Algae 91:101591.

Troch, M. D., V. Chepurnov, H. Cheerardyn, A. Vanreusel, E. Olafsson. 2005. Is diatom size selection by harpacticoid copepods related to grazer body size? Journal of Experimental Marine Biology and Ecology 332:1-11.

Troutman, J. P., D. A. Rutherford, and W. E. Kelso. 2007. Patterns of habitat use among vegetation-dwelling littoral fishes in the Atchafalaya River Basin, Louisiana. Transactions of the American Fisheries Society 136:1063-1075.

Tsai, J., Y. Chuang, Z. Wu, M. Kuo, and H. Lin. 2014. The effects of storm-induced events on the seasonal dynamics of epilithic algal biomass in subtropical mountain streams. Marine and Freshwater Research 65:25-38.

Tunca, H., T. O. Sevindik, D. N. Bal, and S. Arabaci. 2014. Community structure of epiphytic algae on three different macrophytes at Acarlar floodplain forest (northern Turkey). Chinese Journal of Oceanology and Limnology 32:845-857.

Vadeboncoeur, Y. and A. D. Steinman. 2002. Periphyton function in lake ecosystems. The Scientific World JOURNAL 2:1449-1469.

Van den Brink, F. W. B., M. M. van Katwijk, G. Van der Velde. 1994. Impact of hydrology on phyto- and zooplankton community composition in floodplain lakes along the Lower Rhine and Meuse. Journal of Plankton Research 16:351-373.

Vesterinen, J., S. P. Devlin, J. Syvaranta, and R. I. Jones. 2015. Accounting for littoral primary production by periphyton shifts a highly humic boreal lake towards net autotrophy. Freshwater Biology 61:265-276.

Walley, R. C. 2007. Environmental factors affecting the distribution of native and invasive aquatic plants in the Atchafalaya River Basin, Louisiana, USA.

Wan Maznah, W. O. and M. Mansor. 2002. Aquatic pollution assessment based on attached diatom communities in the Pinang River Basin, Malaysia. Hydrologia 487:229-241.

Wang, B., Y. J. Xu, W. Xu, H. Cheng, Z. Chen, and W. Zhang. 2020. Riverbed changes of the uppermost Atchafalaya River, USA – A case study of channel dynamics in large man-controlled alluvial river confluences. Water 12:2139.

Ward, D. P., N. E. Pettit, M. Adame, M. M. Douglas, S. A. Setterfield, and S. E. Bunn. 2016. Seasonal spatial dynamics of floodplain macrophyte and periphyton abundance in the Alligator Rivers region (Kakadu) of northern Australia. Ecohydrology 9:1675-1686.

Wehr, J. D., R. G. Sheath, and J. P. Kociolek (Editors.). 2015. Freshwater algae of North America: ecology and classification. Academic Press, San Diego, CA.

Weilhoefer, C. L., Y. Pan, S. Eppard. 2008. The effects of river floodwaters on floodplain wetland water quality and diatom assemblages. Wetlands 28:473-486.

Wetzel, R. G. 1964. A comparative study of the primary productivity of higher aquatic plants, periphyton, and phytoplankton in a large, shallow lake. Internationale Revue der Gesamten Hydrobiolotie 49:1-61.

Wetzel, R. G. 1983. Attached algal-substrata interactions: Fact or myth, and when and how? Periphyton of Freshwater Ecosystems. Springer, Netherlands 17:207-215.

Wujek, D. E. 2013. A new freshwater chrysophyte, *Chrysomorula cohaerens* gen. et sp. nov. (Chrysophyceae, Chrysocapsaceae) from North America. Phytotaxa 93:61-64.

Yang, W., C. Catalanotti, T. M. Wittkopp, M. C. Posewitz, A. R. Grossman. 2015. Algae after dark: mechanisms to cope with anoxic/hypoxic conditions. The Plant Journal 82:481-503.

Zarfl, C., A. E. Lumsdon, J. Berlekamp, L. Tydecks, and K. Tockner. 2015. A global boom in hydropower dam construction. Aquatic Sciences 77:161-170.

Zarfl, C., J. Berlekamp, F. He, S. C. Jähnig, W. Darwall, and K. Tockner. 2019. Future large hydropower dams impact global freshwater megafauna. Scientific Reports 9:1-10.

Zhang, M., J. Xu, and L. A. Hansson. 2015. Local environment overrides regional climate influence on regime shift in a north temperate lake. Aquatic Ecology 49:105-113.

Zhang, W., H. Shen, J. Zhang, J. Y, P. Xie, and J. Chen. 2020. Physiological differences between free-floating and periphytic algae, and specific submerged macrophytes induce proliferation of filamentous algae: A novel implication for lake restoration. Chemosphere 239.124702.

VITA

Kamela De Gallardo was born in Oklahoma City, Oklahoma in September 1989. She was homeschooled K-12 and attended Sinclair Community College in Dayton, OH, her Freshman and Sophomore years. In 2010, Kamela transferred to Bowling Green State University, where she pursued a B.S. in Biological Sciences. She volunteered as an undergraduate research in the labs of Drs. Moira van Staaden and Robert Huber and studied agonistic behavior in Malawi cichlid fish. She graduated summa cum laude and honors in Biology in 2012 and continued with Dr. van Staaden for her M.S., which she attained in 2014. After working as a technician for Dr. Mark Benfield in the Department of Oceanography and Coastal Sciences at Louisiana State University, Kamela enrolled in the graduate program in the School of Renewable Natural Resources under Drs. William Kelso and Allen Rutherford and is now a doctoral candidate.